```
21.6 15.2 7.4 3.8 352.9 76.4 302.9 -28.4 14.3 4.6 7.5 58.0 111.9 349.9 2
40.0 8.4 10.2 3.7 157.0 234.0 292.9 -28.0 26.9 11.8 5.3 178.0 139.0 34.0 2
21.9 0 25.6 0 0 312.9 0 0.0 0 11.5 0 0 194.0 0 1
17.4 24.5 25.4 4.0 130.0 217.9 110.1 -6.6 4.4 8.1 0.8 204.6 143.6 345.5 2
26.5 14.7 8.9 4.5 137.9 177.2 53.6 8.2 9.5 11.7 2.0 204.0 106.1 91.9 2
11.4 0 2.5 0 0 287.4 0 10.3 0 10.3 0 0 306.2 0 1
-26.3 0 15.6 0 0 85.0 0 -25.8 0 8.7 0 0 146.0 0 1
17.0 50.0 28.2 2.0 13.0 231.0 146.0 -39.7 7.7 14.4 5.4 250.0 97.0 77.0 2
-4.6 0 11.2 0 0 21.0 0 -6.1 0 9.1 0 0 316.9 0 1
-2.6 3.9 3.6 1.7 335.9 276.6 287.9 -12.5 5.6 7.4 5.0 240.0 121.8 10.0 2
-4.5 8.2 3.0 9.6 273.9 322.4 10.0 -5.5 6.3 14.5 13.5 320.9 82.1 351.9 2
-94.4 0 106.1 0 0 152.0 0 -45.3 0 23.8 0 0 238.0 0 1
0 0 0 0 0 0 0 0 0 0 0 0 0 0
-10.6 14.9 42.2 1.9 238.9 260.0 214.0 -31.7 14.3 20.0 2.6 260.0 226.0 138.0 2
0 0 0 0 0 0 0 0 0 0 0 0 0 0
-30.3 0 55.3 0 0 17.0 0 7.3 0 43.8 0 0 313.7 0 1
0 0 0 0 0 0 0 0 0 0 0 0 0 0
0 0 0 0 0 0 0 0 0 0 0 0 0 0
0 0 0 0 0 0 0 0 0 0 0 0 0 0
5.3 47.8 11.7 11.2 157.0 218.0 17.0 -23.6 25.5 18.6 7.5 165.0 116.0 307.9 2
0.0 0 11.9 0 0 260.5 0 7.4 0 2.6 0 0 251.7 0 1
15.1 13.4 45.1 12.7 67.0 100.0 14.0 15.2 42.9 39.8 19.5 185.0 203.0 24.0 2
34.4 0 34.5 0 0 130.7 0 0.0 0 25.6 0 0 38.6 0 1
0 0 0 0 0 0 0 0 0 0 0 0 0 0
0 0 0 0 0 0 0 0 0 0 0 0 0 0
7.7 59.5 30.3 6.5 173.0 188.0 145.0 -23.1 31.0 12.8 10.3 174.0 134.0 28.0 2
2.3 8.5 9.1 8.8 133.0 198.0 349.9 -1.0 2.0 3.3 3.4 219.0 196.3 319.9 2
13.4 9.5 38.1 16.7 312.9 73.8 16.0 25.7 21.9 22.3 19.8 185.0 171.6 35.0 2
50.1 0 13.0 0 0 79.3 0 -1.8 0 16.5 0 0 16.1 0 1
22.2 0 10.9 0 0 42.0 0 16.2 0 19.6 0 0 11.0 0 1
0 0 0 0 0 0 0 0 0 0 0 0 0 0
-19.4 13.7 36.2 9.1 153.0 153.0 20.0 -56.3 30.9 27.6 12.4 206.0 90.0 321.9 2
-8.1 0 11.4 0 0 1.0 0 -11.2 0 45.6 0 0 266.0 0 1
-19.1 34.2 39.4 25.5 164.0 77.6 329.9 -25.4 19.7 39.6 29.0 229.0 194.6 26.0 2
0 0 0 0 0 0 0 0 0 0 0 0 0 0
1.7 0 0.0 0.0 251.0 0 5.5 0 35.0 0 0 290.0 0 1
```

File FAR2 (F-Region)

```
8.4 57 17 11.1 329.5 37.6 317 -3.9 23.2 8.4 4.4 239 145 201 2
15.1 16.2 28.6 18.5 314.9 286.9 17 -35.4 11.7 7.6 8.2 26 134 9 2
4.7 14.8 10.4 15.6 312.6 228.7 9.5 -8 1.7 7.9 5.7 350.1 64.7 345.6 2
-19.6 16.7 21.5 19.7 252.6 177.1 18.2 -14.9 8.6 14.4 6.4 277.4 96.5 210 2
-7.3 13.7 4.2 4.1 225.3 252.6 13.9 -10.1 6.3 7.1 3.5 316.7 107.3 322.8 2
-19.1 15.1 14.9 13.2 216.1 141.1 6.1 -4.9 8.2 7.7 5.8 85.9 33.1 277 2
19.4 74.4 18.2 17.2 299.9 41 342.9 -18 33.8 17.1 8.3 224 32 198 2
-4.7 24.5 45.8 13.5 323.9 235.9 351.9 -42.2 13.6 3.1 3.3 4 216 327.9 2
-12 30.9 5.3 15.6 296.5 211 356.9 -22.9 10.6 12.3 8.3 17.2 52.8 334.5 2
-46.5 11.8 27.5 25.9 254.5 185.7 24.7 -27.5 6.6 22.6 12 10.5 57.8 210.7 2
-19.4 20.8 6.6 9.4 243.5 225.1 8.8 -25.7 10.7 9 5.2 346.6 90.8 342.7 2
-16.7 41.8 3.4 18.5 257.6 217.9 350.7 -12.1 21.6 19 13.3 26.2 29.6 296.7 2
29.6 6.3 26 14.2 283.9 35 338.9 -7.8 24.9 19 8.2 259 215 181 2
34.9 15.5 14.3 18.2 214 312.9 32 -18 14 8.2 7.7 148 163 344.9 2
1.8 17.7 5.8 26.3 347.5 235.1 11 .7 6.7 16.5 12.5 272.3 62.3 331.4 2
-4.2 12.7 11.2 5.7 213.8 326 332.3 -4.3 5.0 13.3 10.5 244.9 213.4 30.5 2
-5 5.6 10 3.8 284 327.7 26.2 -5 5.6 5.9 8.6 295 1 352.4 2
12.5 29.9 15.2 5.8 72 107.8 21 18 20.1 5.9 1.6 152 306.9 205 2
16.5 61.2 4.1 20.8 301.9 88 328.9 3.1 20.3 3.5 9.6 260 168 238 2
10.4 23.4 12.2 16.2 347.9 246 6 -18.9 8 7.1 20.3 179 122 45 2
-3.9 9.4 9 19.2 281.1 215.8 11.7 -4.2 3.3 12.9 9.8 165.1 91.8 357.5 2
21.2 26.7 23.3 7 190.5 39.5 120.8 8.5 14.2 12.6 14.8 294.8 147.1 329.5 2
-3.4 10.8 1 7.2 204.8 56.7 325.4 -9.3 2.8 5.9 5.6 306.5 85.7 347.2 2
-13.0 32.4 17.9 9.3 98 257.7 297.9 1.9 14.1 9.2 2.2 115 230.4 205 2
13.5 75.8 18.5 16.7 293.9 23 348.9 -8.7 38.5 11.7 6.7 227 149 217 2
0 40 18.6 16.5 317.9 306.9 331.9 -35.3 16.1 16.6 12.8 2 86 32 2
-10.2 18.5 15.2 25.4 333.9 243 20.8 -17.4 11 13.8 10.4 4.8 63.4 329.1 2
-17.3 5.1 11.2 6.2 223.4 329.8 341.2 -12.6 11.3 10.9 12.1 246.3 117.6 356.2 2
-2.6 13.7 7.5 14.3 299.6 331 6.8 -4.4 19.6 8.1 8.8 6.8 43.1 28.7 2
-30.8 13.7 15 12.7 209 195.9 3 -6.3 3.1 5.4 11 40 340.8 333.9 2
16 69.1 19.7 12.6 339.3 35.4 298.7 -7.1 19.2 7.2 6.2 239 21 197 2
8.2 37.1 23.2 9.5 354.9 276.9 13 -44.6 8.2 5.6 2 343.9 212 274.9 2
-3.6 22.1 17.6 6.1 298.9 203.8 331.9 -28.6 3.9 18.2 4.3 234 108 9 2
-26.6 18.4 26.2 9.4 248.9 239.5 5.5 -17.2 3.1 14 6.9 280.3 154.5 250.7 2
-27.6 27.6 8.8 8.7 236.1 249.4 20.8 -26.8 3 16.9 5.1 355.1 95.6 300.4 2
-26.8 45.4 10.3 23.5 256.9 126.7 16.9 -20.6 19 25.4 12.6 29.3 38 294 2
-11.8 31.1 25.4 7.1 283.9 60.8 338.9 -3.9 12.5 9.8 4.1 260 215 18 2
43.9 0 10.4 0 0 26 0 -30.3 10.3 0 0 160 0 0 1
4.6 23.5 5.5 11.2 313.9 218.3 22 -5.6 9.1 12.5 4.2 200.8 102 318.9 2
```

-10.2	10.1	20.9	11.1	308.7	243.1	301.7	3.2	11.2	10.6	8.2	203.8	143	273.3	2
-8.3	22	12	5.8	182	303.9	49.9	-2.2	15.7	5.7	8.2	218.2	102.2	355.8	2
-18.5	21	8.4	12.4	258	212	67	2.5	7.4	9.9	10.4	229	103.9	4	2
13.7	28.7	10.4	14.3	13.5	48.8	292.1	2.3	3	15	9.7	277.9	165	272.9	2
38.6	0	7.1	0	0	358.9	0	-26	0	25.8	0	0	227	0	1
-3.2	18.1	21.9	8.6	290.3	235.1	10.1	-8.4	7.5	17.8	7.9	166.8	117.1	355	2
2.8	9.5	3.3	4	211.8	177.8	.4	-16.3	7.2	12.3	8.7	248	153.2	249.4	2
1.2	19.4	7	9.7	177.8	217.3	15	8.6	10	7.9	2.8	213.9	163	351.5	2
10.3	83.8	29.3	6.8	80	20	349.9	6.2	31.6	5.7	1.4	96	307.9	58	2
12.3	19.5	12.5	15.2	304.9	338.9	6	-11.9	22	6.4	11.1	142	176	278.9	2
26.2	22.4	16	10.9	353.9	281.9	322.9	-35.8	18	18.5	10.4	35	85	93	2
-5.1	22.8	24.7	23.5	342.9	253	34	-28.1	8.3	16.3	11.4	356.9	94	2	2
-8	25	19.1	11.2	270.3	266.6	350.9	-9.8	2.9	10.1	.4	136.6	170.1	101.1	2
-23.7	20.1	4.5	2.3	239.2	262.9	40.4	1.5	4.2	7.6	6.8	300.8	102.8	348.3	2
-56.5	0	28.7	0	0	294.3	0	-5.4	0	27.3	0	0	259.1	0	1
0	0	0	0	0	0	0	0	0	0	0	0	0	0	0
-13.1	13.6	51.5	3.6	270	282.9	110	-34.4	14.6	16.1	4.3	39	200	317.9	2
-11	24.1	5.2	7.8	272.7	185.9	328.1	-12.8	11.3	5.3	7.7	57	55.7	334.5	2
-17.9	0	51	0	0	323.1	0	-9.5	0	94.6	0	0	85.2	0	1
-28.3	6.3	2.3	11.3	301.1	121	6.6	-24.6	10.2	5.6	7.5	336	337.9	3.8	2
0	0	0	0	0	0	0	0	0	0	0	0	0	0	0
0	0	0	0	0	0	0	0	0	0	0	0	0	0	0
17.1	46.8	4.5	23.8	185	207	60	-13.4	14.8	13	6	140	110	28	2
-6	7.6	14.5	15.4	97.8	198	23.4	5.1	6.5	15.4	7.9	232.2	72.4	290.1	2
39.6	44.2	40	10.2	207	65	356.9	-4.5	11	15.9	37	295.9	180	41	2
-24.2	12.2	8.2	3.7	310.9	305.9	255	-24.4	9	5	4.9	343.9	326.8	27	2
0	0	0	0	0	0	0	0	0	0	0	0	0	0	0
0	0	0	0	0	0	0	0	0	0	0	0	0	0	0
0	0	0	0	0	0	0	0	0	0	0	0	0	0	0
-14.3	5.7	7	6.3	313.5	164.6	355.9	-2.9	6.9	8.5	4.9	215.2	109.4	332.4	2
34.8	32.1	53.3	21.9	179	26	116	24.2	23.2	7.8	25.5	306.9	153	318.9	2
-18.7	4.4	13.5	8.4	278.9	343.9	227	-30.1	5.5	7.5	6	352.9	360	355.9	2
-31	0	63.5	0	0	33	0	-5.7	0	13.2	0	0	61	0	1
0	0	0	0	0	0	0	0	0	0	0	0	0	0	0
-7.3	47.8	16.6	23.4	235.9	225	276.9	-20.4	25.9	18.5	14.8	329.9	140	16	2
-19.4	5.9	27.3	21.9	297.2	194	22.8	-11.6	4.5	17.9	8.5	240.6	108.8	276.9	2
23.3	22.8	24.5	9.9	140	46	331.9	-6.4	39.4	23	35.3	262	200.8	6	2
2.7	30.8	2.9	6.6	11.7	54.6	338.3	12.3	30.3	6.3	5.1	25.9	31.4	343.9	2
0	0	0	0	0	0	0	0	0	0	0	0	0	0	0

Chapter 4 IRI-90: Graphs

Contents

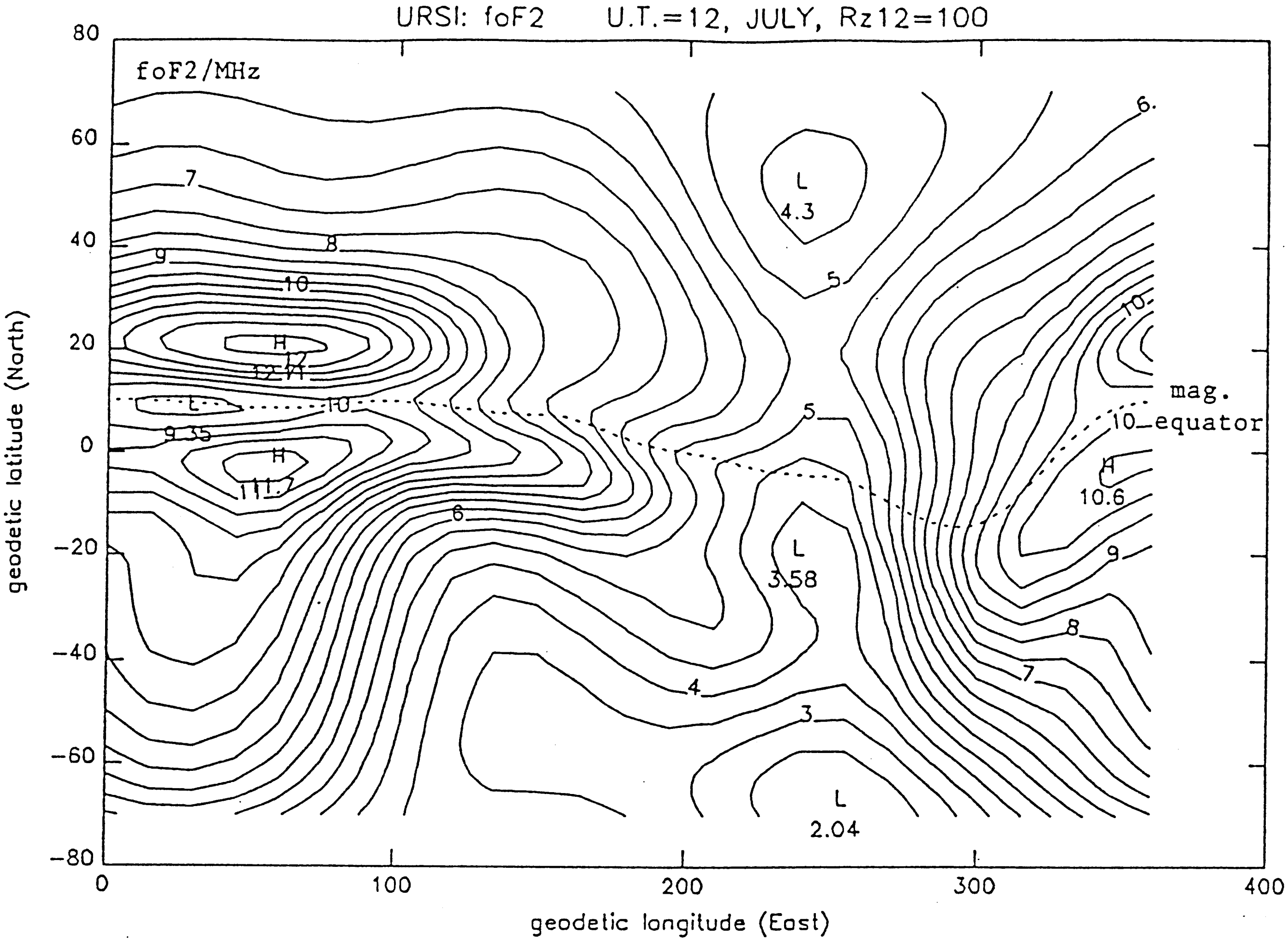
URSI: foF2 U.T.=12, JULY, Rz12=100
foF2/MHz
geodetic latitude (North)
geodetic longitude (East)
mag. equator
L
4.3
H
11.7
10.6
3.58
2.04

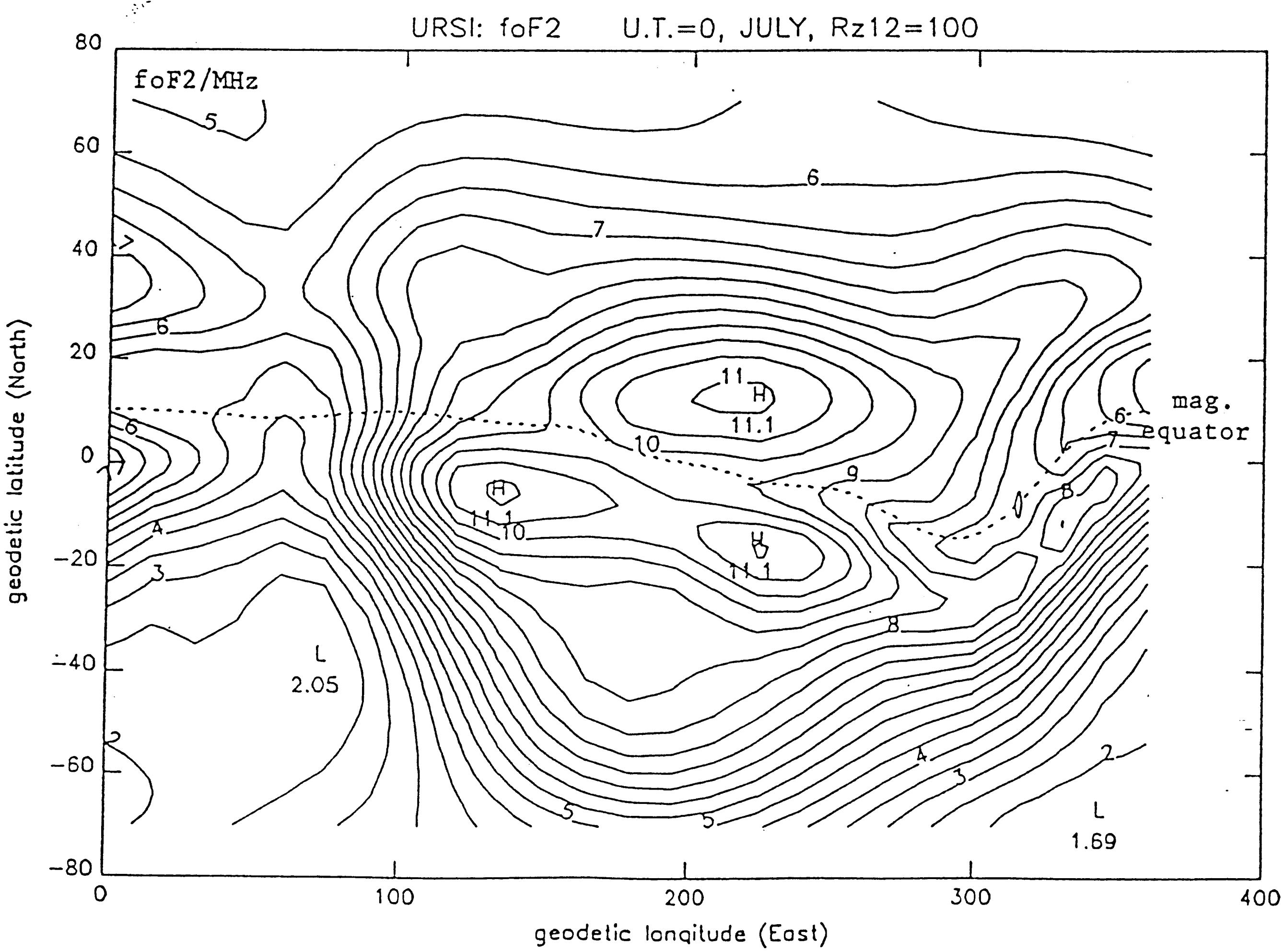
URSI: foF2 U.T.=0, JULY, Rz12=100
foF2/MHz
geodetic latitude (North)
geodetic longitude (East)
mag. equator
H
11.1
L
2.05
1.69

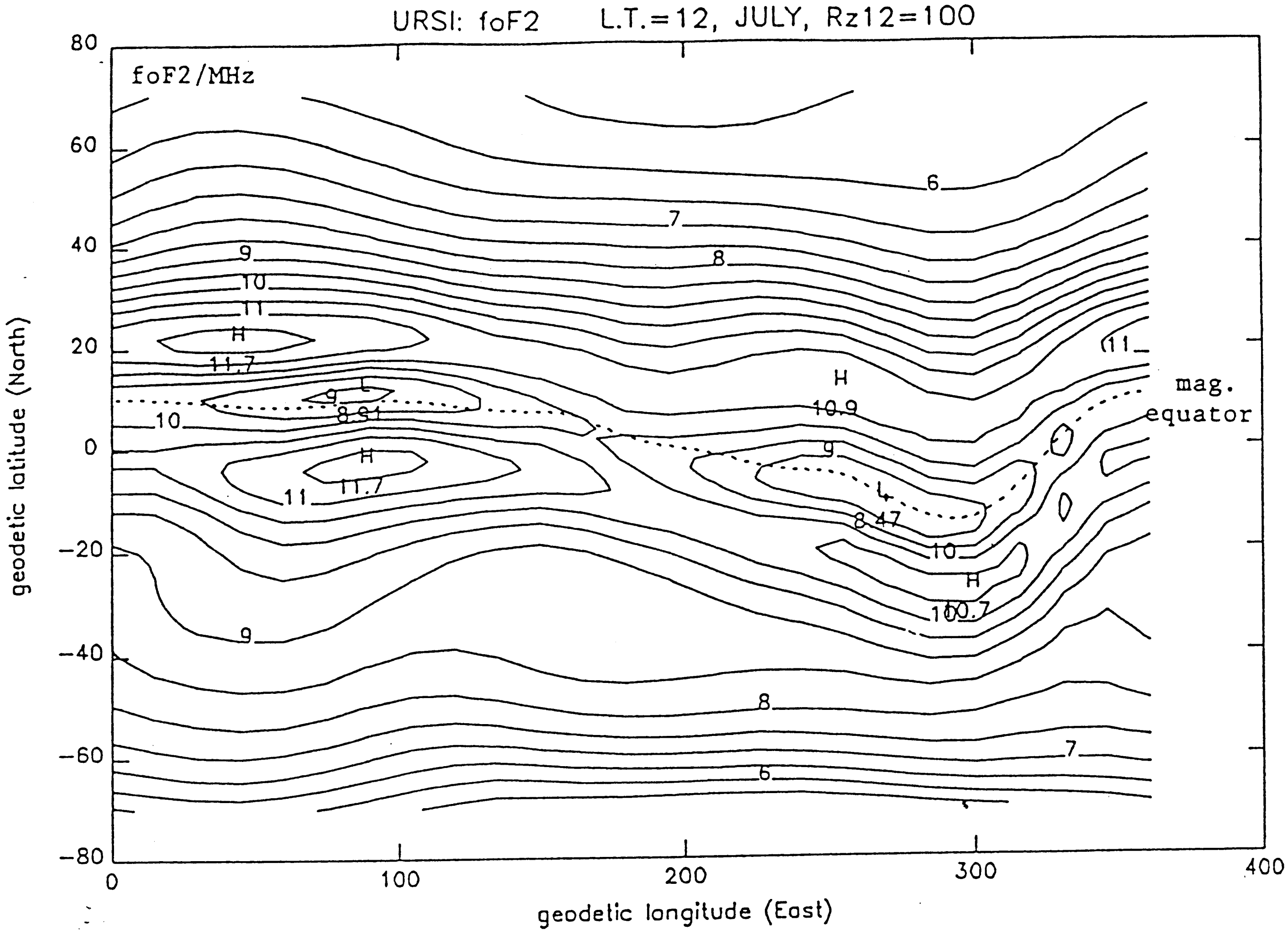
URSI: foF2 L.T.=12, JULY, Rz12=100
foF2/MHz
mag. equator
geodetic latitude (North)
geodetic longitude (East)
H
11.7
L
8.91
H
11.7
H
10.9
L
8.47
H
10.7

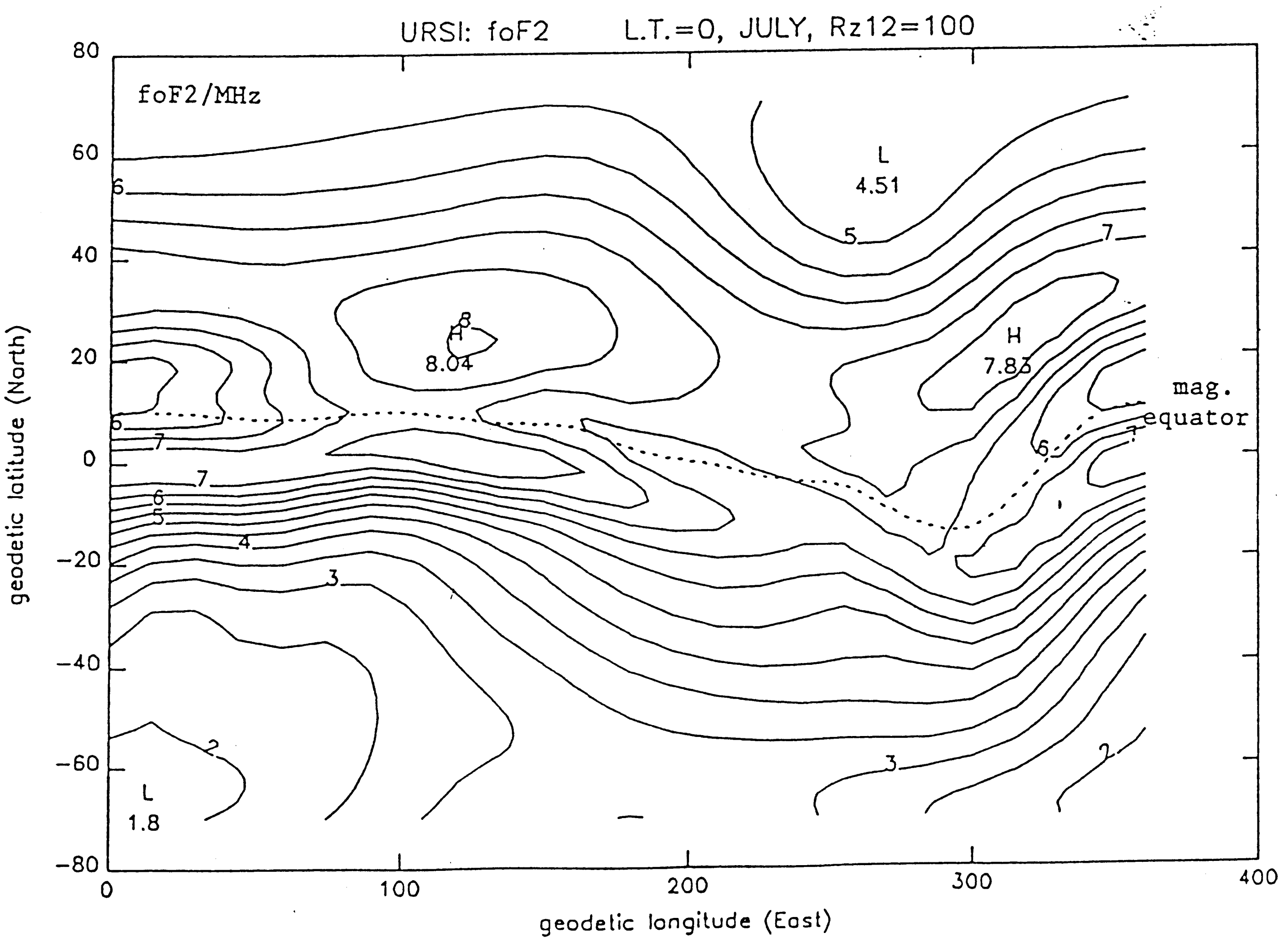
URSI: foF2 L.T.=0, JULY, Rz12=100
foF2/MHz
mag. equator
geodetic latitude (North)
geodetic longitude (East)
L
4.51
H
8.04
H
7.83
L
1.8

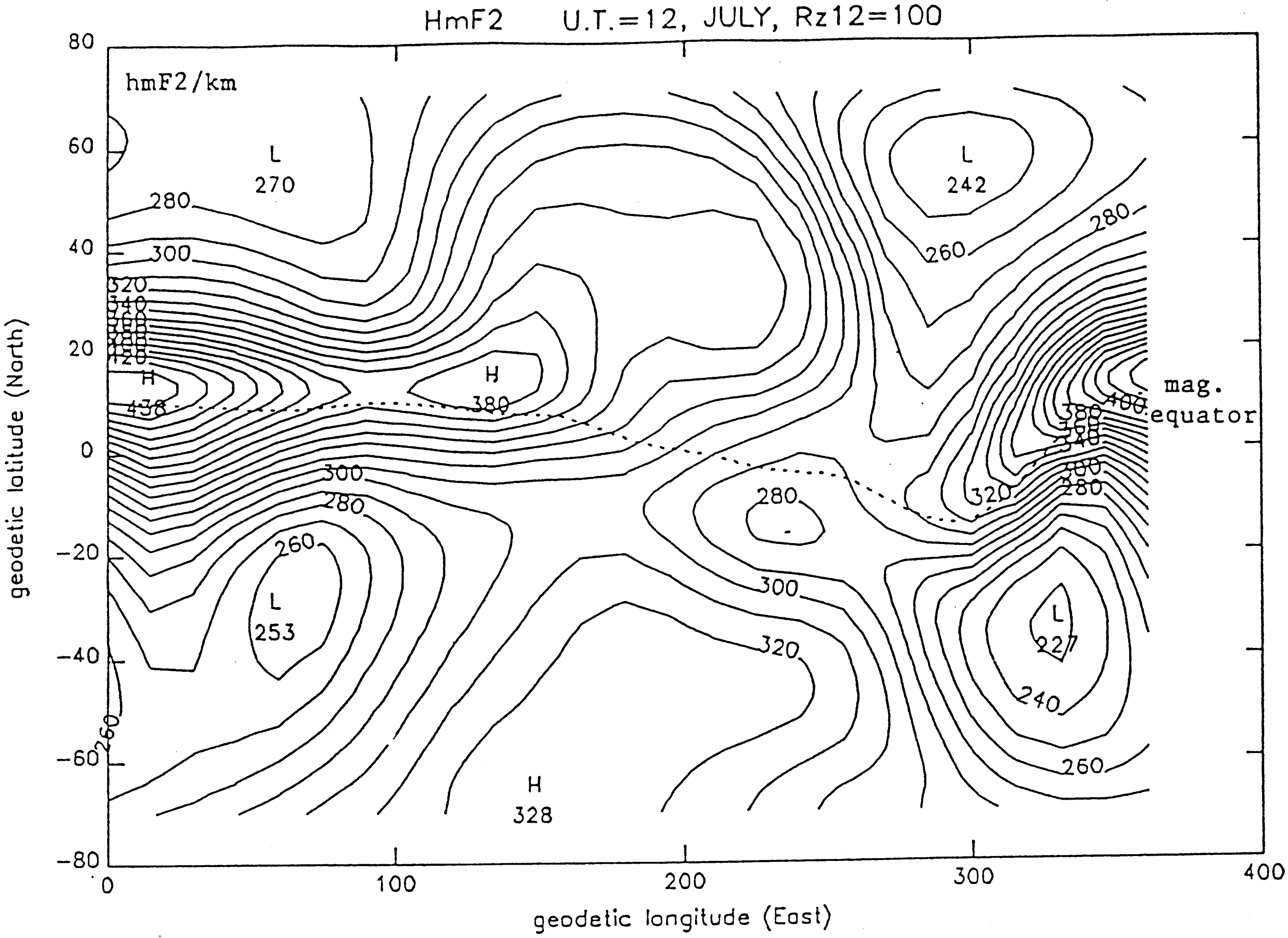
HmF2 U.T.=12, JULY, Rz12=100
hmF2/km
geodetic latitude (North)
geodetic longitude (East)
mag. equator
L 270
L 242
H 436
H 380
L 253
L 227
H 328
280
300
320
340
260
240
400
0
100
200
300
400
80
60
40
20
-20
-40
-60
-80

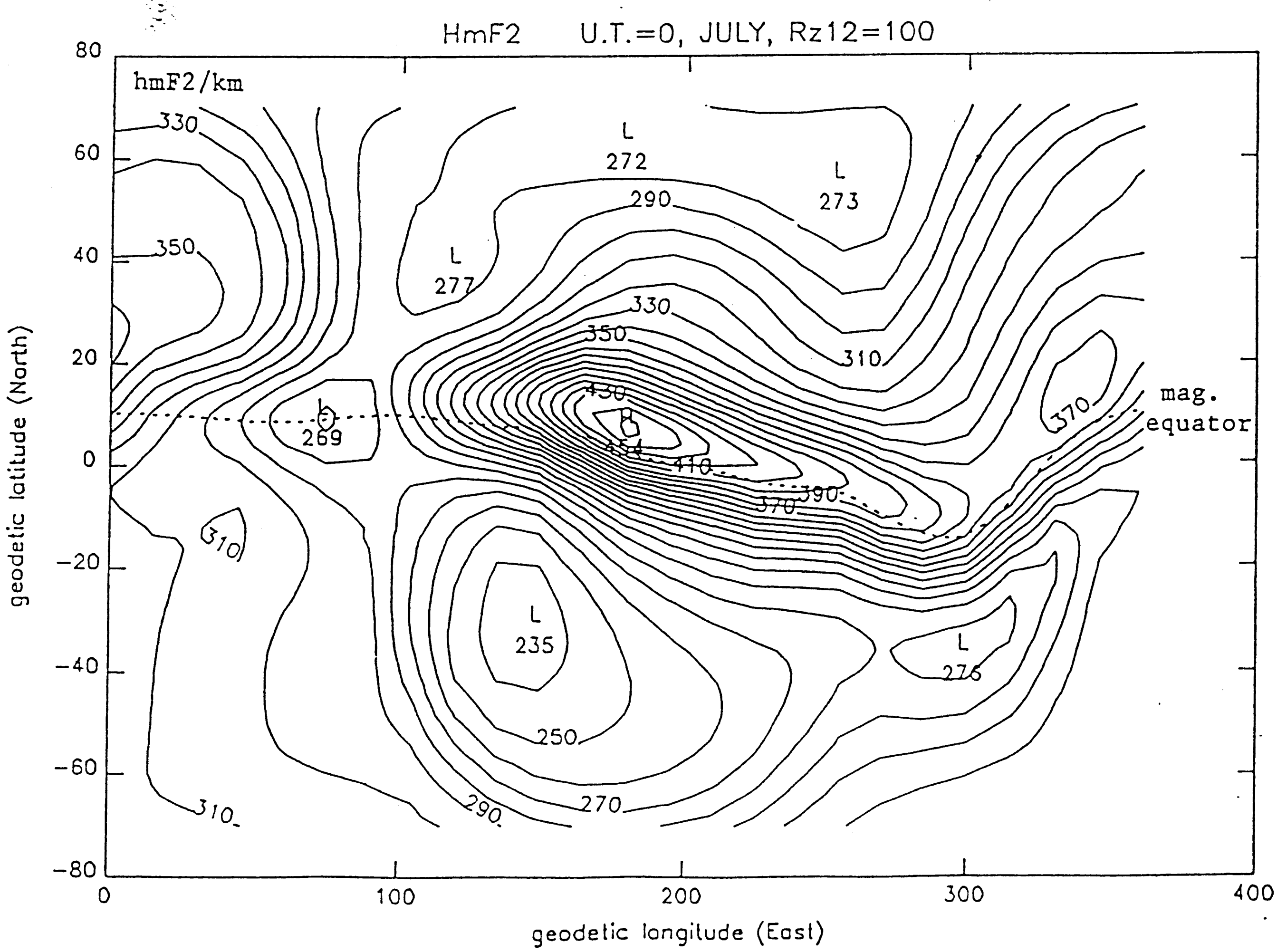
HmF2 U.T.=0, JULY, Rz12=100
hmF2/km
geodetic latitude (North)
geodetic longitude (East)
mag. equator
L 272
L 273
L 277
L 269
H 454
L 235
L 276
330
350
290
310
370
390
410
430
250
270
0
100
200
300
400
80
60
40
20
-20
-40
-60
-80

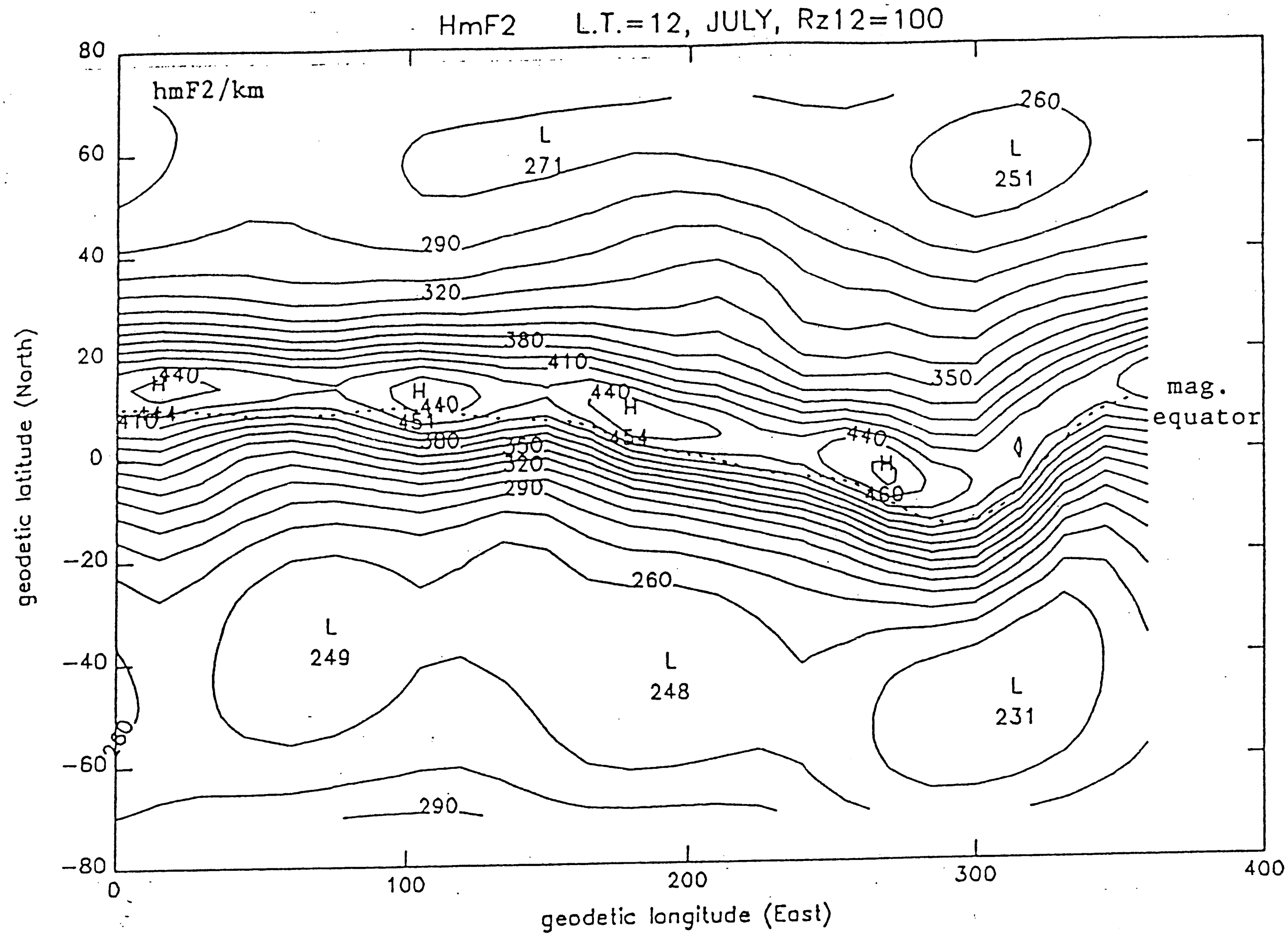
HmF2 L.T.=12, JULY, Rz12=100
hmF2/km
mag.
equator
geodetic latitude (North)
geodetic longitude (East)
260
L
271
L
251
290
320
380
410
350
440
H
440
451
454
440
460
380
350
320
290
260
L
249
L
248
L
231
280
290
0
100
200
300
400
80
60
40
20
0
-20
-40
-60
-80

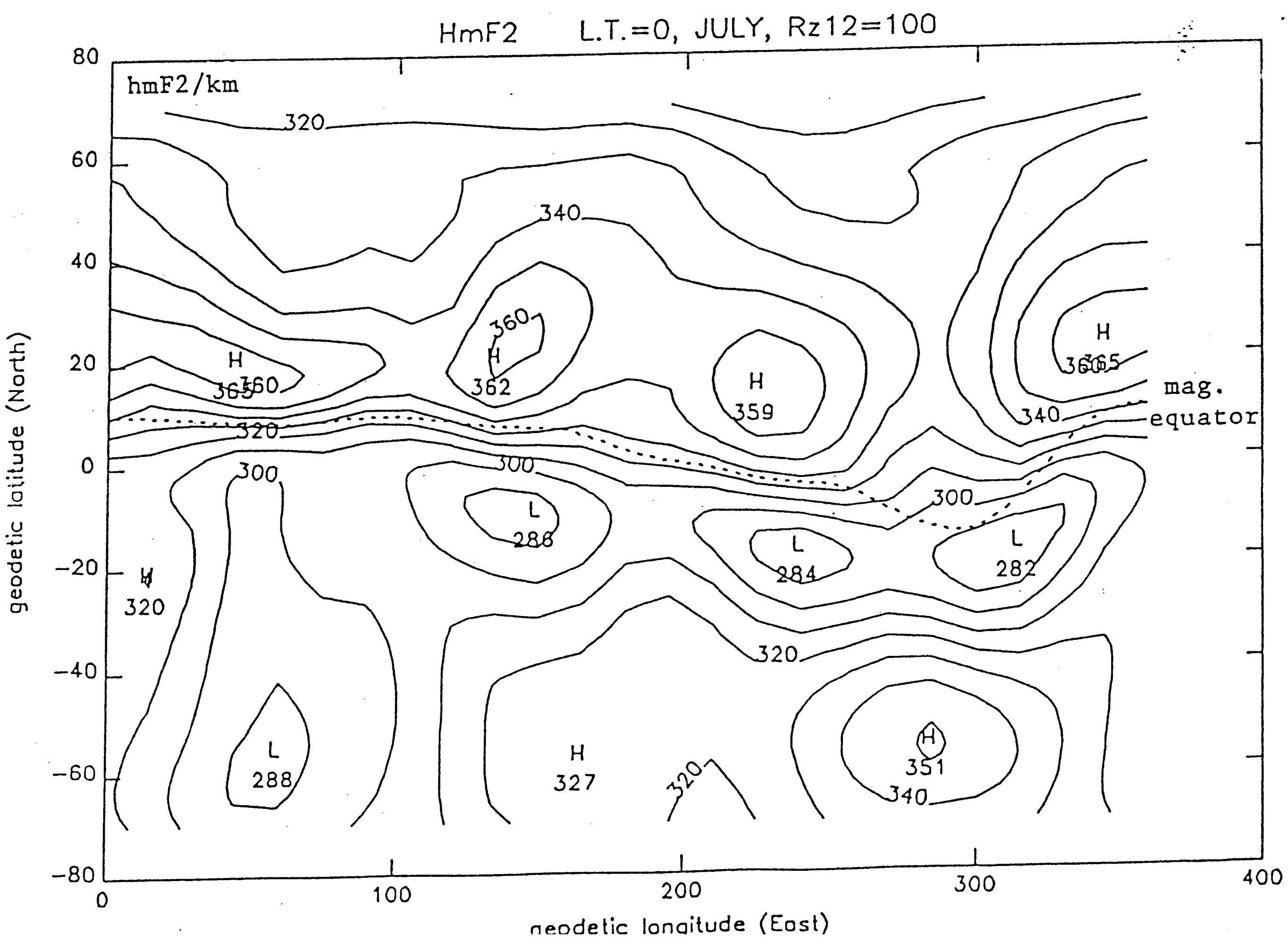
HmF2 L.T.=0, JULY, Rz12=100
hmF2/km
mag.
equator
geodetic latitude (North)
geodetic longitude (East)
320
340
360
H
362
H
359
H
365
360
H
365
360
340
320
300
300
300
L
286
L
284
L
282
H
320
320
L
288
H
327
320
H
351
340
0
100
200
300
400
80
60
40
20
0
-20
-40
-60
-80

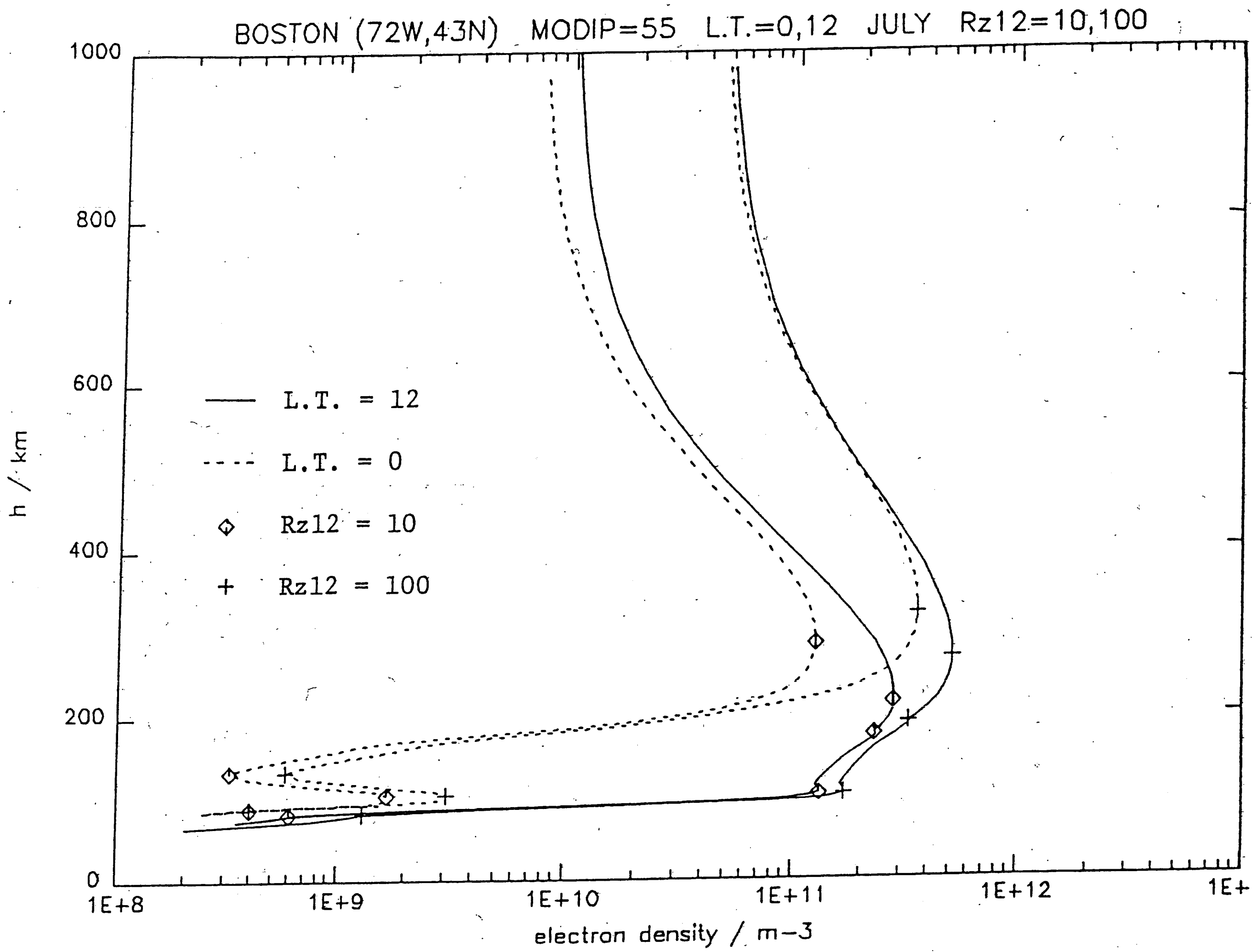
BOSTON (72W,43N) MODIP=55 L.T.=0,12 JULY Rz12=10,100
1000
800
600
400
200
0
h / km
L.T. = 12
L.T. = 0
Rz12 = 10
Rz12 = 100
1E+8
1E+9
1E+10
1E+11
1E+12
1E+
electron density / m-3

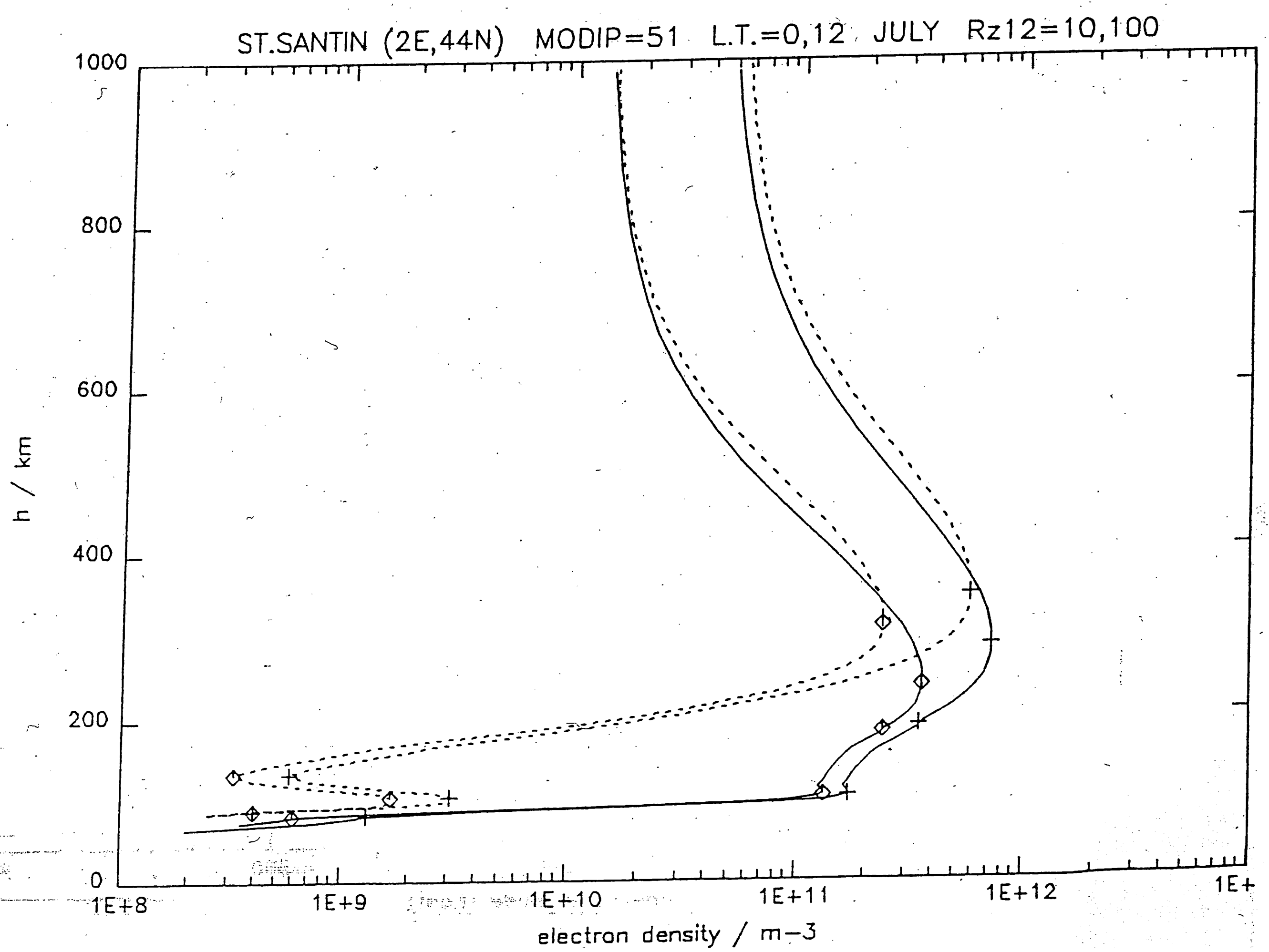
ST.SANTIN (2E,44N) MODIP=51 L.T.=0,12 JULY Rz12=10,100
1000
800
600
400
200
0
h / km
1E+8
1E+9
1E+10
1E+11
1E+12
1E+
electron density / m-3

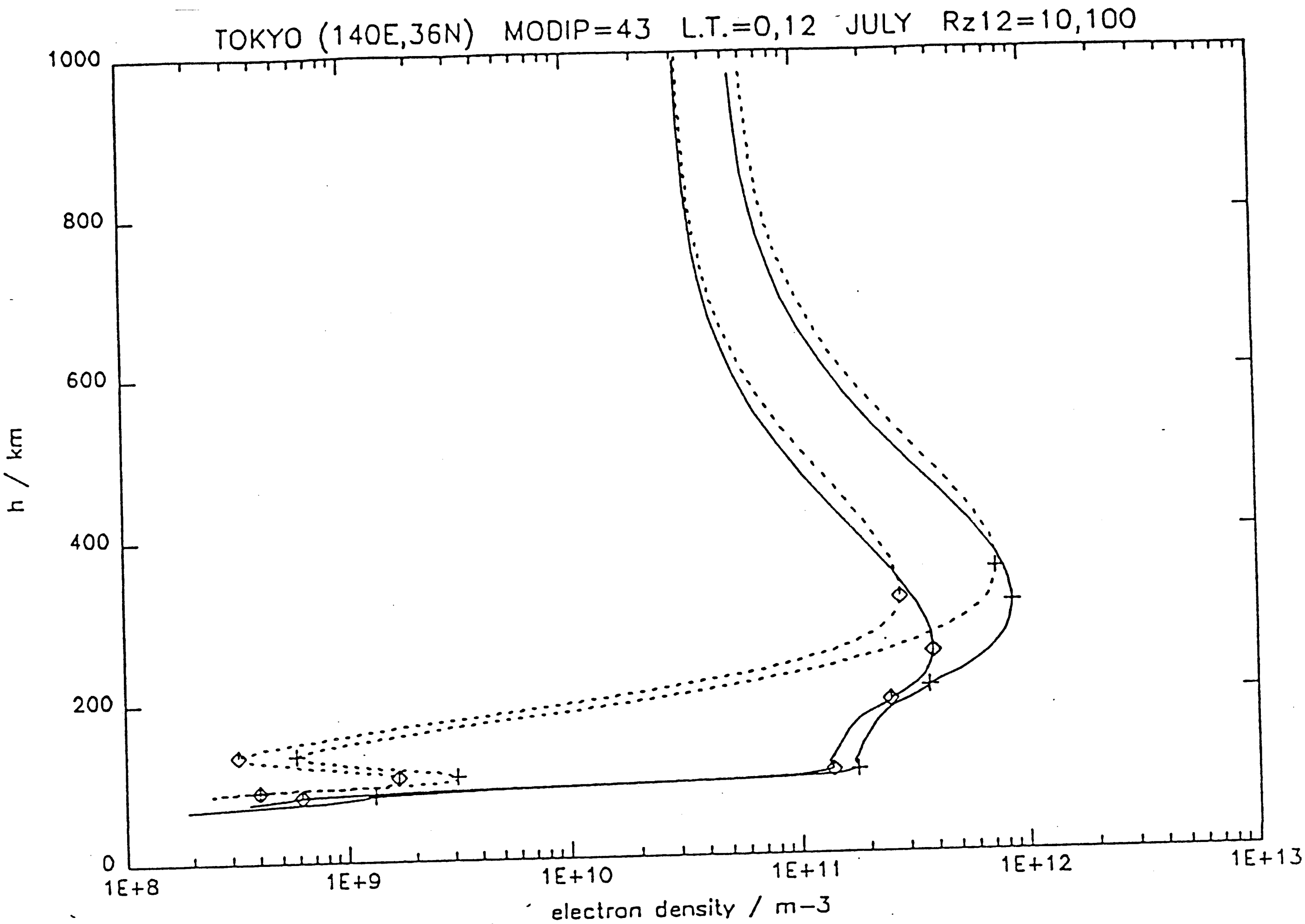

BOSTON	Rz12=10 noon h/km	N/m-3	midnight h/km	N/m-3	Rz12=100 noon h/km	N/m-3	midnight h/km	N/m-3
F2-peak	215.9	2.830E+11	286.8	1.250E+11	268.9	5.165E+11	322.6	3.567E+11
F1-peak	176.4	2.330E+11	0.0	0.000E+00	191.3	3.304E+11	0.0	0.000E+00
E-F-conn.	157.5	1.939E+11	229.8	9.176E+10	167.2	2.560E+11	247.4	2.407E+11
Valley-top	121.5	1.332E+11	170.4	1.707E+09	121.5	1.720E+11	170.4	3.090E+09
Valley-base	114.7	1.271E+11	133.0	3.244E+08	114.7	1.640E+11	133.0	5.871E+08
E-peak	105.0	1.332E+11	105.0	1.707E+09	105.0	1.720E+11	105.0	3.090E+09
D-point	81.0	6.141E+08	88.0	4.000E+08	81.0	1.316E+09	88.0	4.000E+08

ST.SANTIN	Rz12=10 noon h/km	N/m-3	midnight h/km	N/m-3	Rz12=100 noon h/km	N/m-3	midnight h/km	N/m-3
F2-peak	236.9	3.599E+11	308.9	2.407E+11	285.2	7.243E+11	347.0	5.844E+11
F1-peak	183.2	2.423E+11	0.0	0.000E+00	190.4	3.509E+11	0.0	0.000E+00
E-F-conn.	166.4	1.925E+11	239.2	1.094E+11	166.0	2.556E+11	262.7	3.046E+11
Valley-top	120.8	1.321E+11	169.6	1.707E+09	120.8	1.706E+11	169.6	3.090E+09
Valley-base	114.3	1.262E+11	133.0	3.244E+08	114.3	1.630E+11	133.0	5.871E+08
E-peak	105.0	1.321E+11	105.0	1.707E+09	105.0	1.706E+11	105.0	3.090E+09
D-point	81.0	6.117E+08	88.0	4.000E+08	81.0	1.311E+09	88.0	4.000E+08

TOKYO	Rz12=10 noon h/km	N/m-3	midnight h/km	N/m-3	Rz12=100 noon h/km	N/m-3	midnight h/km	N/m-3
F2-peak	250.0	3.822E+11	317.3	2.760E+11	310.9	8.454E+11	352.6	7.191E+11
F1-peak	191.7	2.506E+11	0.0	0.000E+00	208.3	3.663E+11	0.0	0.000E+00
E-F-conn.	174.7	1.987E+11	247.9	1.229E+11	184.1	2.637E+11	261.0	3.032E+11
Valley-top	119.1	1.373E+11	167.4	1.707E+09	119.1	1.772E+11	167.4	3.090E+09
Valley-base	113.3	1.319E+11	133.0	3.244E+08	113.3	1.702E+11	133.0	5.871E+08
E-peak	105.0	1.373E+11	105.0	1.707E+09	105.0	1.772E+11	105.0	3.090E+09
D-point	81.0	6.214E-08	88.0	4.000E+08	81.0	1.332E+09	88.0	4.000E+08

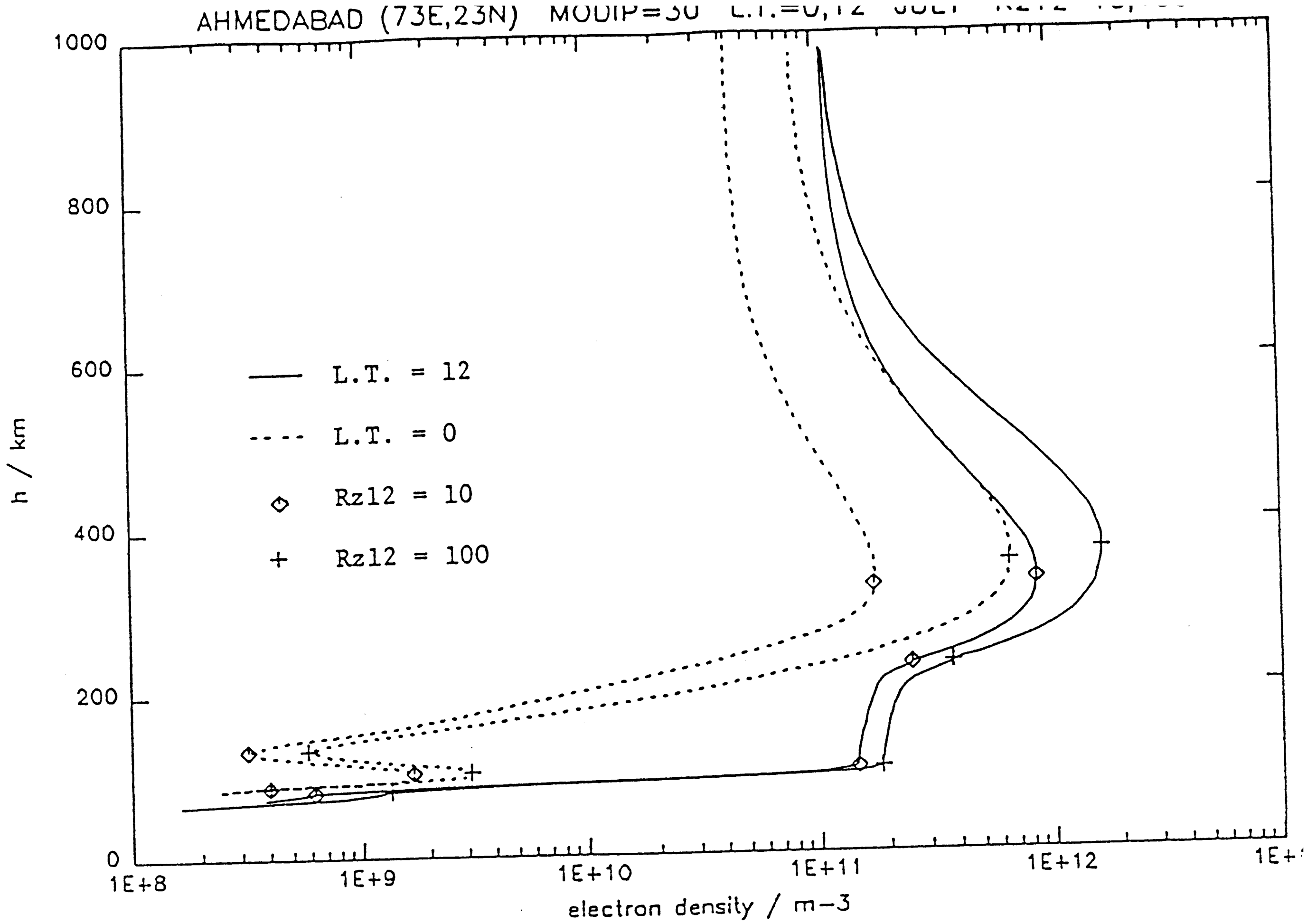

AHMEDABAD (73E,23N)
L.T. = 12
L.T. = 0
Rz12 = 10
Rz12 = 100
h / km
electron density / m-3
1E+8
1E+9
1E+10
1E+11
1E+12
0
200
400
600
800
1000

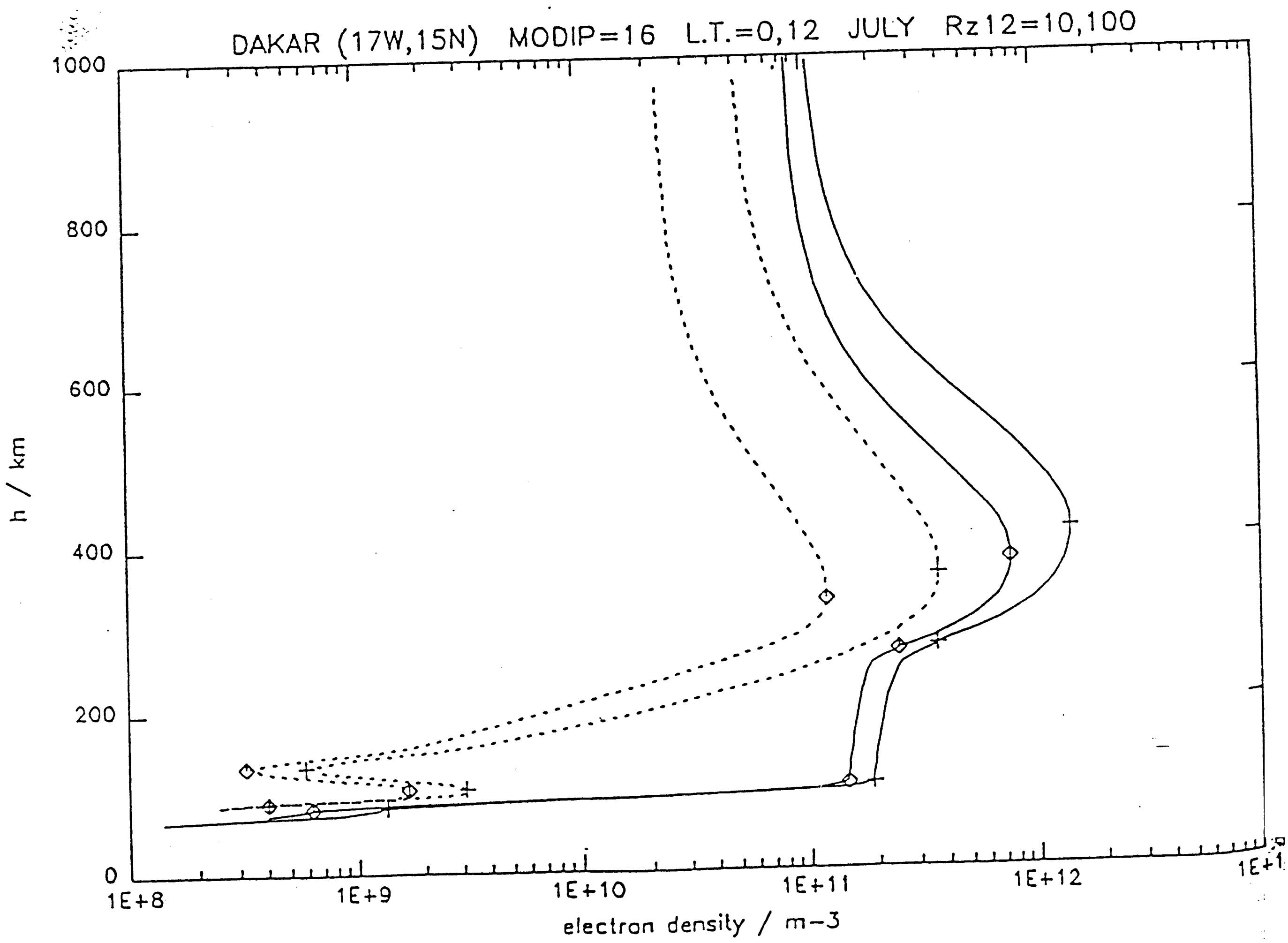

DAKAR (17W,15N) MODIP=16 L.T.=0,12 JULY Rz12=10,100
h / km
electron density / m-3
1E+8
1E+9
1E+10
1E+11
1E+12
0
200
400
600
800
1000

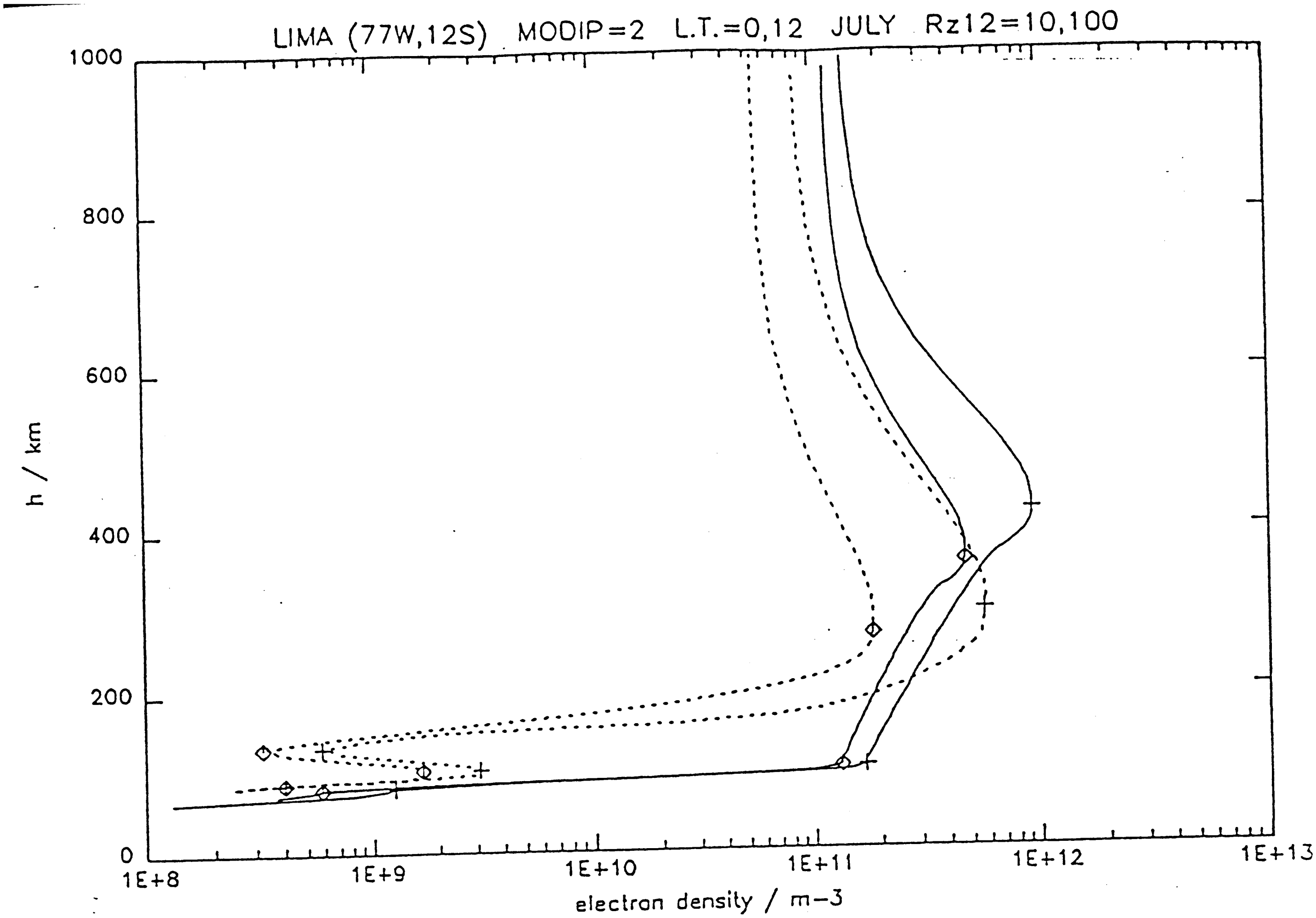

AHMEDABAD	Rz12=10 noon h/km	N/m-3	midnight h/km	N/m-3	Rz12=100 noon h/km	N/m-3	midnight h/km	N/m-3
F2-peak	329.6	8.342E+11	325.0	1.743E+11	366.6	1.635E+12	353.4	6.519E+11
F1-peak	228.4	2.532E+11	0.0	0.000E+00	230.0	3.708E+11	0.0	0.000E+00
E-F-conn.	213.9	1.974E+11	260.7	8.318E-10	208.3	2.565E+11	261.0	2.789E+11
Valley-top	113.9	1.445E+11	161.0	1.707E+09	113.9	1.866E+11	161.0	3.090E+09
Valley-base	110.2	1.410E+11	133.0	3.244E+08	110.2	1.820E+11	133.0	5.871E+08
E-peak	105.0	1.446E+11	105.0	1.707E+09	105.0	1.866E+11	105.0	3.090E+09
D-point	81.0	6.269E+08	88.0	4.000E+08	81.0	1.343E+09	88.0	4.000E+08

DAKAR	Rz12=10 noon h/km	N/m-3	midnight h/km	N/m-3	Rz12=100 noon h/km	N/m-3	midnight h/km	N/m-3
F2-peak	377.4	7.517E+11	329.9	1.202E+11	412.7	1.417E+12	359.1	3.682E+11
F1-peak	266.9	2.498E+11	0.0	0.000E+00	272.5	3.637E+11	0.0	0.000E+00
E-F-conn.	253.4	1.983E+11	270.0	6.065E+10	252.9	2.685E+11	269.2	1.716E+11
Valley-top	109.1	1.470E+11	155.1	1.707E+09	109.1	1.898E+11	155.1	3.090E+09
Valley-base	107.4	1.453E+11	133.0	3.244E+08	107.4	1.876E+11	133.0	5.871E+08
E-peak	105.0	1.470E+11	105.0	1.707E+09	105.0	1.898E+11	105.0	3.090E+09
D-point	81.0	6.258E+08	88.0	4.000E+08	81.0	1.341E+09	88.0	4.000E+08

LIMA	Rz12=10 noon h/km	N/m-3	midnight h/km	N/m-3	Rz12=100 noon h/km	N/m-3	midnight h/km	N/m-3
F2-peak	359.8	4.669E+11	269.5	1.847E+11	422.0	9.190E+11	297.5	5.680E+11
F1-peak	0.0	0.000E+00	0.0	0.000E+00	0.0	0.000E+00	0.0	0.000E+00
E-F-conn.	328.1	3.757E+11	215.3	1.024E+11	374.3	6.911E+11	261.9	5.432E+11
Valley-top	109.1	1.324E+11	155.1	1.707E+09	109.1	1.709E+11	155.1	3.090E+09
Valley-base	107.4	1.293E+11	133.0	3.244E+08	107.4	1.669E+11	133.0	5.871E+08
E-peak	105.0	1.324E+11	105.0	1.707E+09	105.0	1.709E+11	105.0	3.090E+09
D-point	81.0	5.888E+08	88.0	4.000E+08	81.0	1.262E+09	88.0	4.000E+08

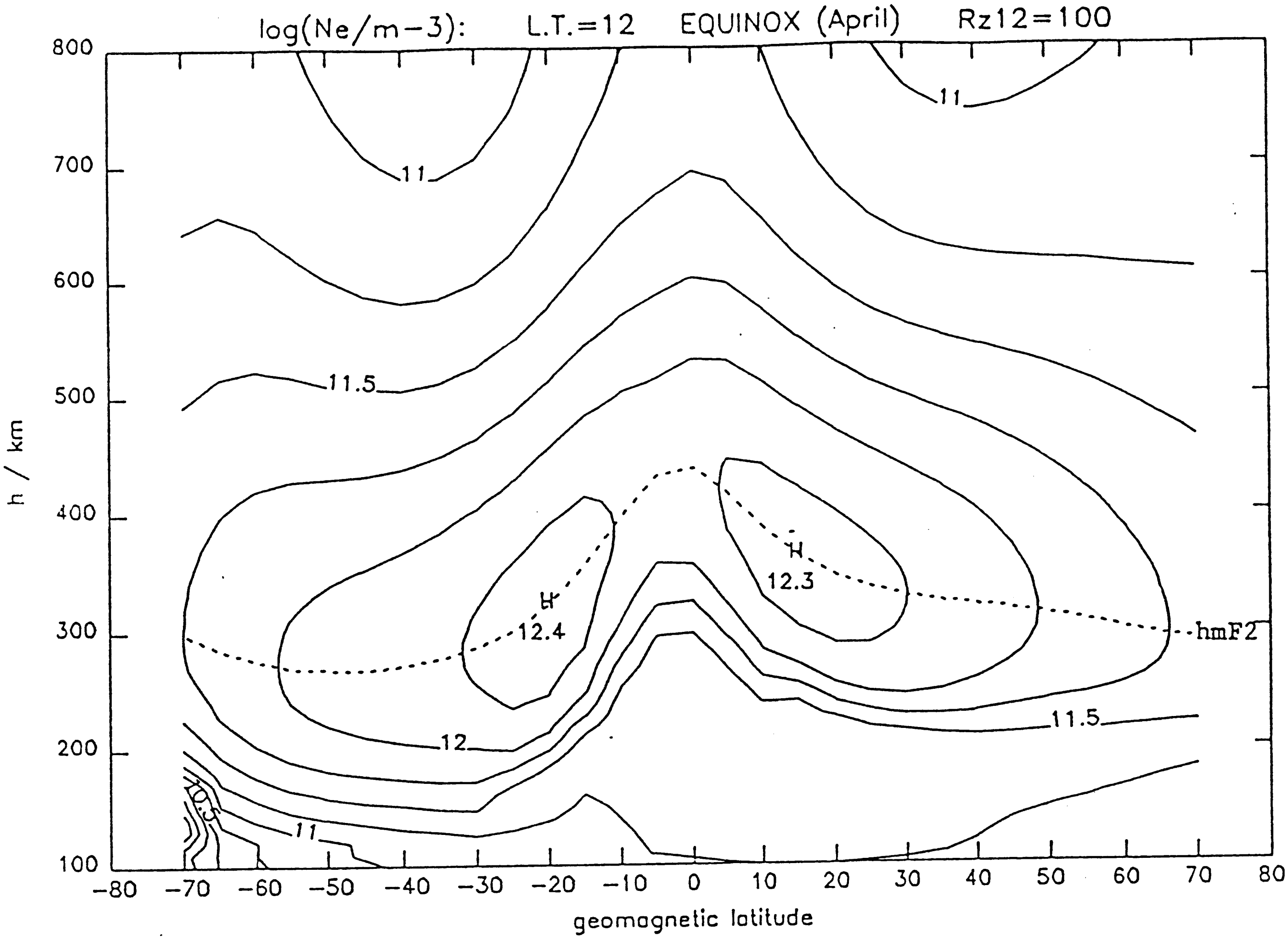
log(Ne/m-3): L.T.=12 EQUINOX (April) Rz12=100
h / km
geomagnetic latitude
hmF2
H
12.4
12.3
12
11.5
11
10.5

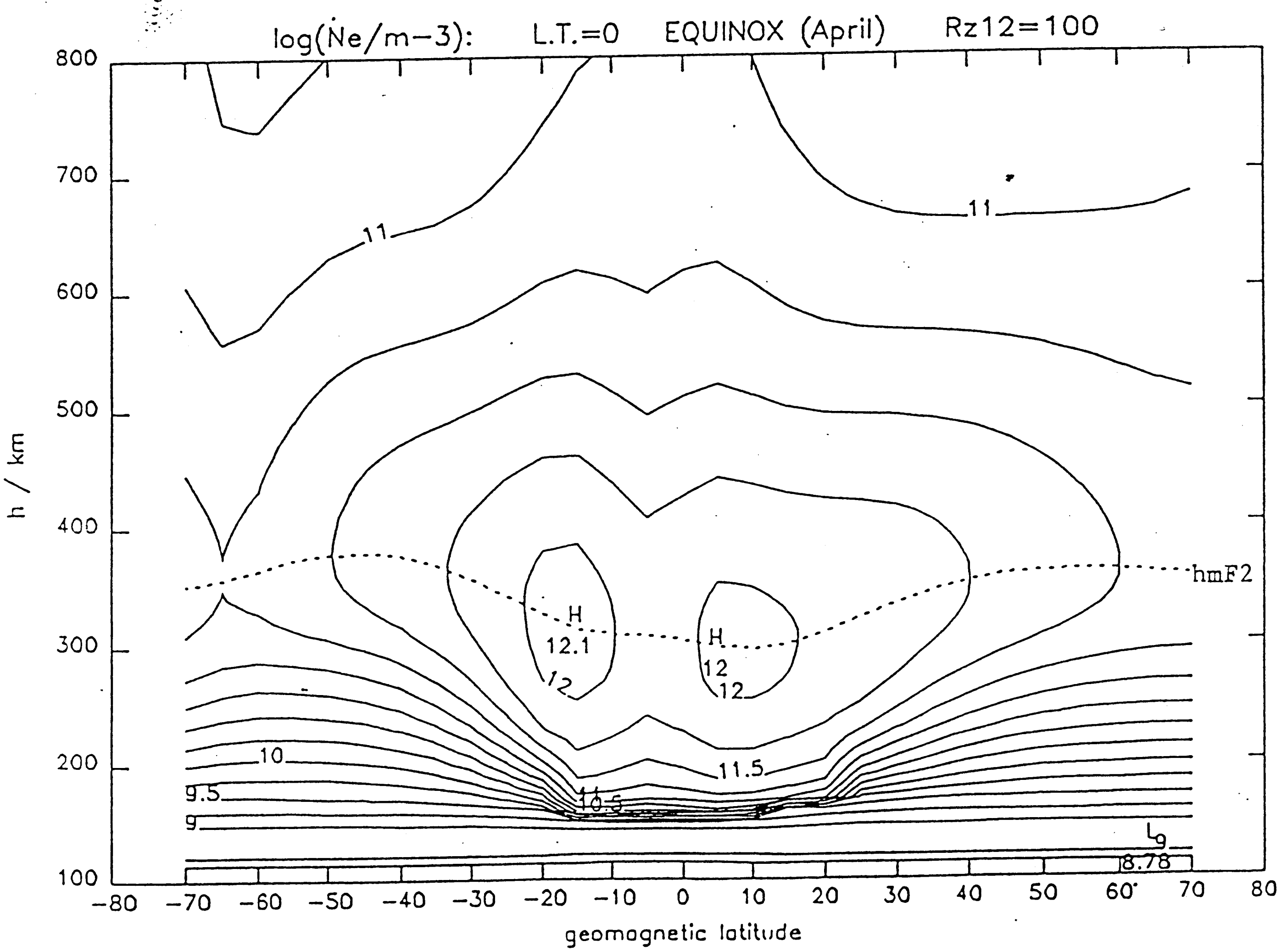
log(Ne/m-3): L.T.=0 EQUINOX (April) Rz12=100
h / km
geomagnetic latitude
hmF2
H
12.1
12
11.5
11
10.5
10
9.5
9
8.78

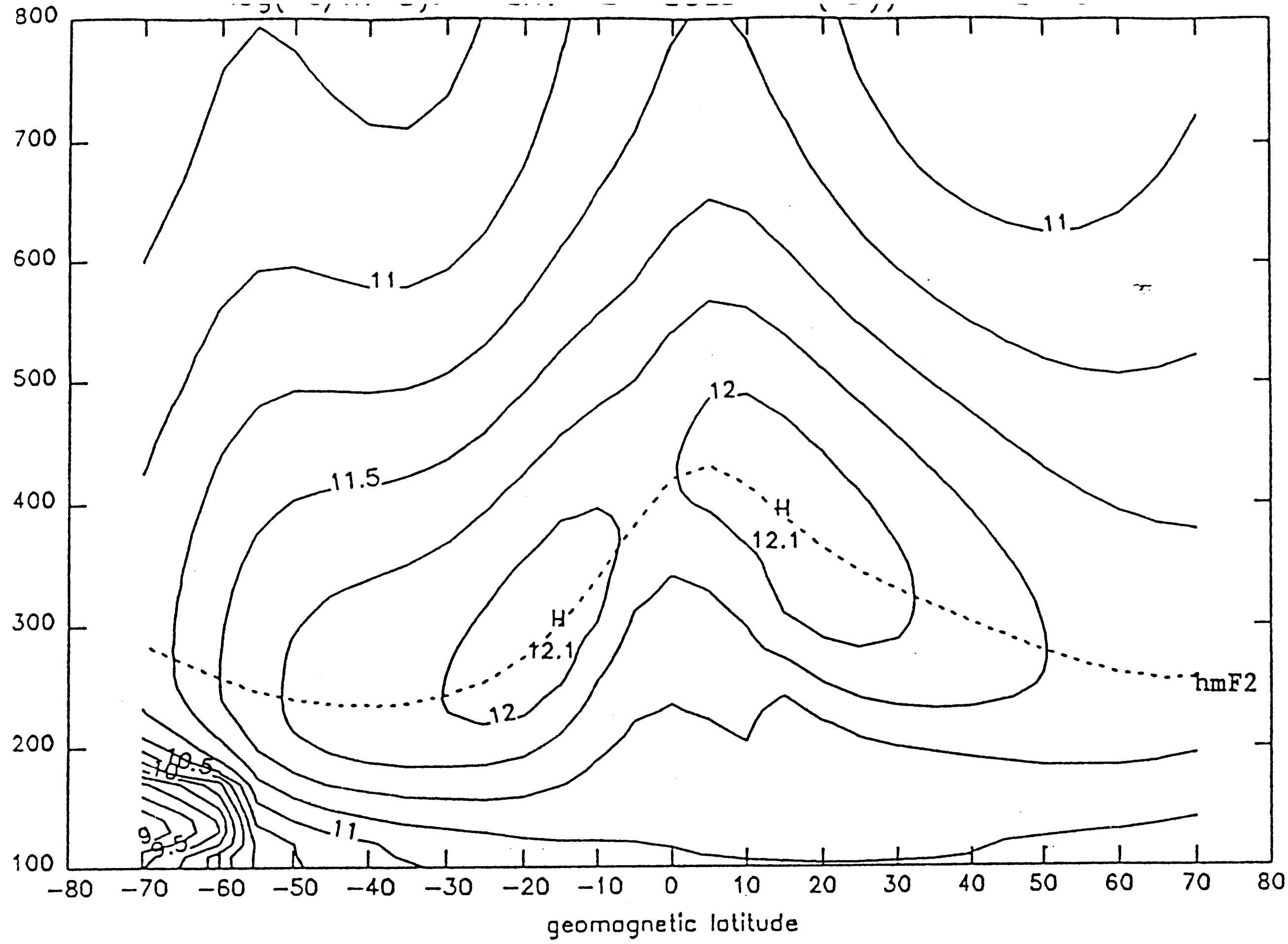

log(Ne/m−3): L.T.=0 SOLSTICE (July) Rz12=100

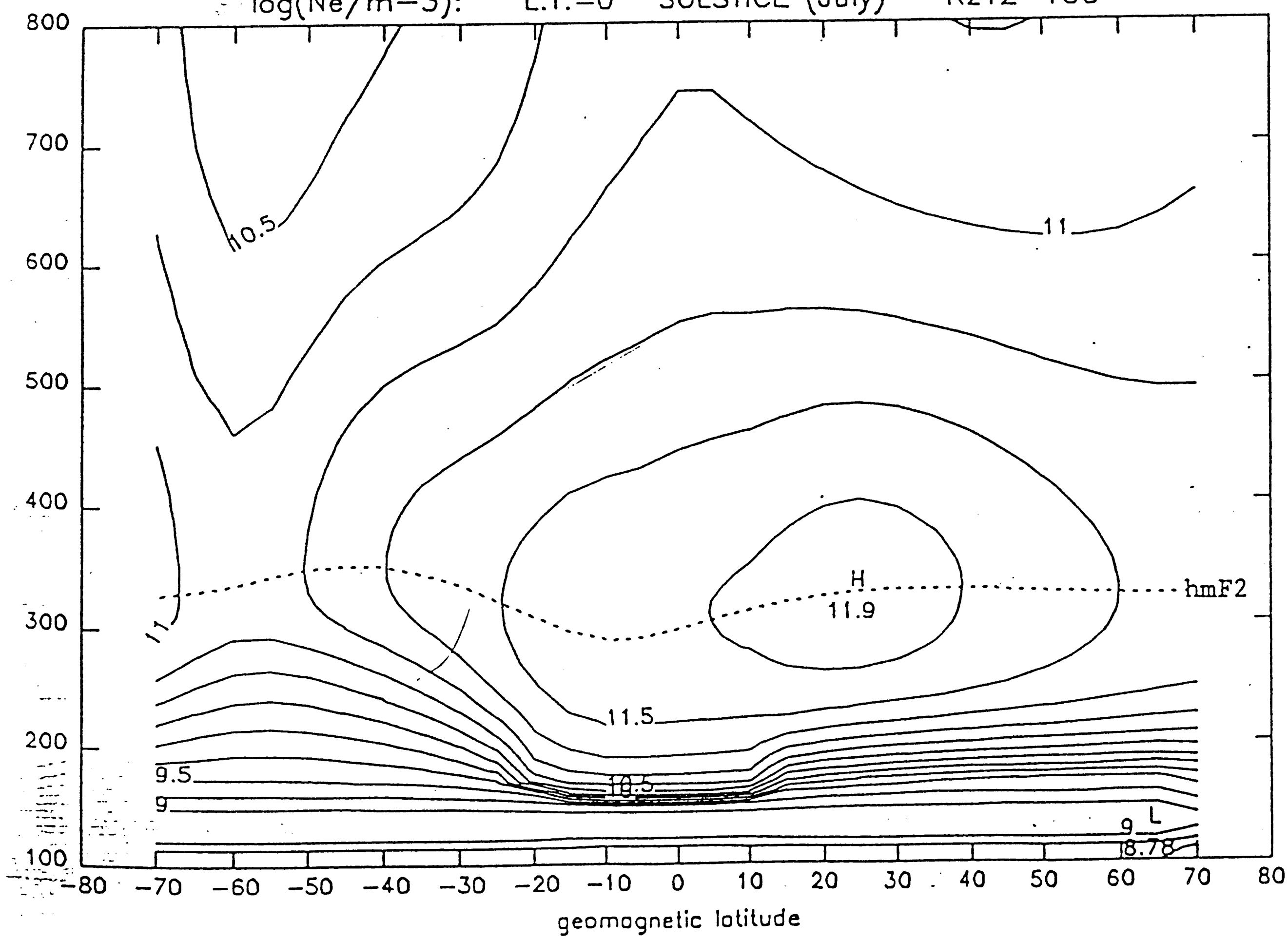

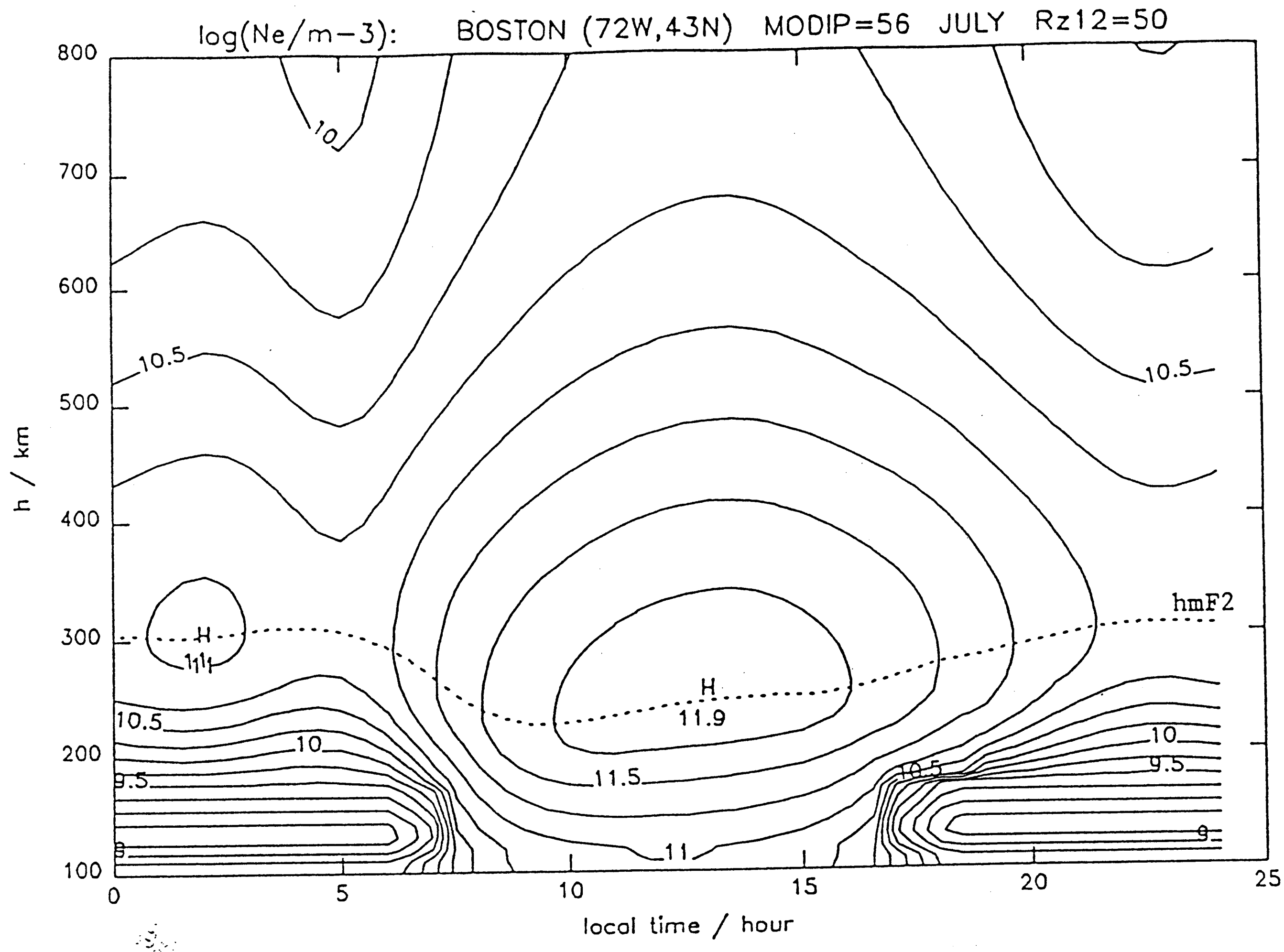
log(Ne/m-3): BOSTON (72W,43N) MODIP=56 JULY Rz12=50
h / km
local time / hour
hmF2
H
11.9
11.5
11
10.5
10
9.5
9

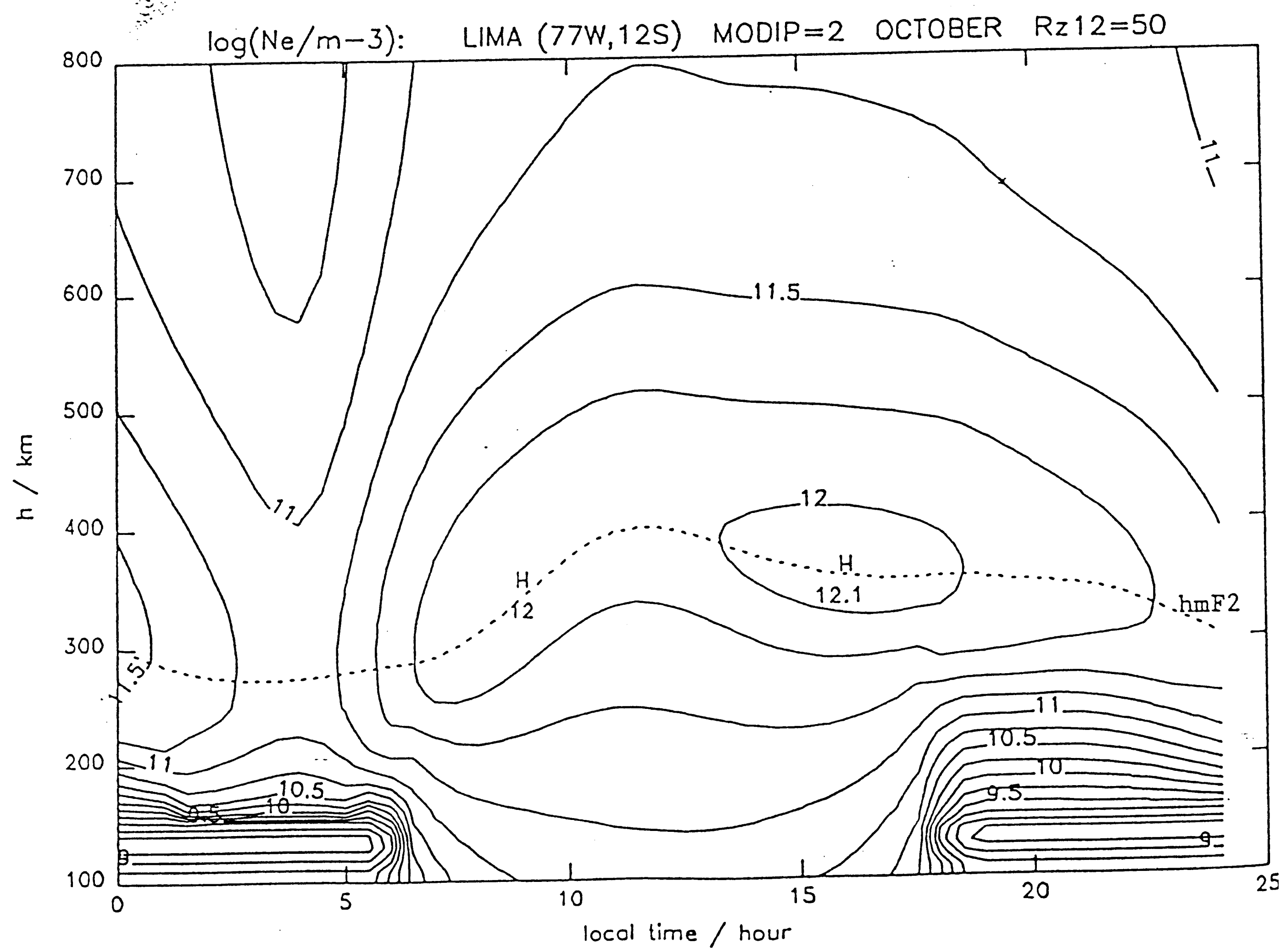
log(Ne/m-3): LIMA (77W,12S) MODIP=2 OCTOBER Rz12=50
h / km
local time / hour
hmF2
H
12.1
12
11.5
11
10.5
10
9.5
9

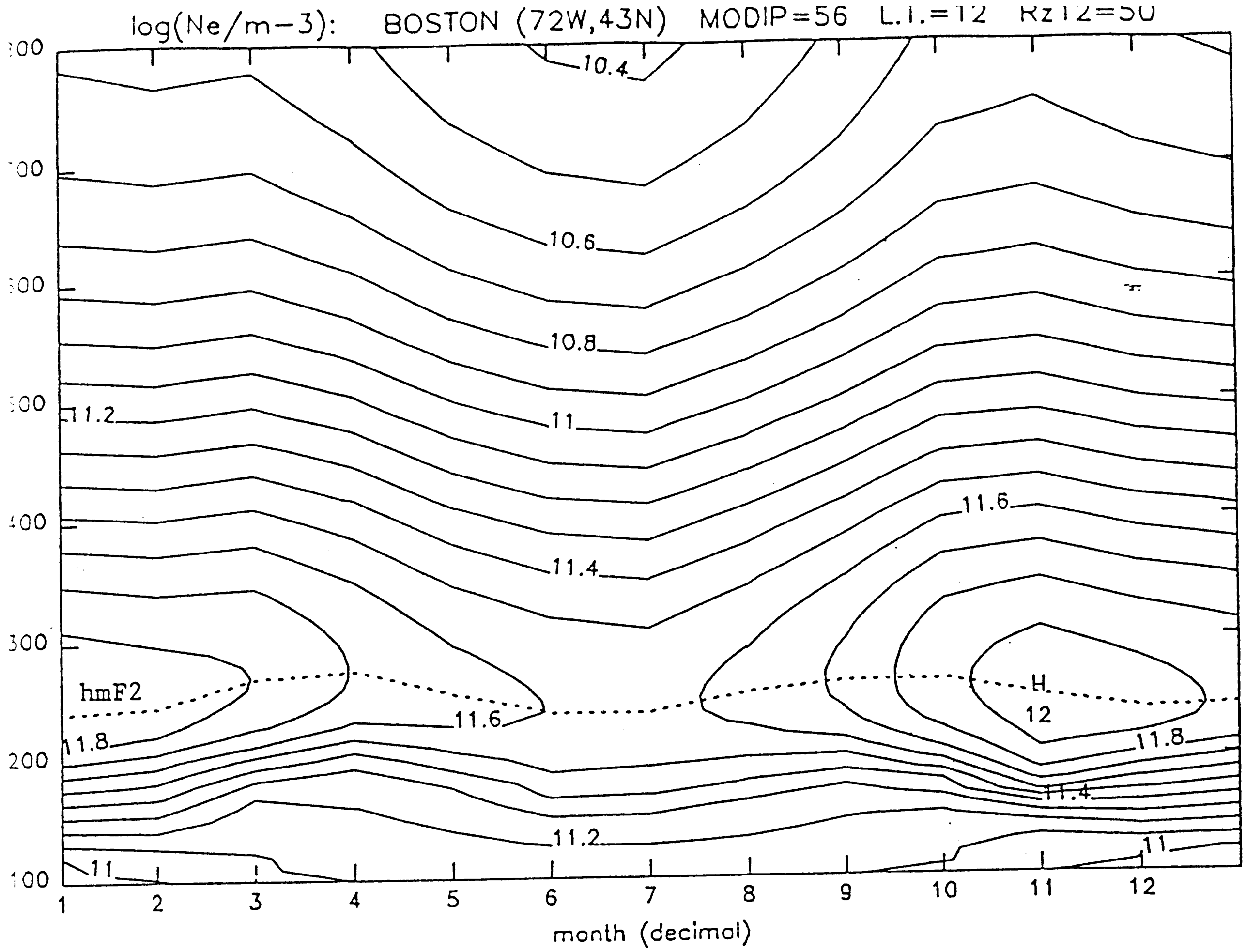
log(Ne/m−3): BOSTON (72W,43N) MODIP=56 L.T.=12 Rz12=50
10.4
10.6
10.8
11.2
11
11.6
11.4
hmF2
11.6
H
12
11.8
11.8
11.4
11.2
11
11
100
200
300
400
1 2 3 4 5 6 7 8 9 10 11 12
month (decimal)

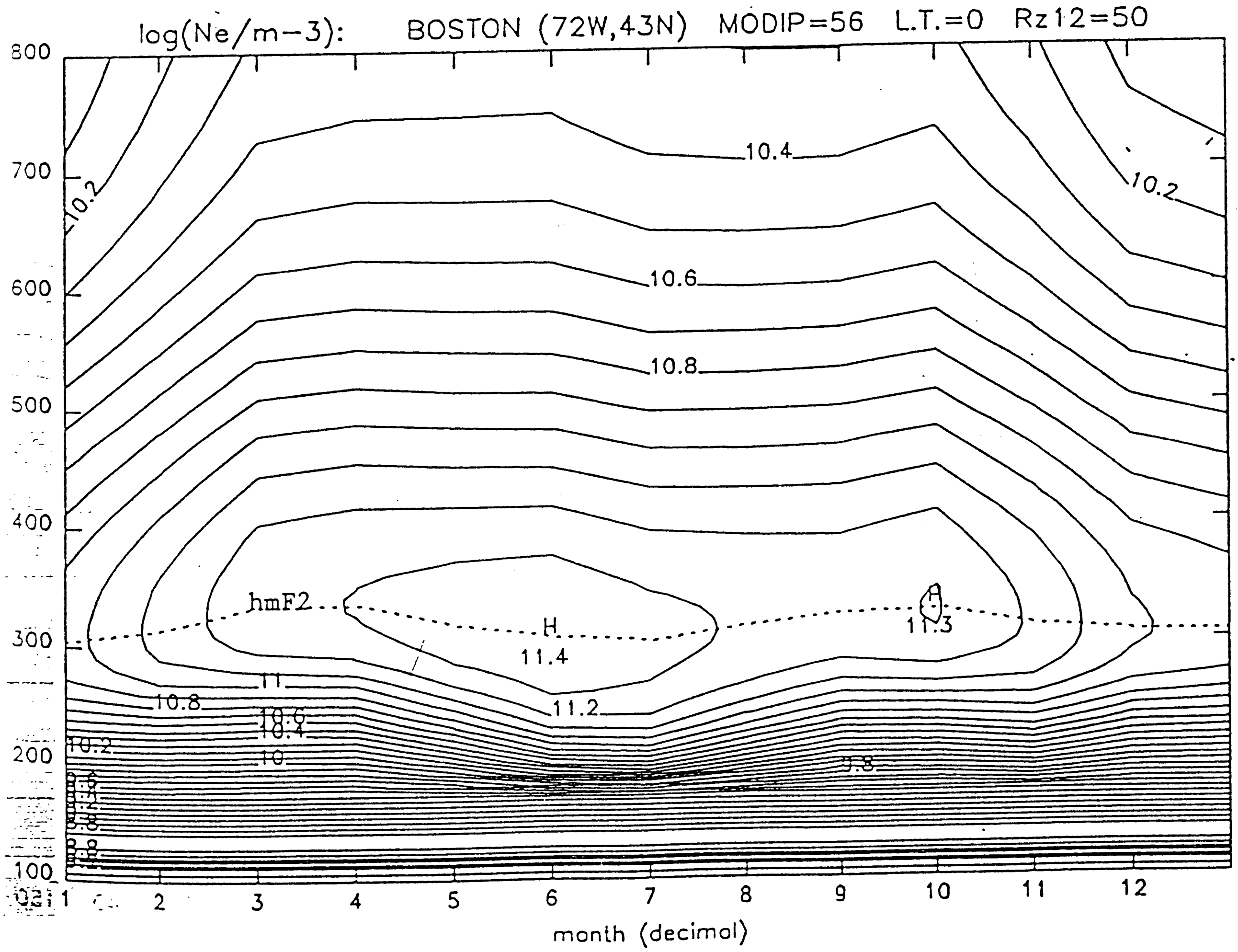
log(Ne/m−3): BOSTON (72W,43N) MODIP=56 L.T.=0 Rz12=50
800
700
600
500
400
300
200
100
10.4
10.2
10.2
10.6
10.8
hmF2
H
11.4
11.3
11
10.8
11.2
10.6
10.4
10.2
10
1 2 3 4 5 6 7 8 9 10 11 12
month (decimal)

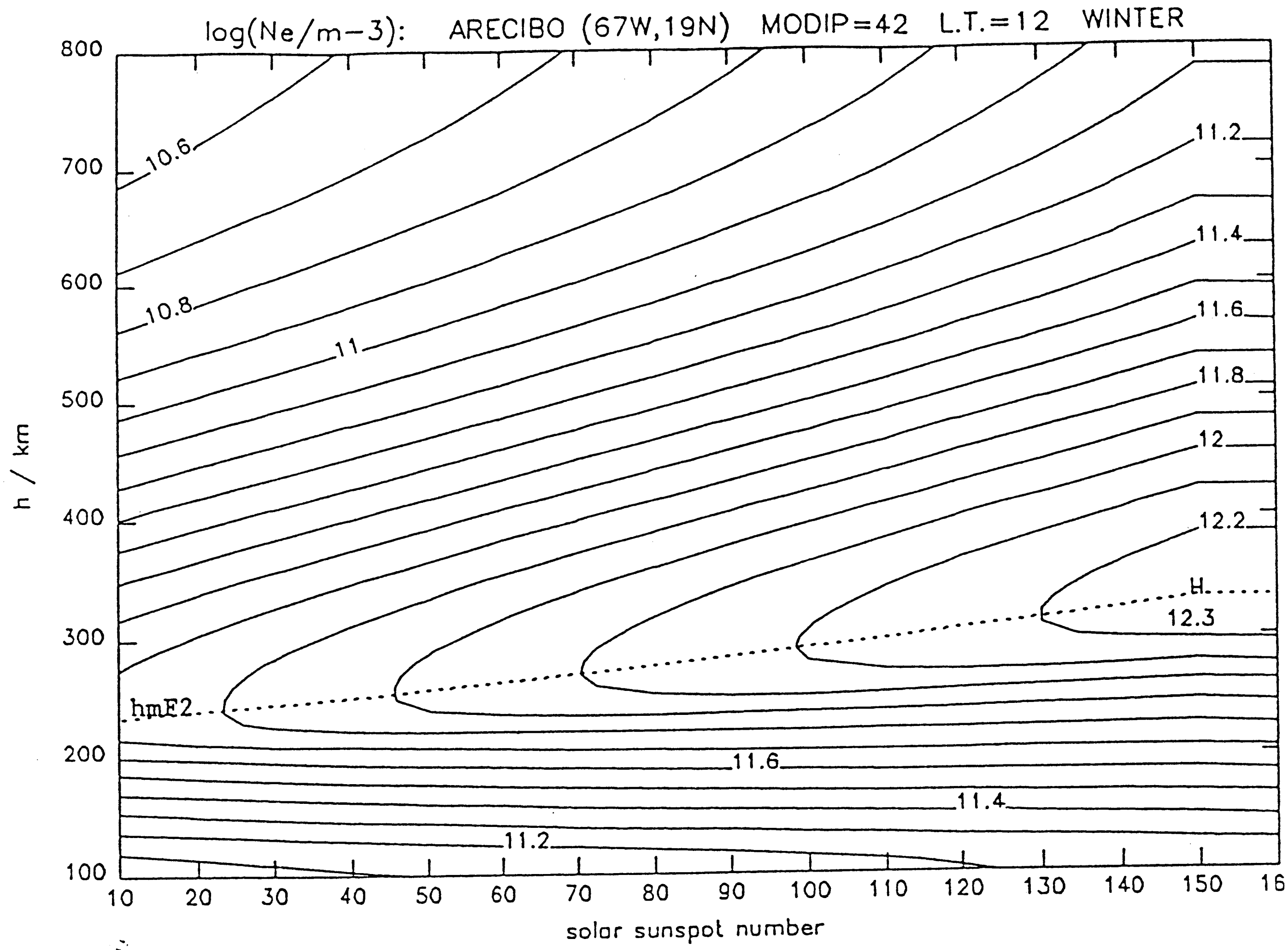
log(Ne/m−3): ARECIBO (67W,19N) MODIP=42 L.T.=12 WINTER
h / km
solar sunspot number
10.6
10.8
11
11.2
11.4
11.6
11.8
12
12.2
12.3
H
hmF2
11.6
11.4
11.2

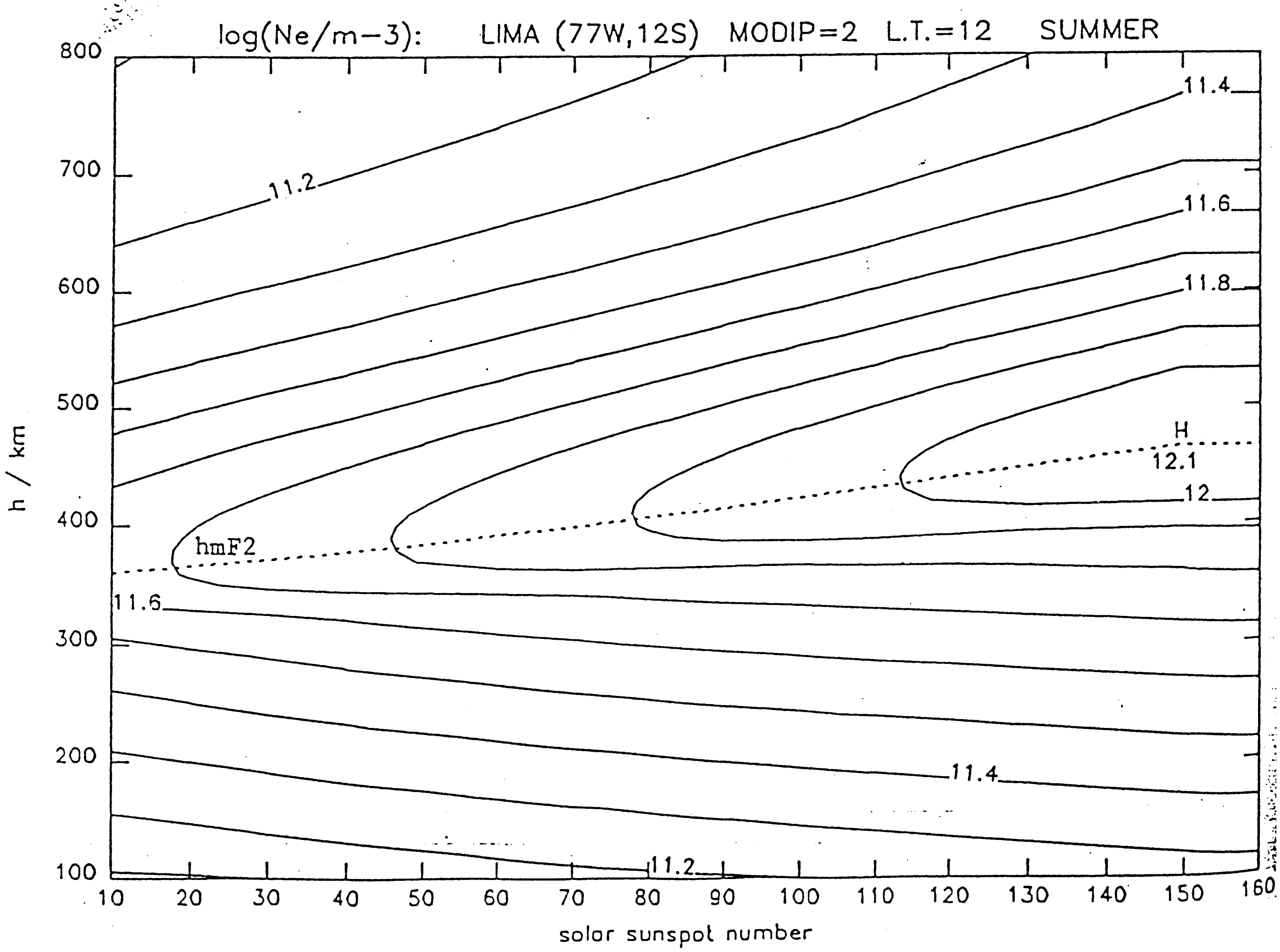
log(Ne/m−3): LIMA (77W,12S) MODIP=2 L.T.=12 SUMMER
h / km
solar sunspot number
11.2
11.4
11.6
11.8
H
12.1
12
hmF2
11.6
11.4
11.2

Bottomside Parameters: LT=12, April, Rz12=50

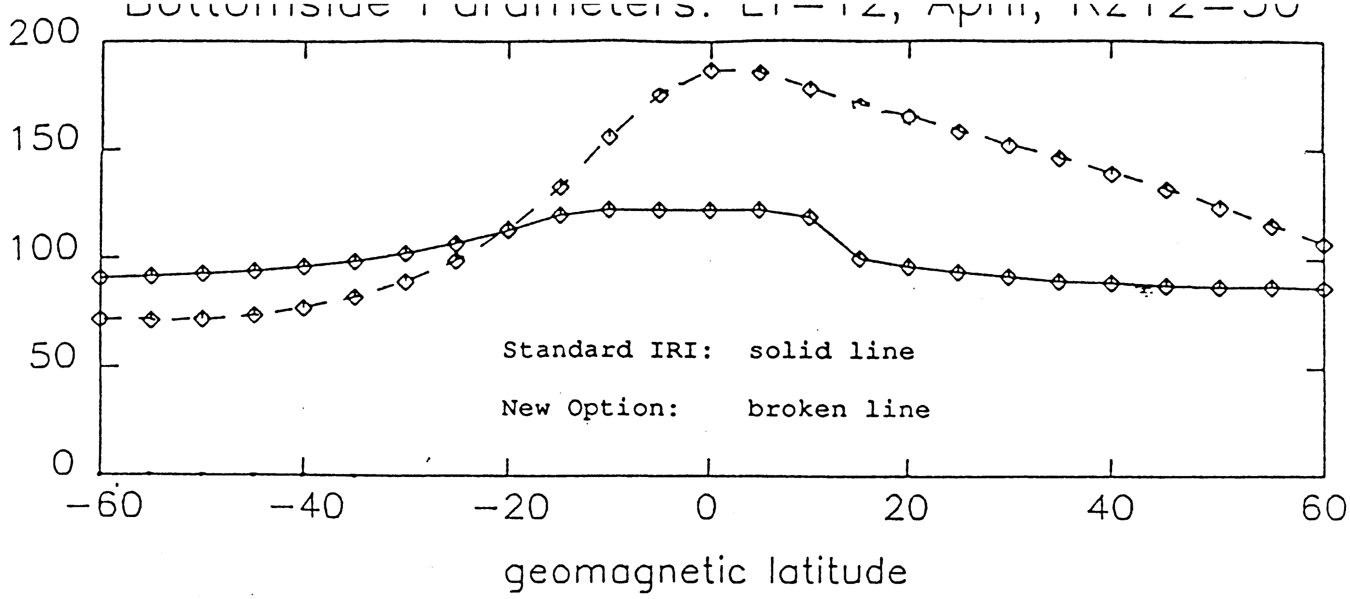

LT=0, April, Rz12=50

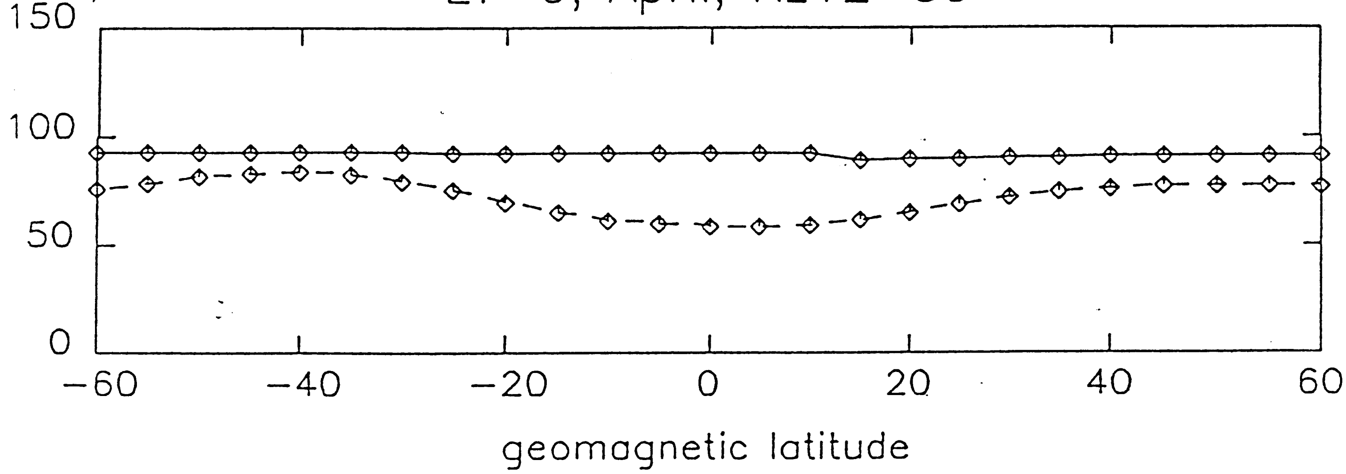

Lima (Modip=2), April, Rz12=50

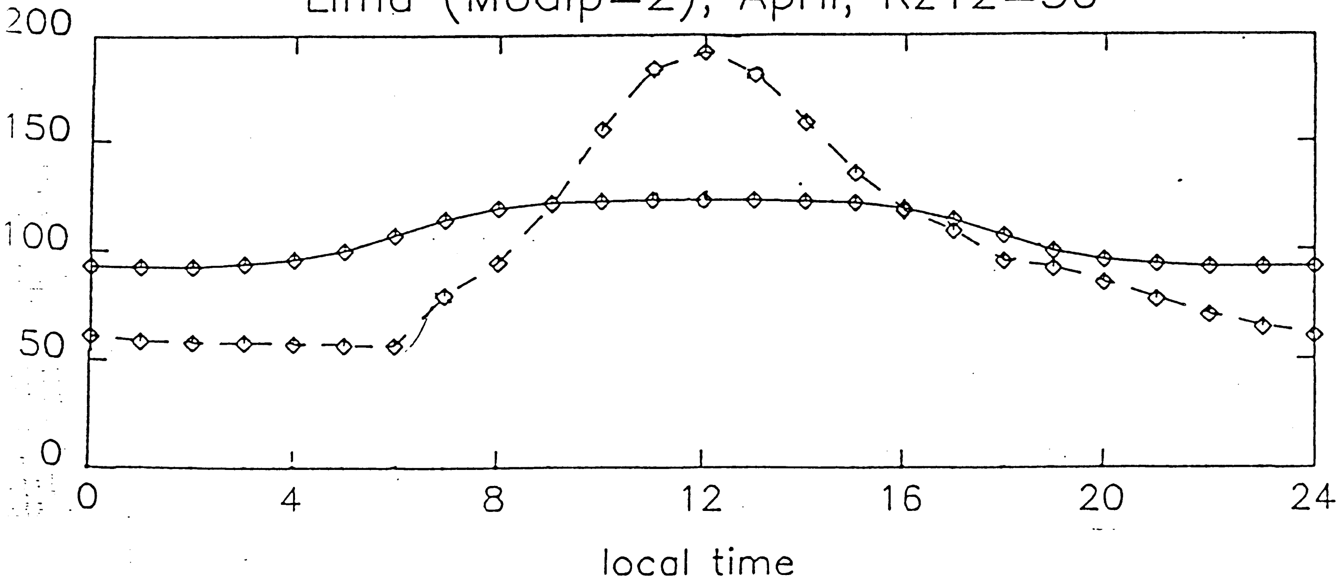

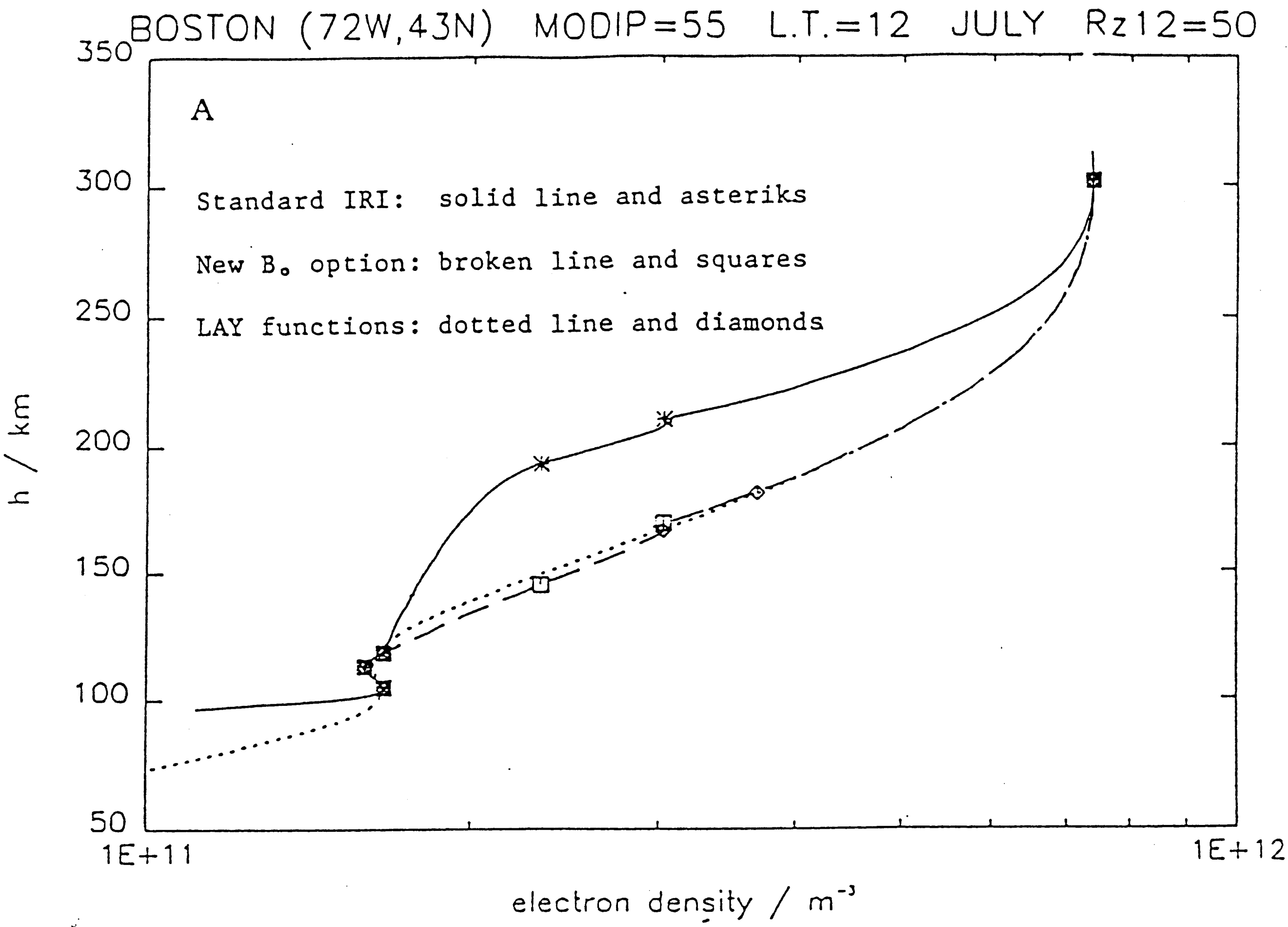
BOSTON (72W,43N) MODIP=55 L.T.=12 JULY Rz12=50
A
Standard IRI: solid line and asteriks
New B₀ option: broken line and squares
LAY functions: dotted line and diamonds
h / km
350
300
250
200
150
100
50
1E+11
1E+12
electron density / m⁻³

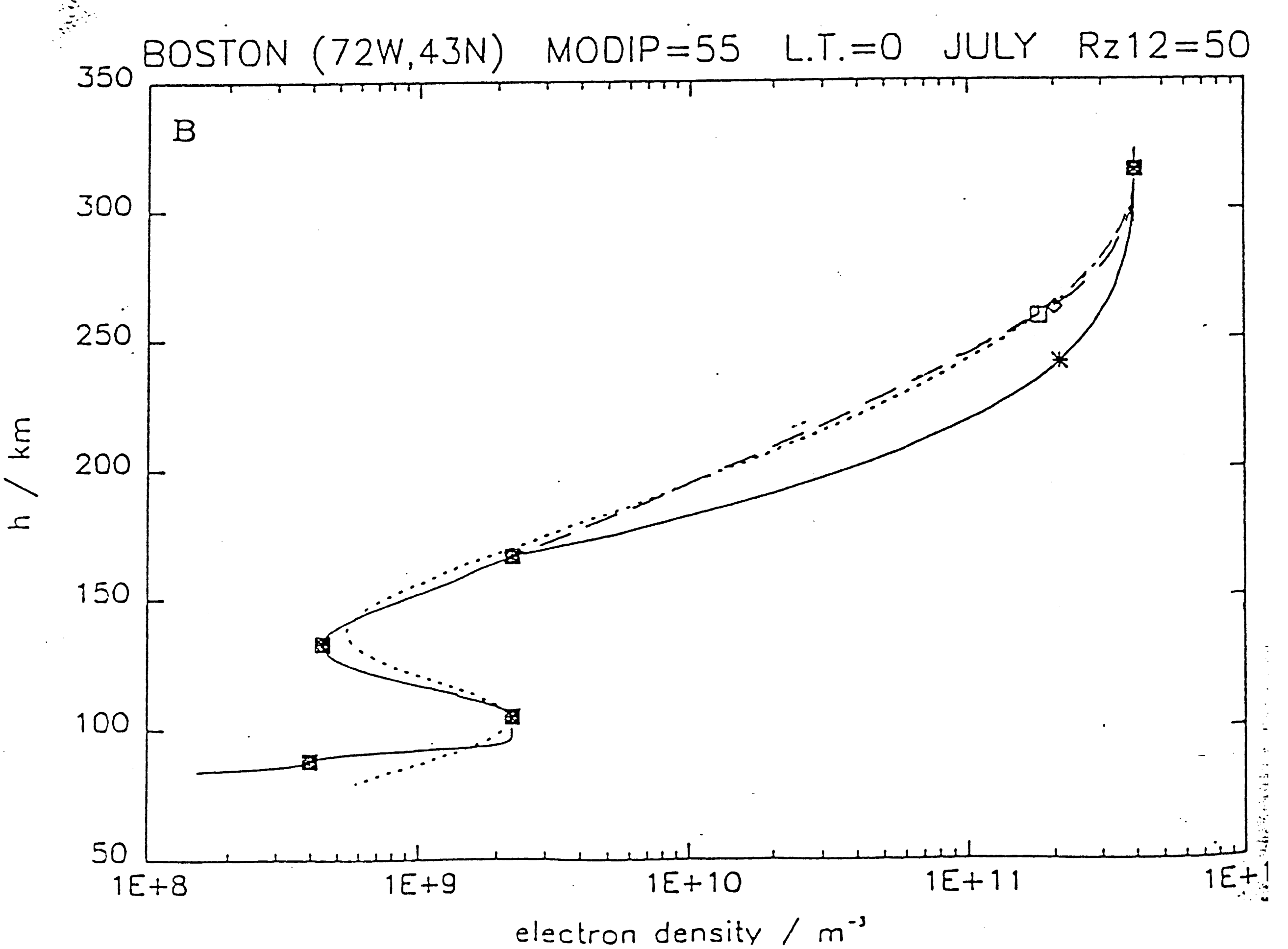
BOSTON (72W,43N) MODIP=55 L.T.=0 JULY Rz12=50
B
h / km
350
300
250
200
150
100
50
1E+8
1E+9
1E+10
1E+11
1E+1
electron density / m⁻³

STANDARD IRI

IRI-86, L.T.=0, July, Rz12=50

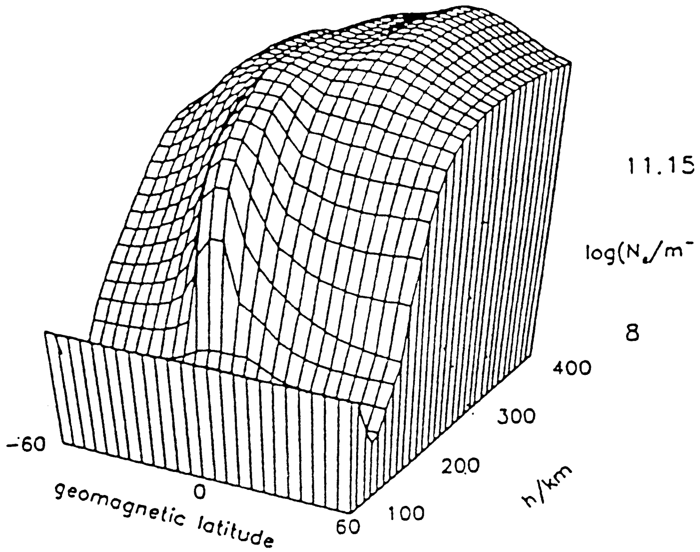

IRI-86, L.T.=12, April, Rz12=50

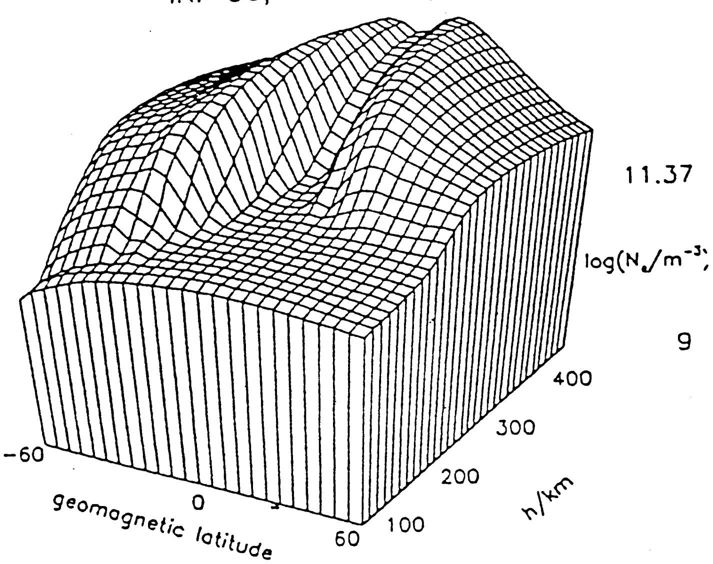

IRI-86, Boston(Modip=56), July, Rz12=50

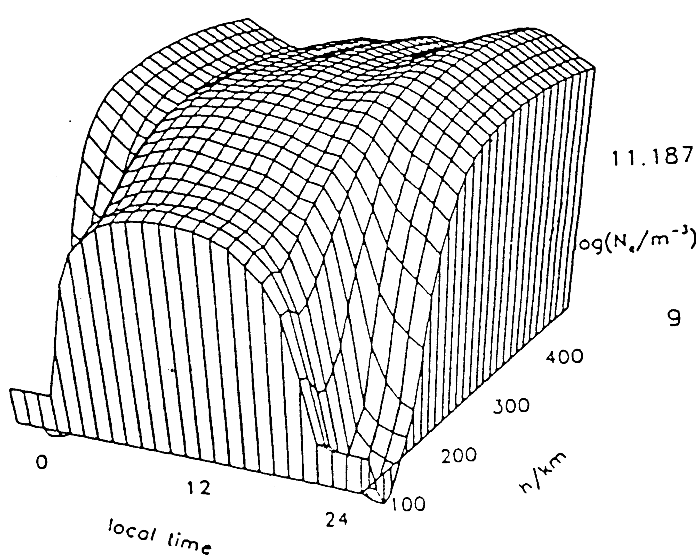

LAY FUNCTIONS

IRI-ANA, L.T.=0, July, Rz12=50

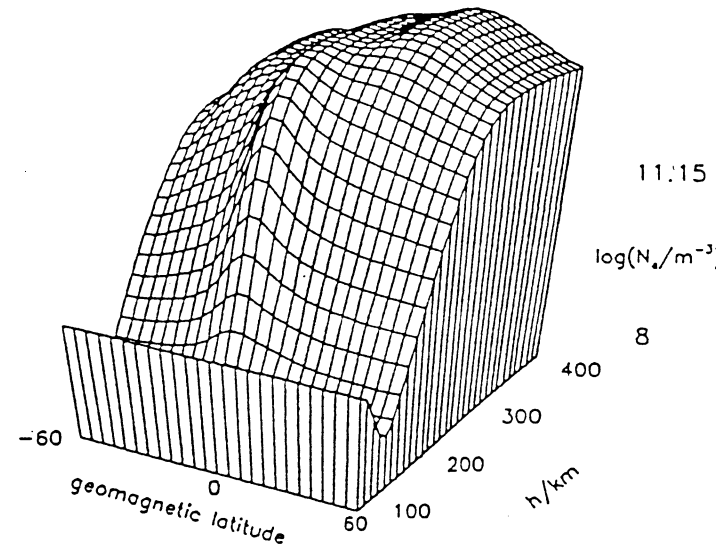

IRI-ANA, L.T.=12, April, Rz12=50

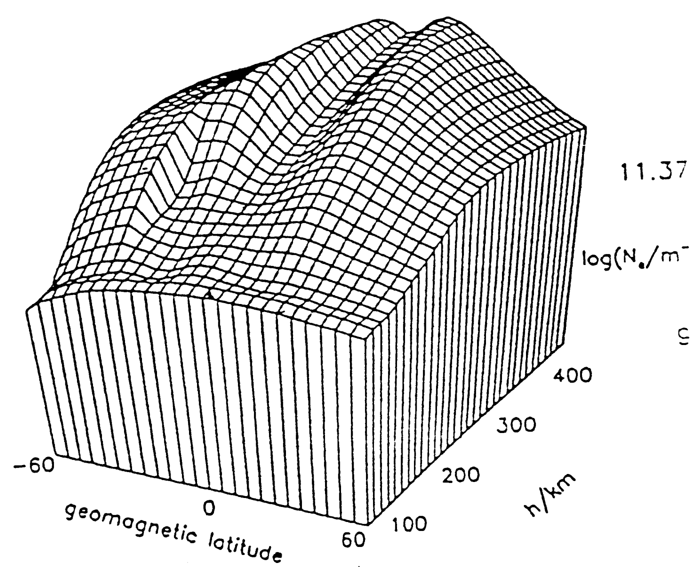

IRI-ANA, Boston(Modip=56), July, Rz12=50

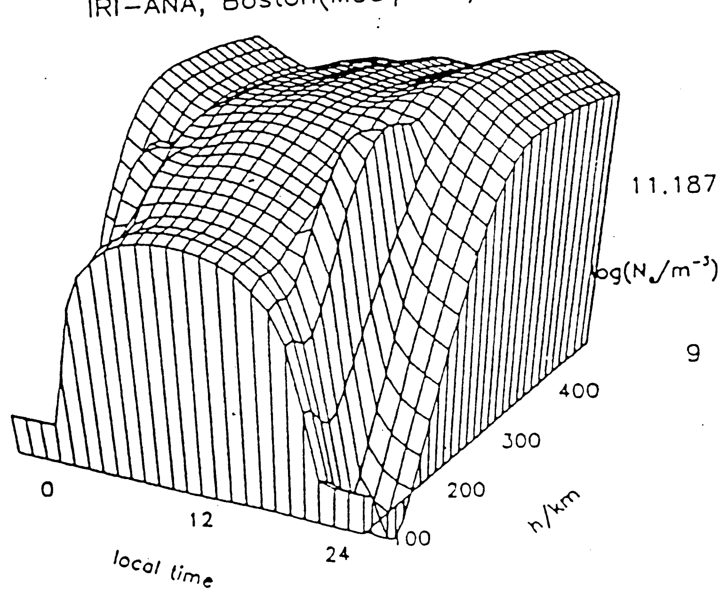

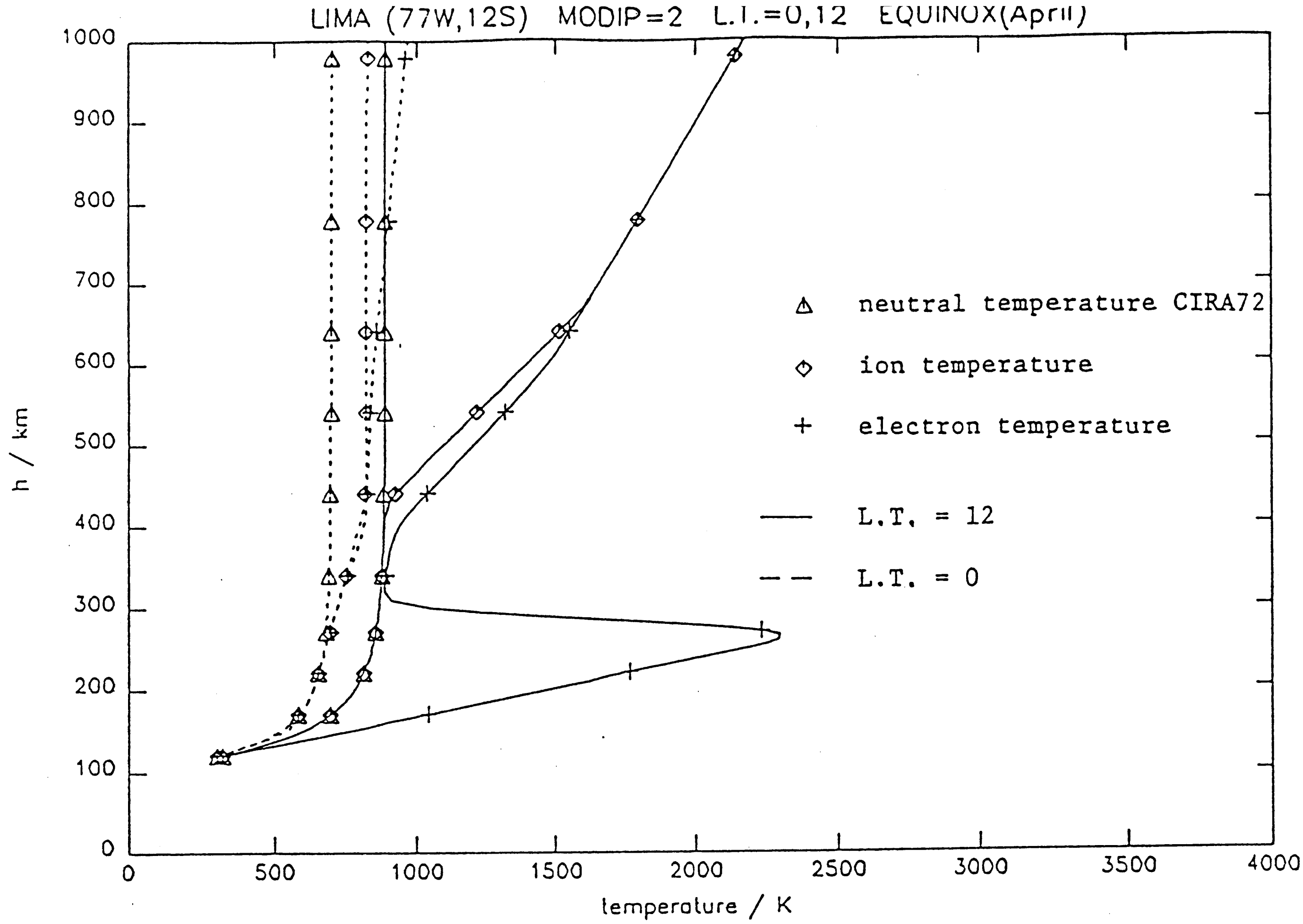

LIMA (77W,12S) MODIP=2 L.T.=0,12 EQUINOX(April)
neutral temperature CIRA72
ion temperature
electron temperature
L.T. = 12
L.T. = 0
h / km
temperature / K

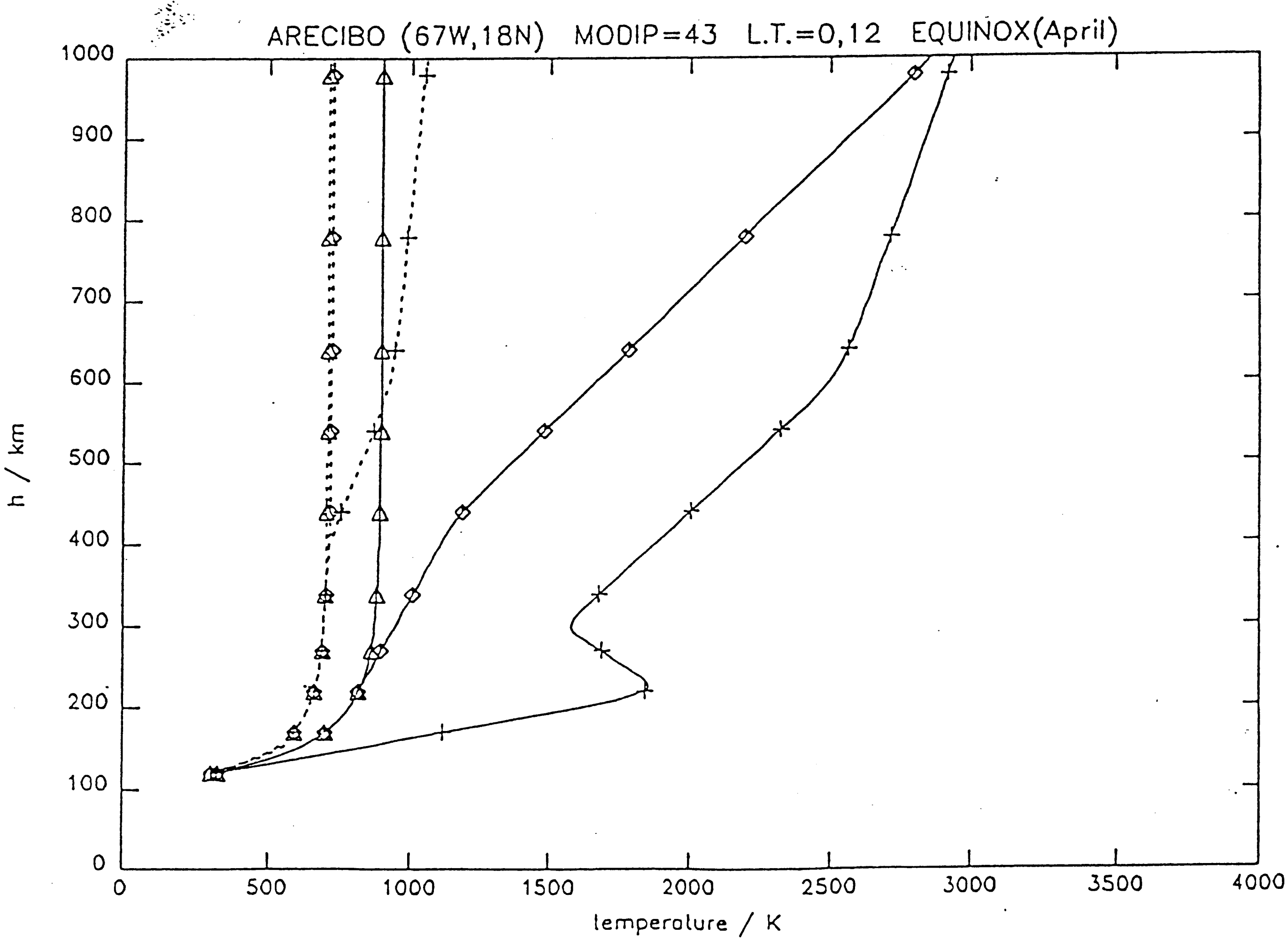

ARECIBO (67W,18N) MODIP=43 L.T.=0,12 EQUINOX(April)
h / km
temperature / K

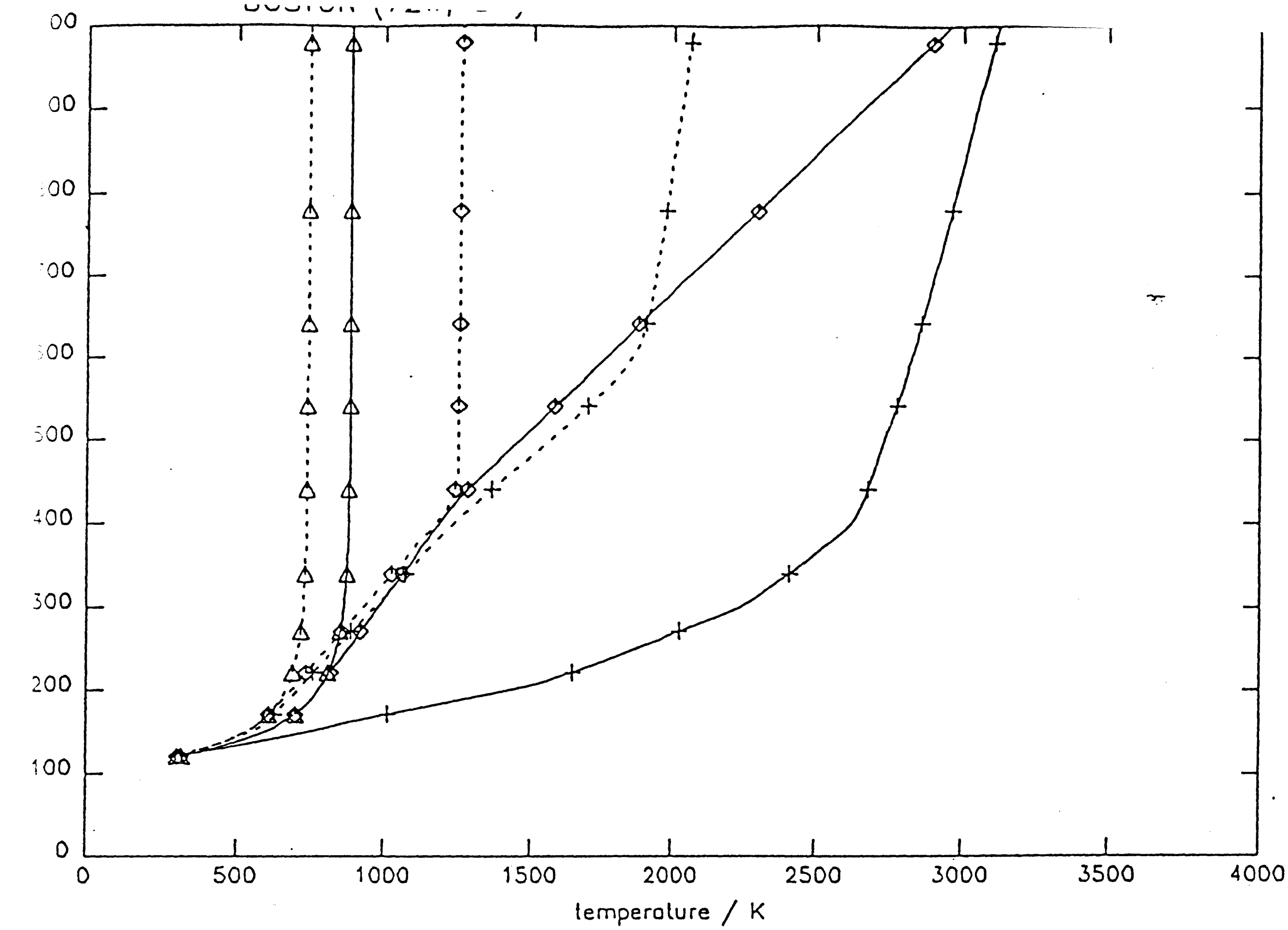

BOSTON (72W,43N) MODIP=55 L.T.=0,12 SOLSTICE(July)

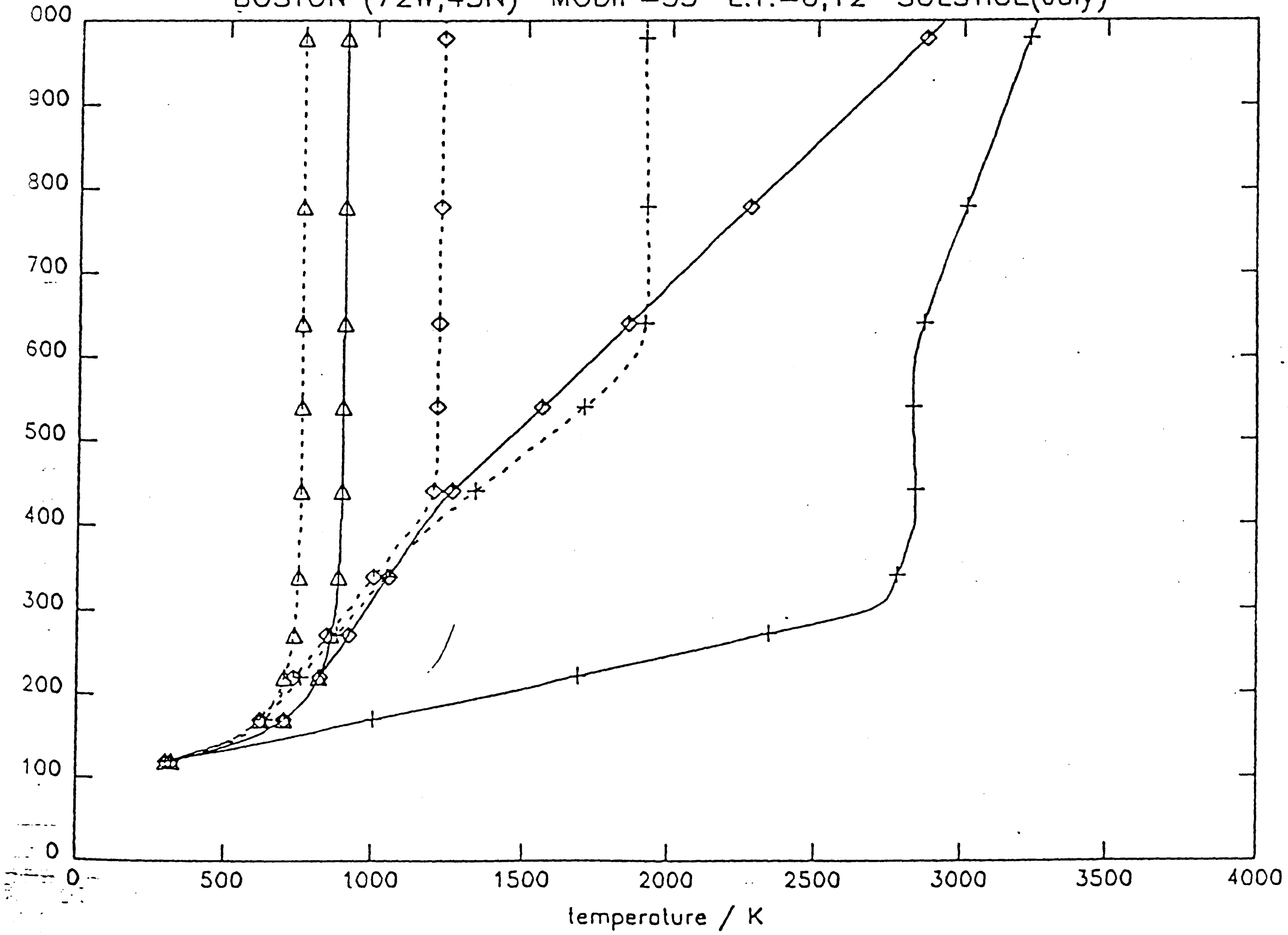

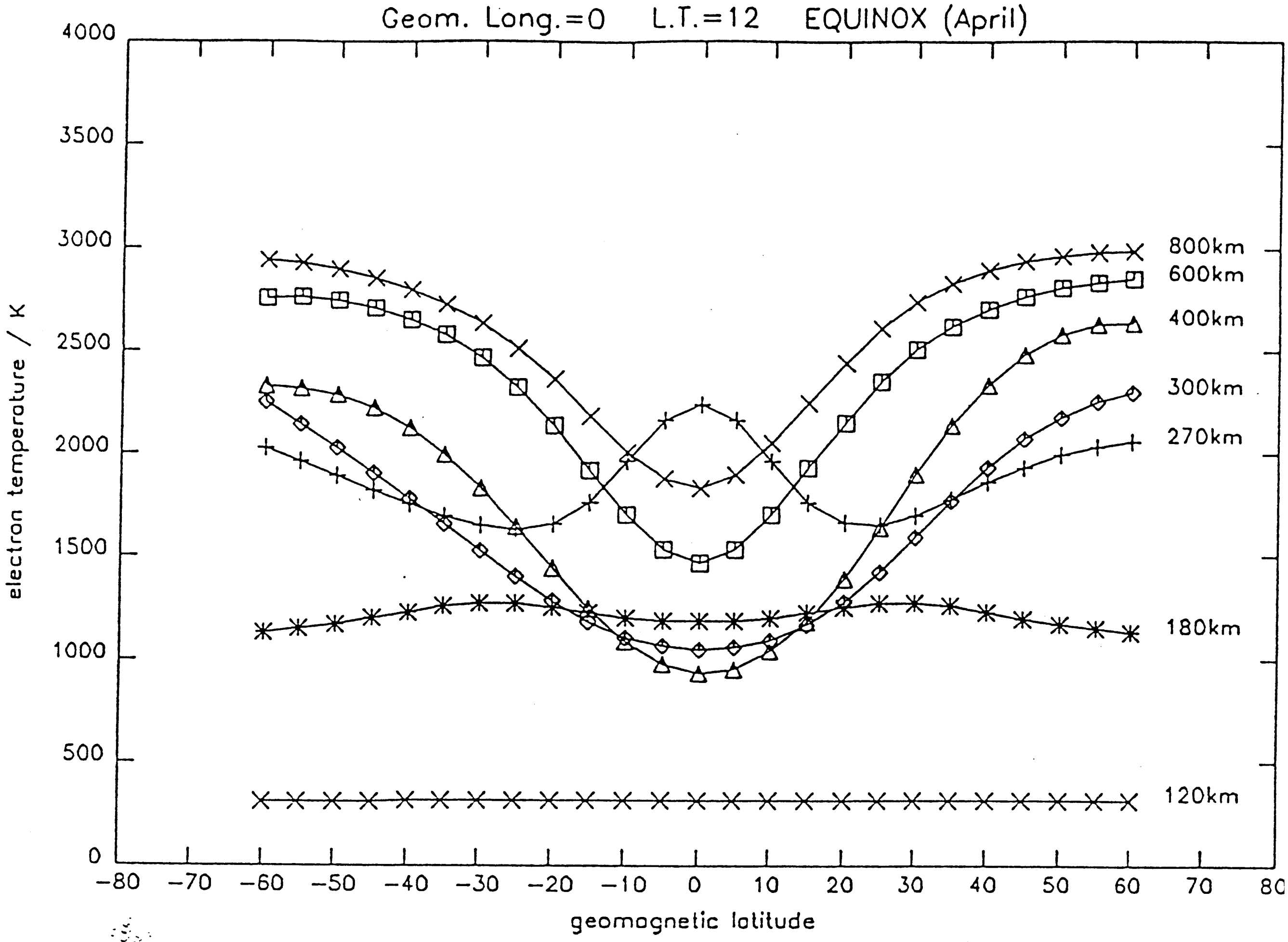

Geom. Long.=0 L.T.=12 EQUINOX (April)
electron temperature / K
geomagnetic latitude
800km
600km
400km
300km
270km
180km
120km

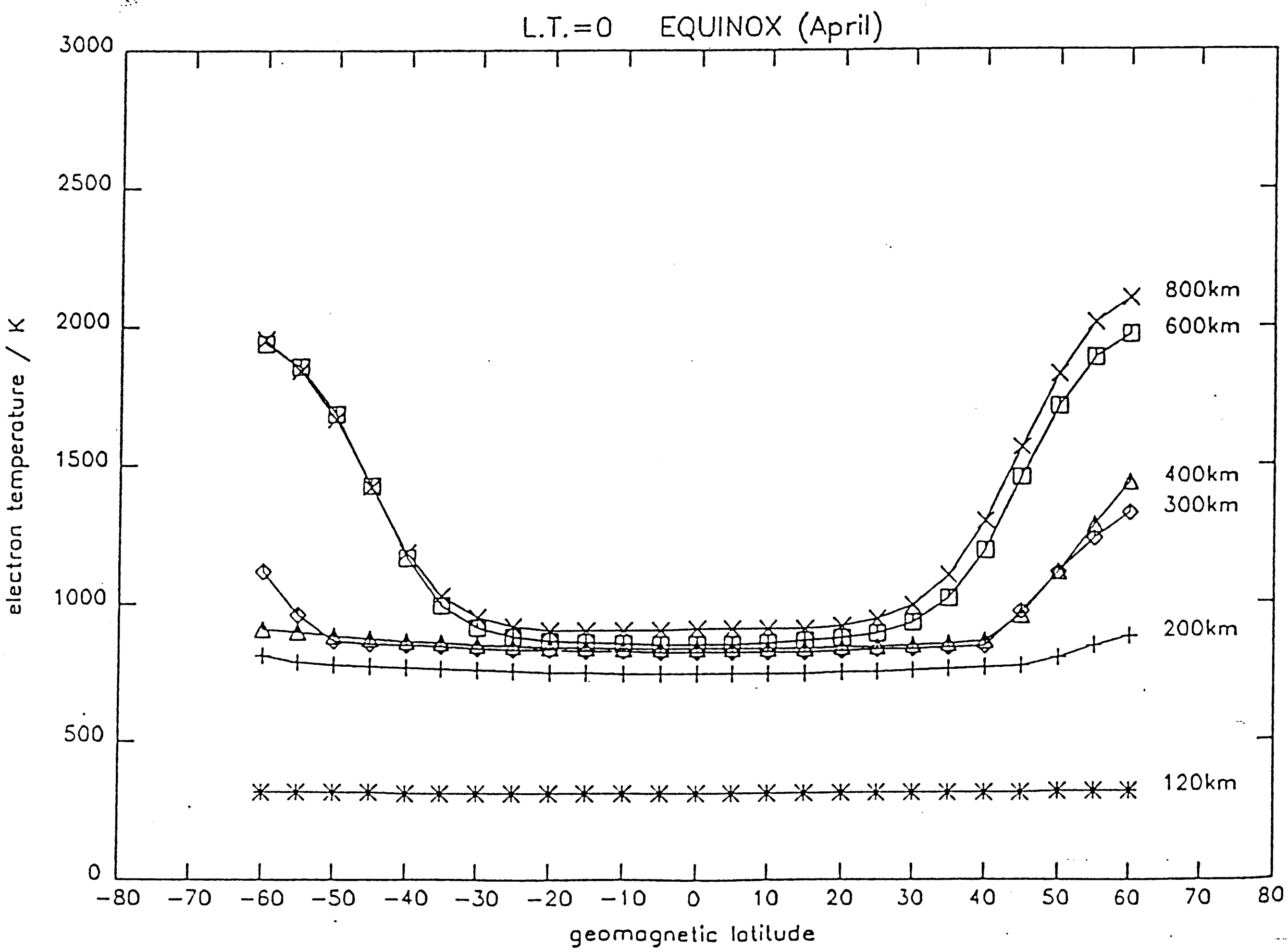

L.T.=0 EQUINOX (April)
electron temperature / K
geomagnetic latitude
800km
600km
400km
300km
200km
120km

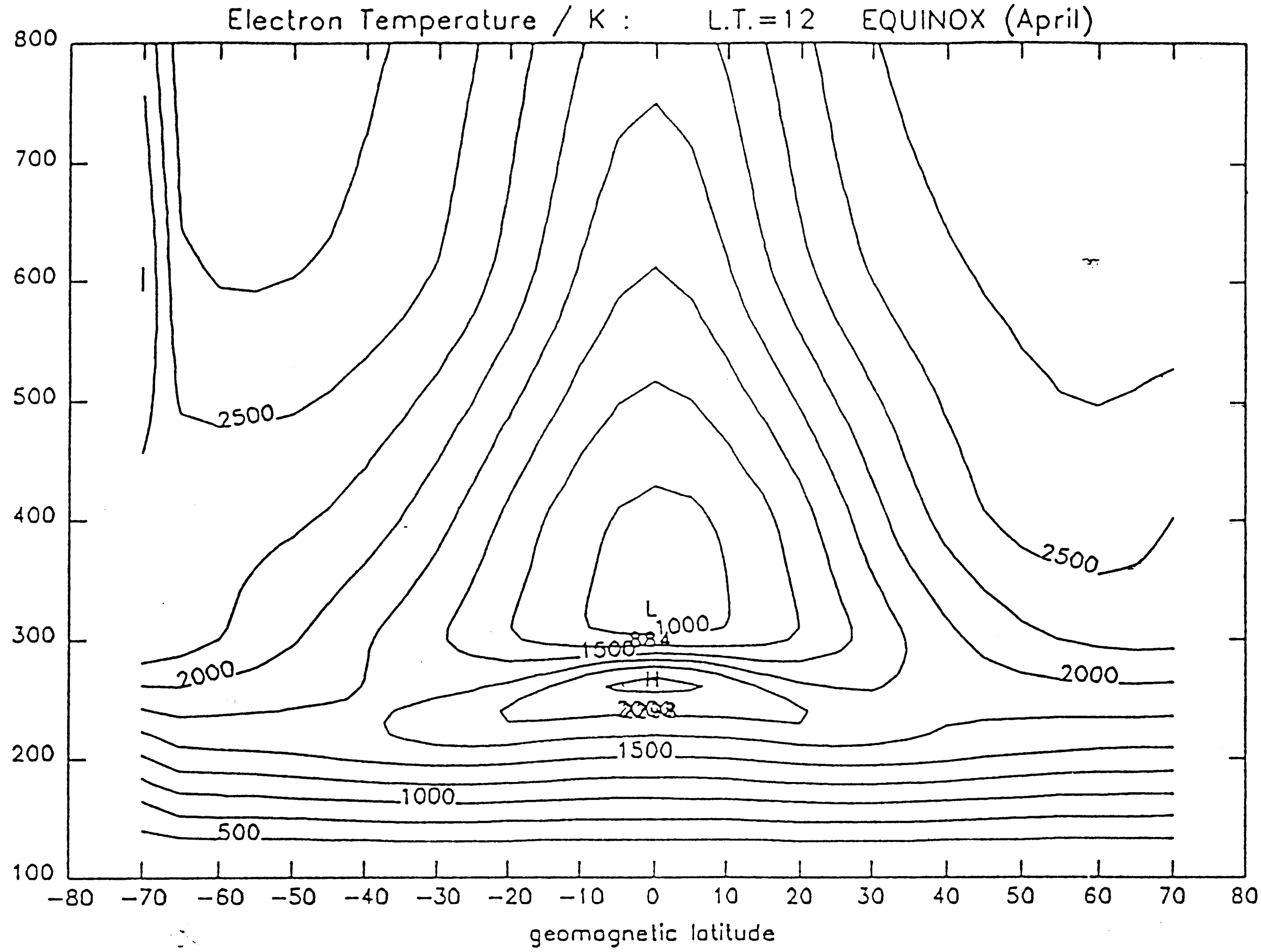
Electron Temperature / K : L.T.=12 EQUINOX (April)
800
700
600
500
400
300
200
100
2500
2000
1000
1500
H
500
-80 -70 -60 -50 -40 -30 -20 -10 0 10 20 30 40 50 60 70 80
geomagnetic latitude

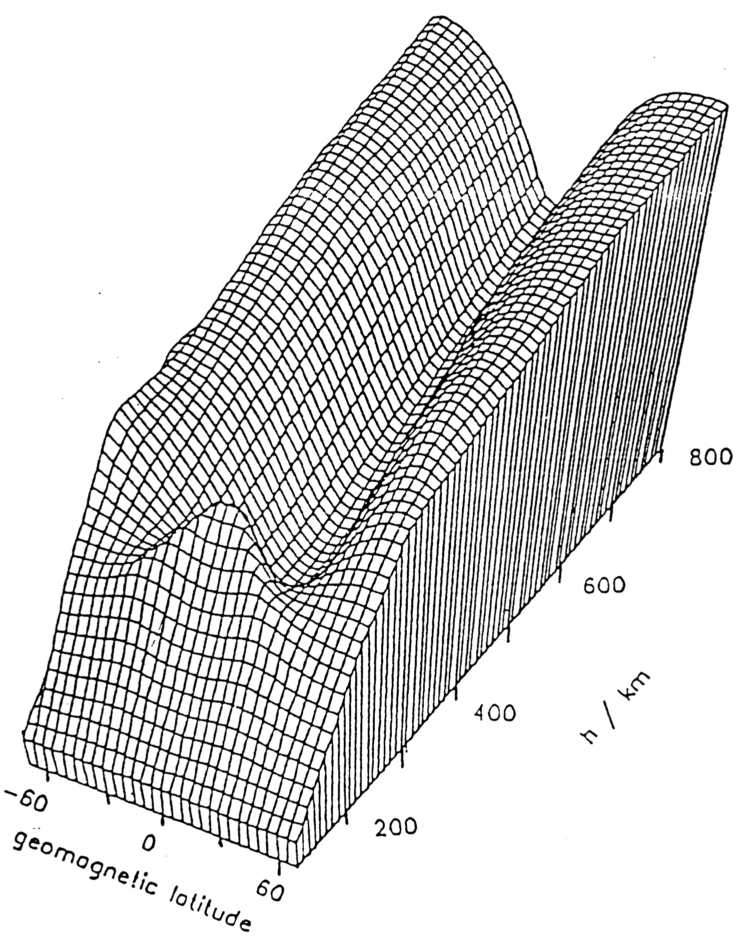
800
600
400
200
h / km
-60
0
60
geomagnetic latitude

LIMA (77W,12S) MODIP=2 EQUINOX (April)

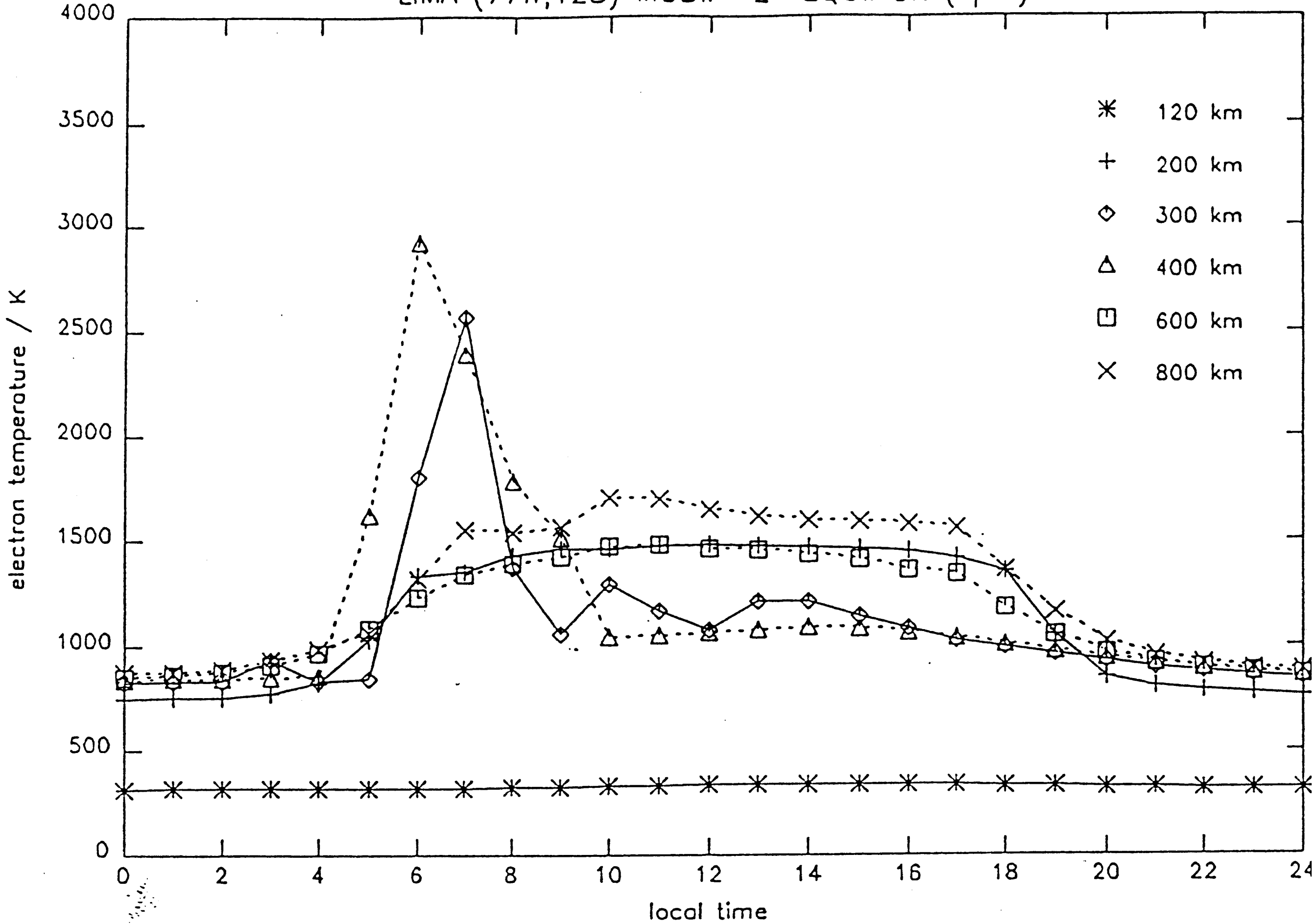

BOSTON (72W,43N) MODIP=55 EQUINOX (April)

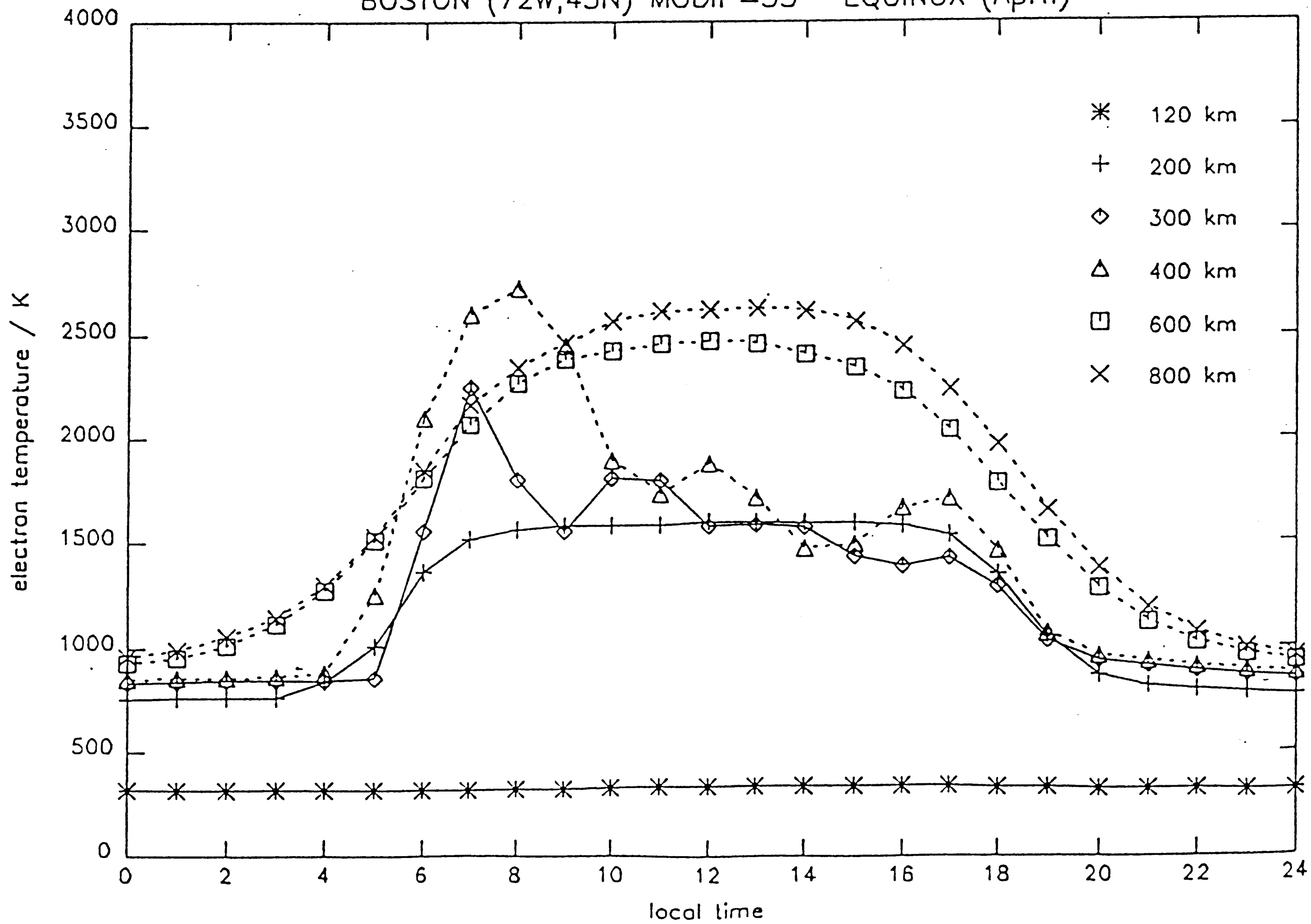

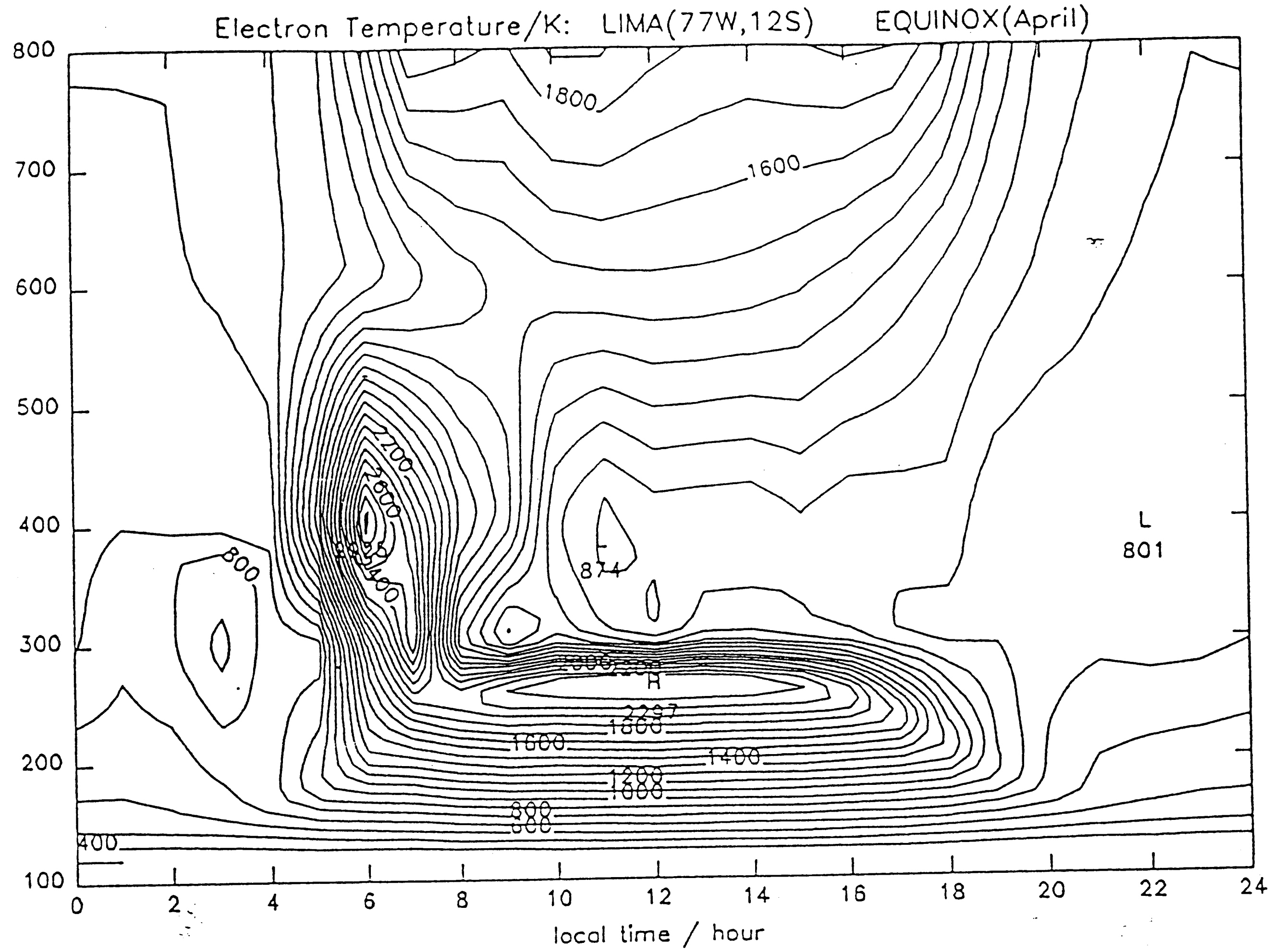
Electron Temperature/K: LIMA(77W,12S) EQUINOX(April)
local time / hour
1800
1600
2200
2600
874
L
801
800
1400
400

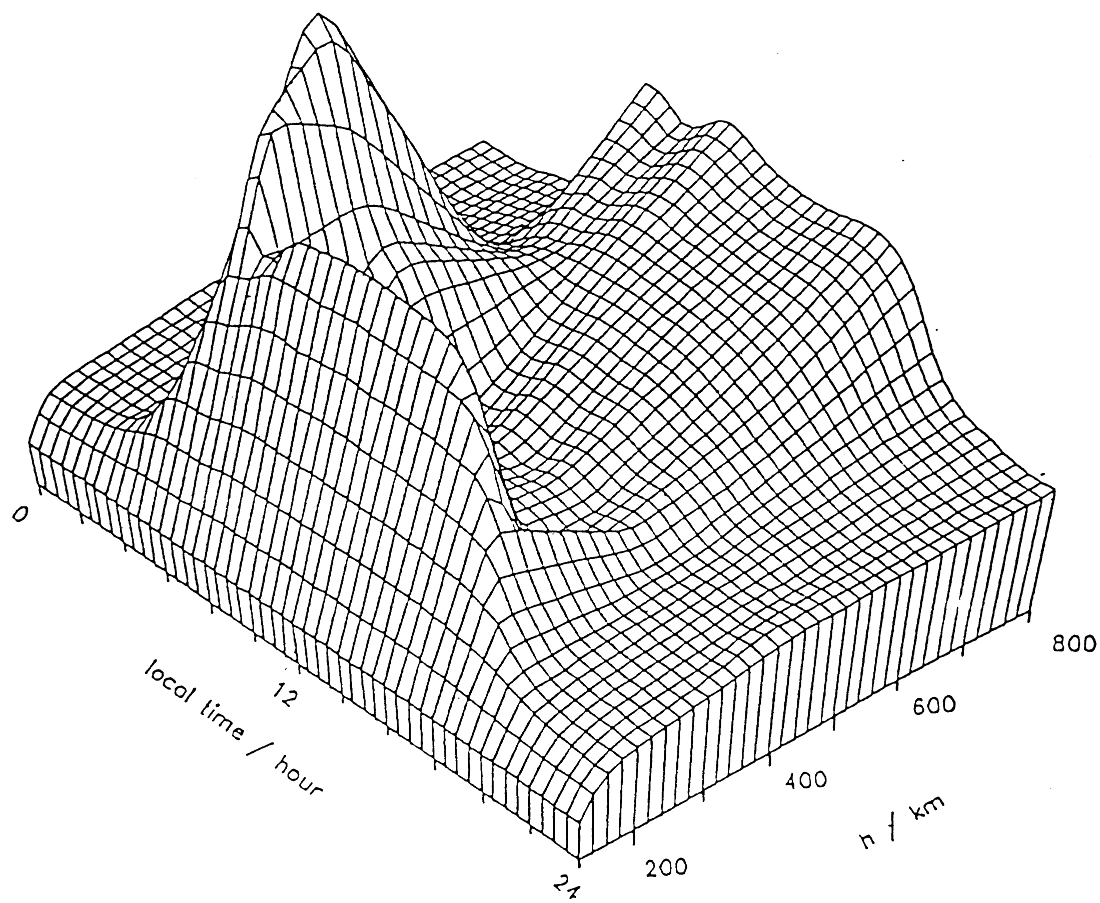
local time / hour
h / km
800
600
400
200

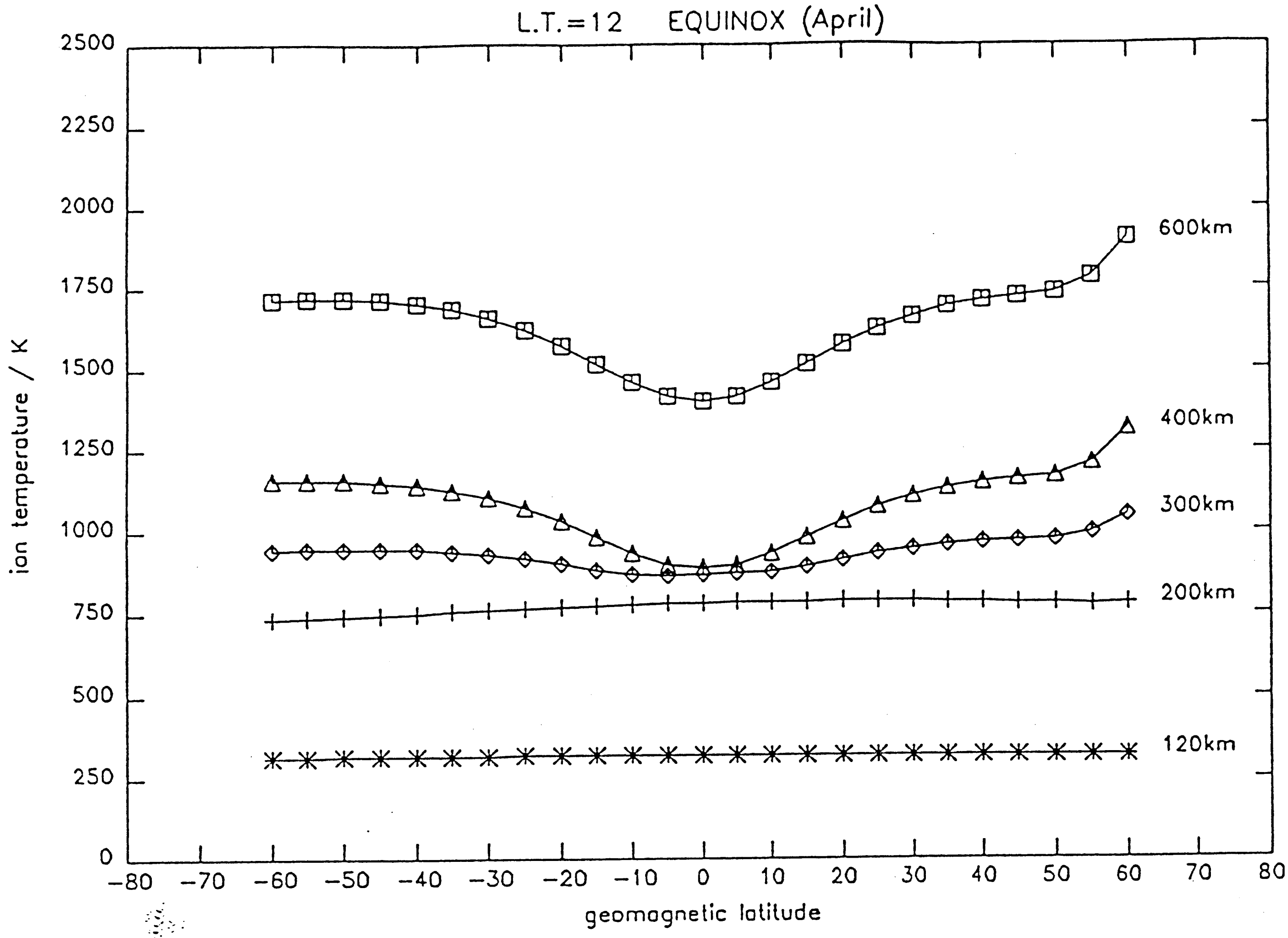
L.T.=12 EQUINOX (April)
ion temperature / K
geomagnetic latitude
600km
400km
300km
200km
120km

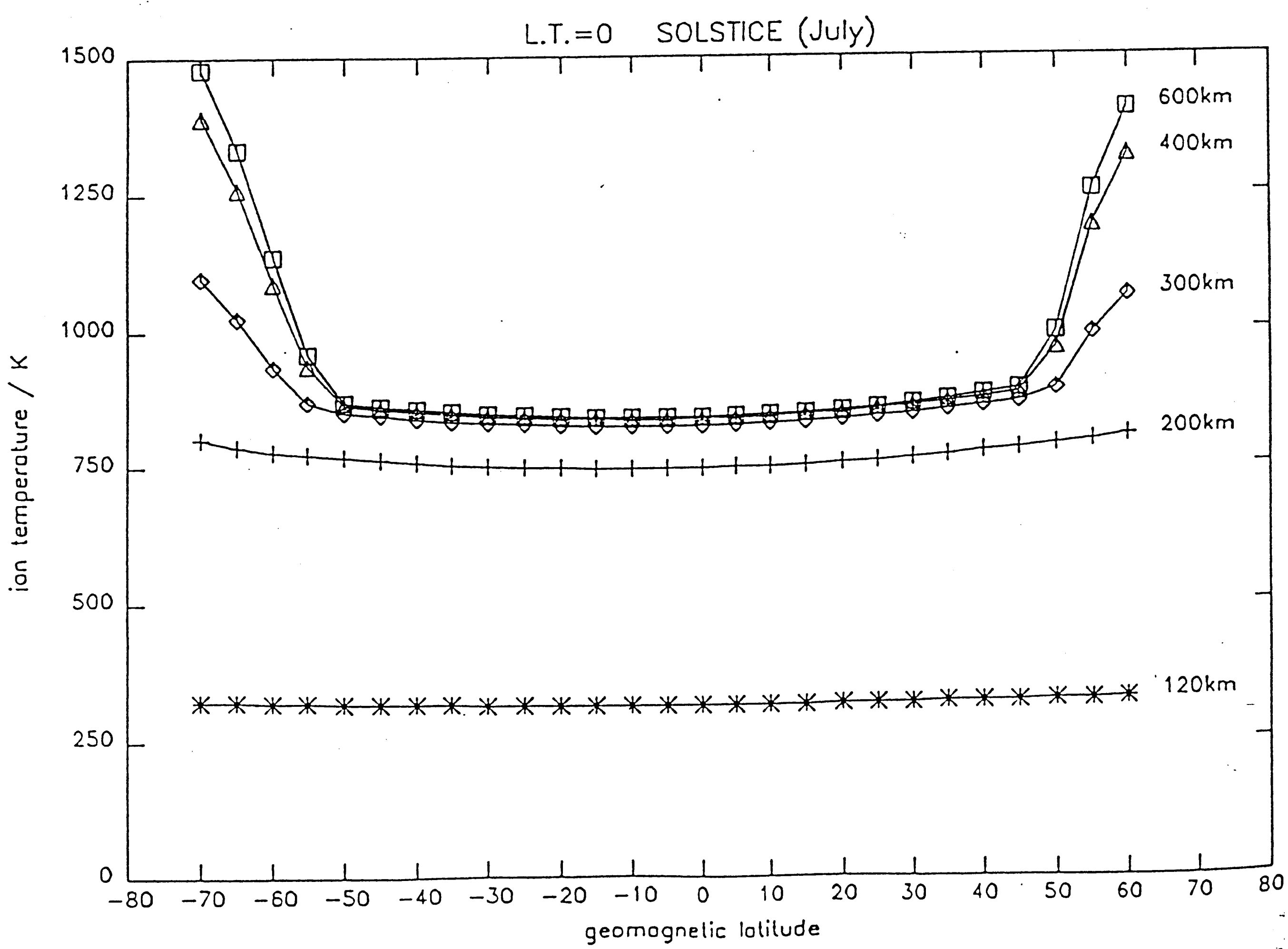
L.T.=0 SOLSTICE (July)
ion temperature / K
geomagnetic latitude
600km
400km
300km
200km
120km

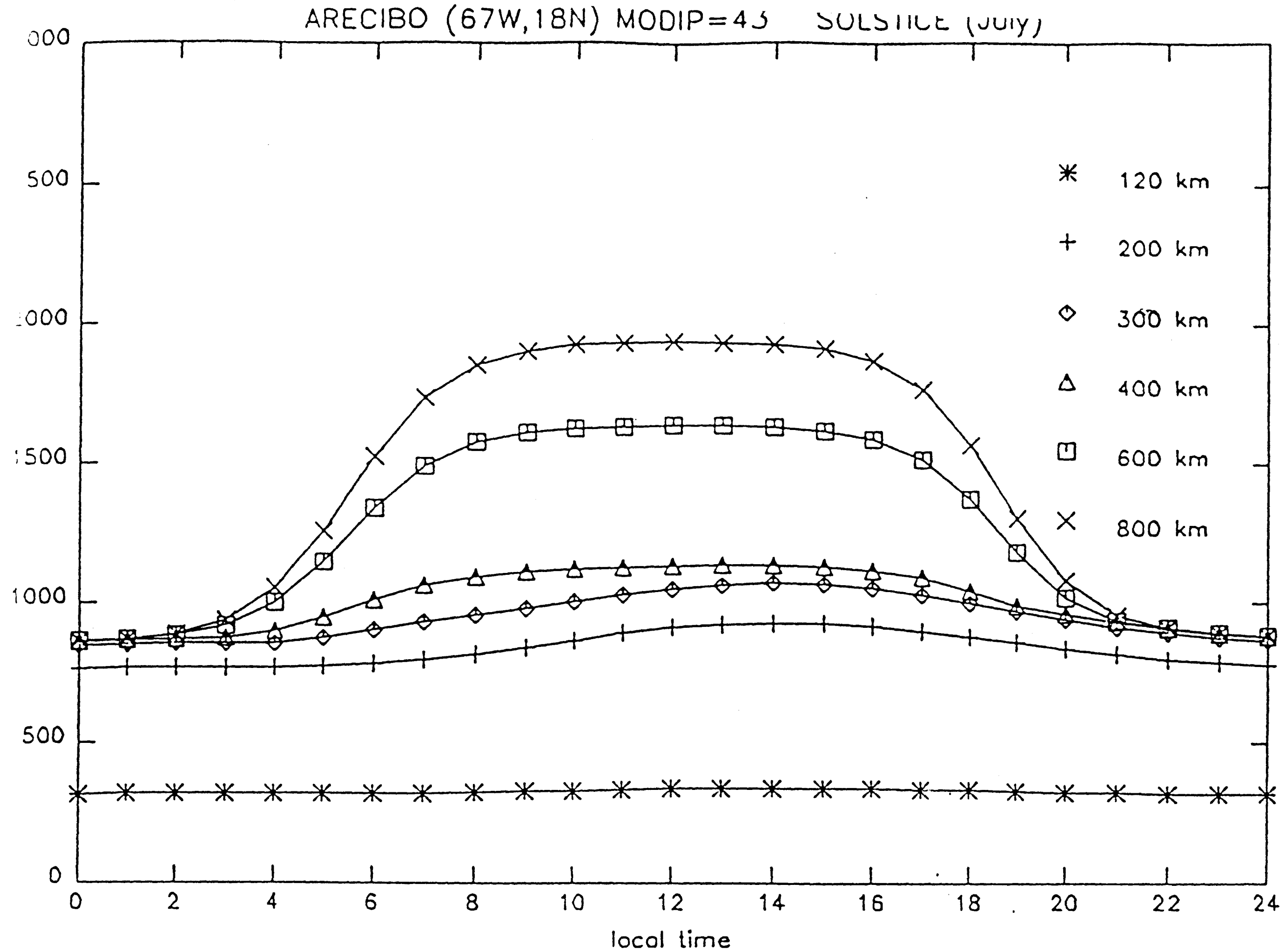
ARECIBO (67W,18N) MODIP=43 SOLSTICE (July)
120 km
200 km
300 km
400 km
600 km
800 km
local time

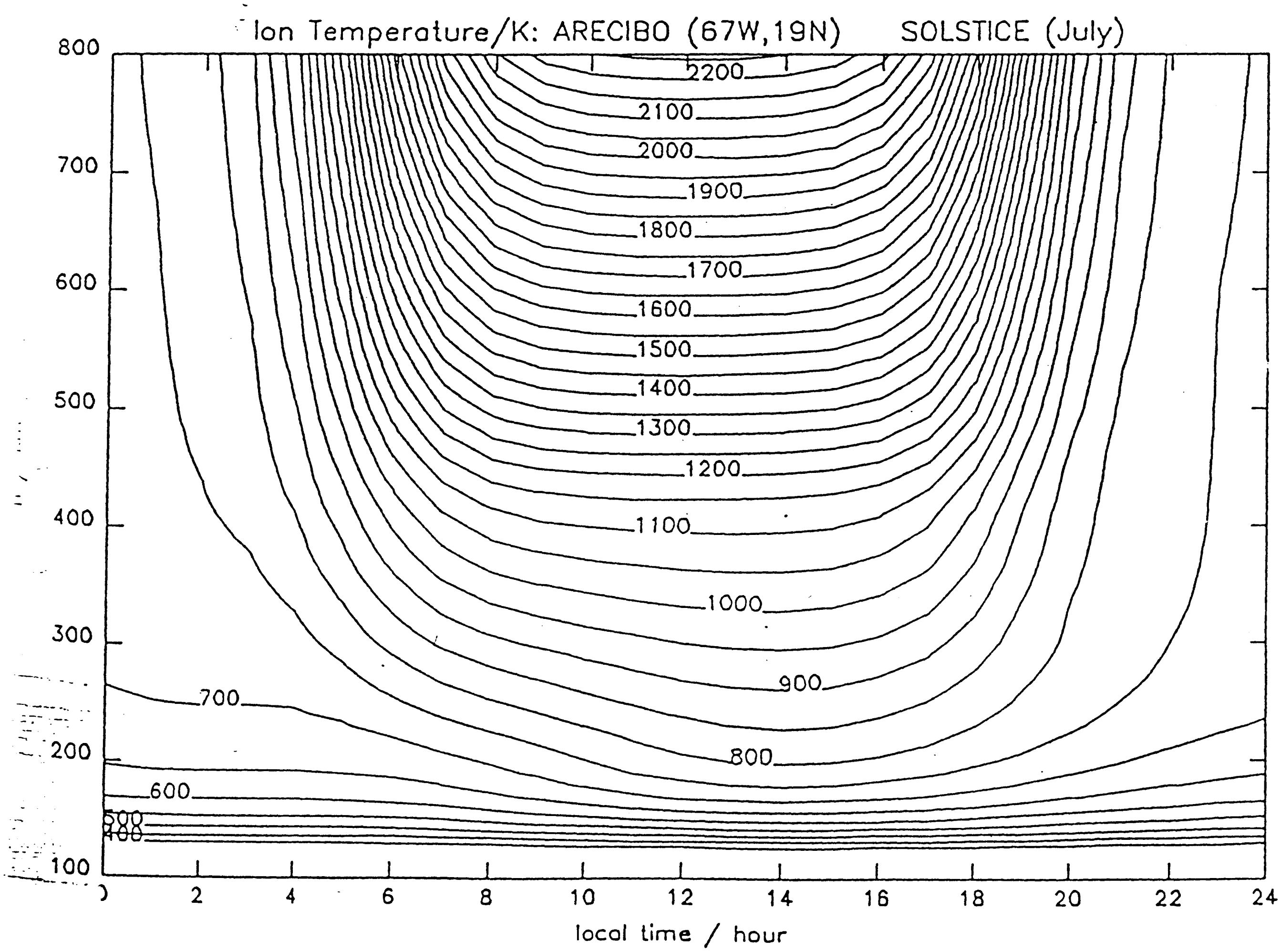
Ion Temperature/K: ARECIBO (67W,19N) SOLSTICE (July)
2200
2100
2000
1900
1800
1700
1600
1500
1400
1300
1200
1100
1000
900
800
700
600
500
400
local time / hour

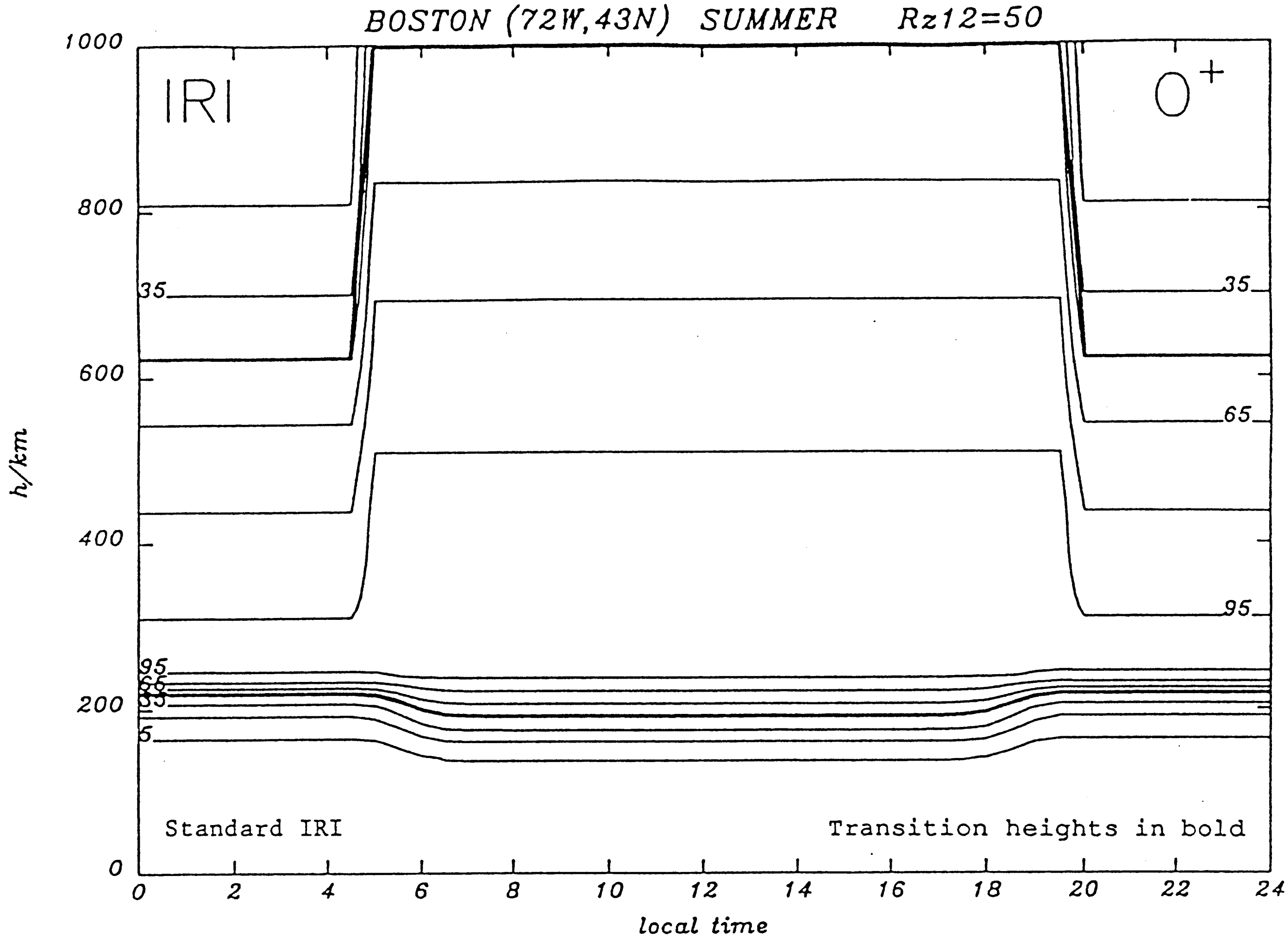
BOSTON (72W,43N) SUMMER Rz12=50
IRI
O+
Standard IRI
Transition heights in bold
h/km
local time

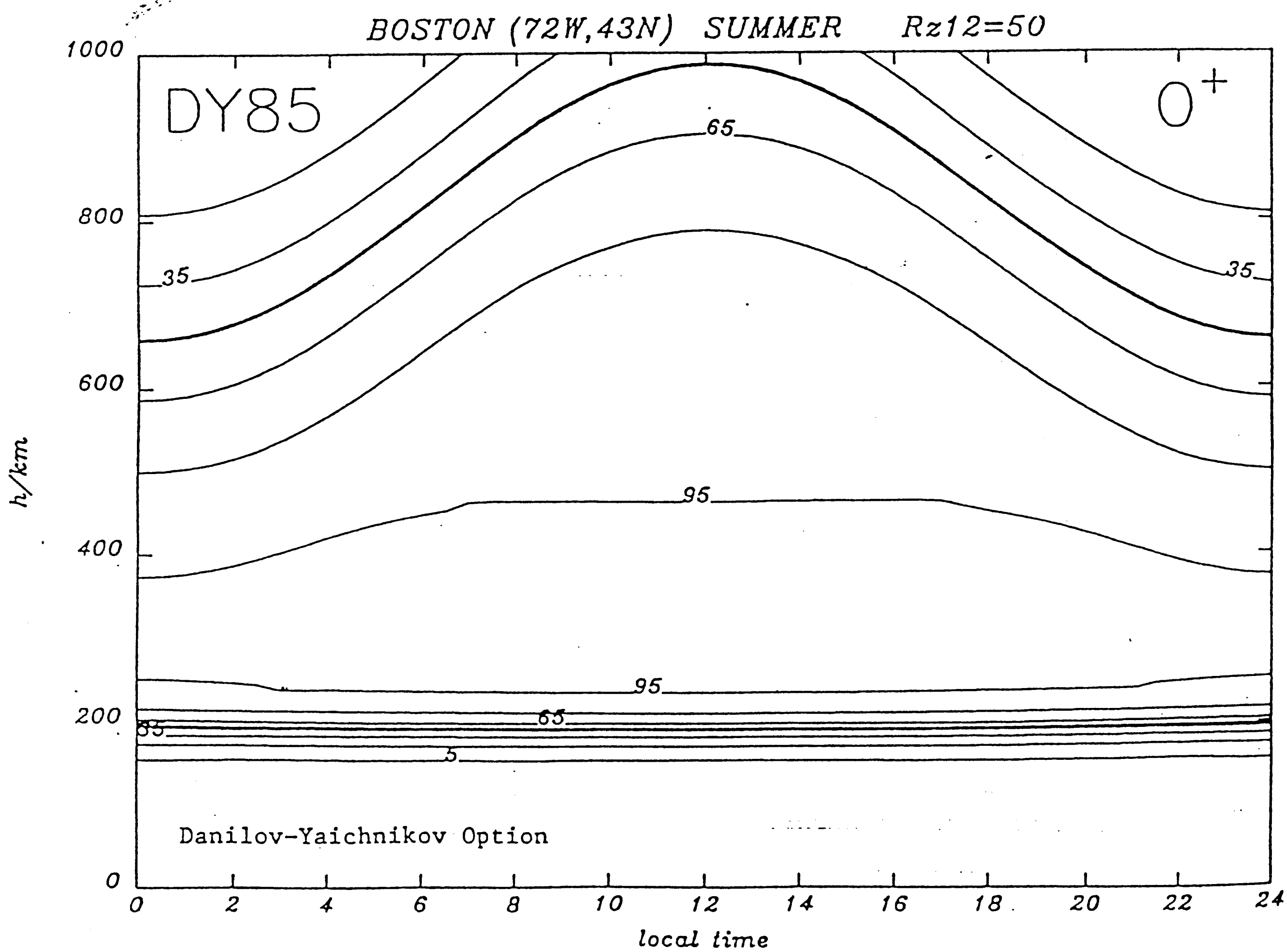
BOSTON (72W,43N) SUMMER Rz12=50
DY85
O+
Danilov-Yaichnikov Option
h/km
local time

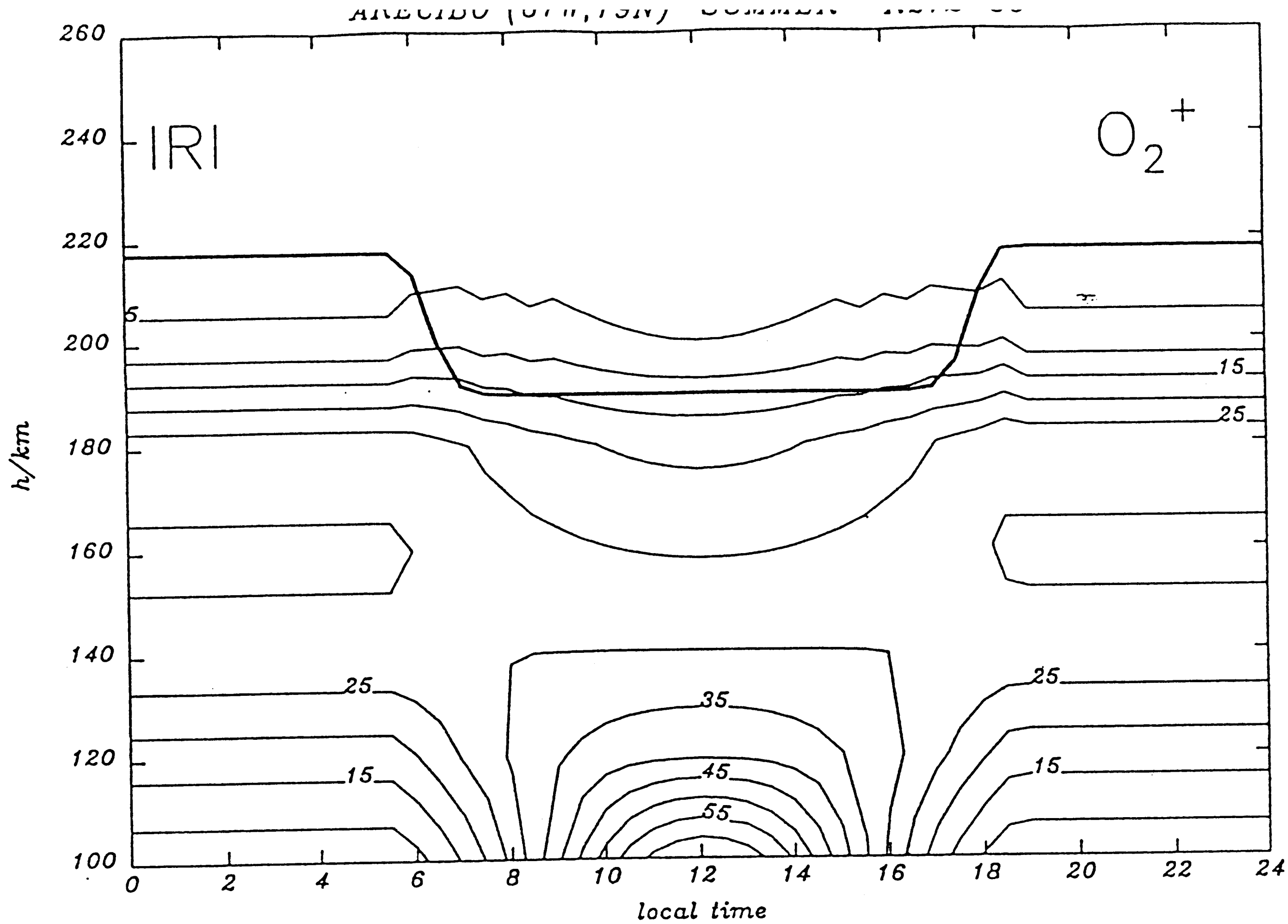

ARECIBO (67W,19N) SUMMER Rz12=50

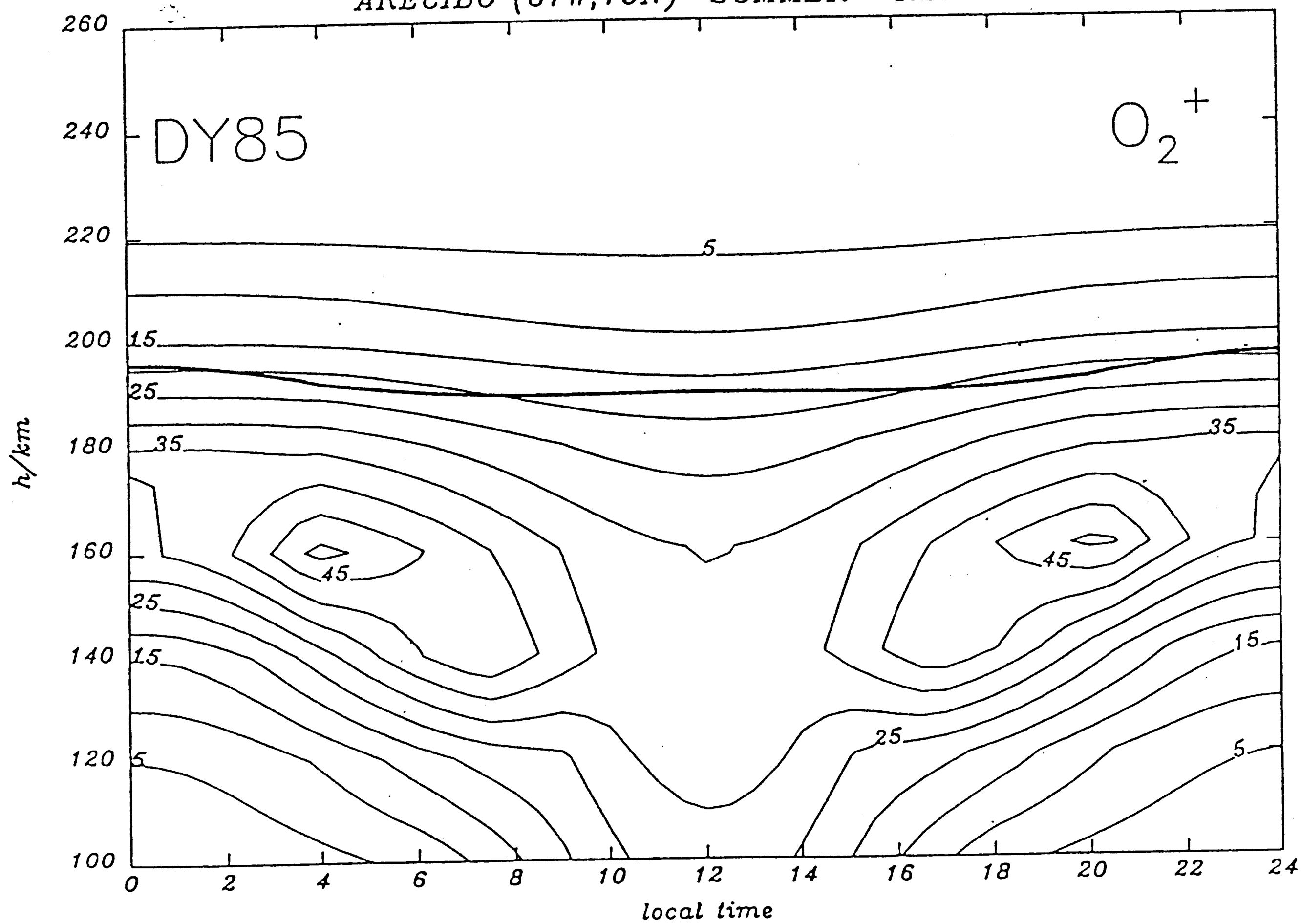

Chapter 5

Tables of Contents of IRI Reports

Contents

5.1 INTERNATIONAL REFERENCE IONOSPHERE 1979

K. Rawer, J. V. Lincoln, and R. O. Conkright (eds.)
World Data Center A for Solar-Terrestrial Physics, *Report UAG-82*, 245 pages, Boulder, Colorado, 1981.

5.2 Experience With and Proposed Improvements of the International Reference Ionosphere

K. Rawer and C. M. Minnis (eds.)
World Data Center A for Solar-Terrestrial Physics, *Report UAG-90*, 235 pages,
Boulder, Colorado, 1984.
Proceedings of the 1980 IRI Workshop in Budapest (Hungary).

1.3 Topside

1.3.1 Rocket and Satellite Measurements Compared with the IRI-79 Electron Density Profiles
E. Neske, S. Ramakrishnan, and C. Rebstock

1.3.2 Comparison Between Plasma Densities Measured with the AEROS-B and S3-1 Satellites and the IRI Model
C. R. Philbrick, P. Lämmerzahl, E. Neske, and A. Dumbs

1.3.3 Comparison of Theoretical Electron Density Profiles at the Magnetic Equator with IRI Model and Incoherent Scatter Data
T. Y. Leshchinskaya and A. V. Mikhailov

1.3.4 Intercomparison of Various Measurements of Thermal Plasma Densities at and Near the Plasmapause
D. V. Williams, M. J. Rycroft, A. J. Smith, V. V. Bezrukikh, K. I. Gringauz, N. C. Maynard, M. J. Morgan, and T. W. Thomas
(This paper was withdrawn by the authors.)

1.3.5 Comparison with IRI of Electron Density and Temperature at the Magnetic Equator
G. F. Deminova and L. A. Yudovich

1.4 Variability

1.4.1 Variability of the Equatorial F-Region
K. Bibl

1.4.2 Construction of Electron Density Profiles for the Flare-Disturbed Ionosphere with Data from Doppler Measurements
I. N. Odintsova and V. D. Novikov

2. Plasma Temperatures

2.1 Electron Temperature

2.1.1 Comparisons of ISIS and AE Satellite Measurements of Electron Temperature with the International Reference Ionosphere
L. H. Brace and R. F. Theis

2.1.2 Proposal of Improvement of the Electron Temperature Model in IRI
K. Hirao

2.1.3 Verification of the International Reference Ionosphere on Electron Temperature Profiles Obtained by Various Methods Below 200 km
Y. K. Chasovitin and N. M. Klyueva

2.1.4 Electron Temperature Modeling in the F-Region and Topside of the Ionosphere: A Proposal for Improving the IRI
K. K. Mahajan and V. K. Pandey

5.3 The Upper Atmospheres of the Earth and Planets

C. A. Barth, D. Offermann, K. Labitzke, J. I. Vette, K. Rawer, H. A. Taylor (eds.)
Advances in Space Research, Volume 2, Number 10, 183-260, 1982.
Proceedings of the 1982 IRI Workshop in Ottawa (Canada).

Section 1 — ELECTRON DENSITY PROFILES

Replacement of the Present Sub-Peak Plasma Density Profile by a Unique Expression
K. Rawer

Implementation of a New Characteristic Parameter into the IRI Sub-Peak Electron Density Profile
T. L. Gulyaeva

In Situ Studies of Electron Density During Equatorial Spread-*F*
S. Prakash, S. Pal, R. Pandey, and B. H. Subbaraya

Equatorial F-Region Ionization Differences Between March and September, 1979
A. DasGupta, D. N. Anderson, and J. A. Klobuchar

Section 2 — THE LOWER IONOSPHERE

D-Region IRI Profiles in Relation to Radio Observations
Y. V. Ramanamurty

Comparison of Al-Absorption Data with Theoretically Computed Values Based on the International Reference Ionosphere (IRI)
G. Datta, S. N. Pradhan, and K. M. Kotadia

Latitudinal Influences on the Quiet Daytime D-Region
W. Swider

Mesospheric Ionization Over Dip Equator at Sunrise
S. P. Gupta

Section 3 — THE PLASMASPHERE

Section 4 — PLASMA TEMPERATURE PROFILES

Section 5 — ION COMPOSITION

5.4 Toward an Improved International Reference Ionosphere

K. Rawer, C. M. Minnis, K. B. Serafimov (eds.)
Advances in Space Research, Volume 4, Number 1, 1-171, 1984.
Proceedings of the 1983 IRI Workshop in Stara Zagora (Bulgaria).

Chapter 1 — ELECTRON DENSITY PROFILES

New Description of the Electron Density Profile
K. Rawer

Geometry of the "Exponential" Middle Ionosphere
T. L. Gulyaeva

Prediction of Total Electron Content Using the IRI
L. F. McNamara

Model Representation of Mid-Latitudinal Electron Density by Means of Interkosmos-19 Data
N. P. Benkova, N. A. Kochenova, A. D. Legenka, M. N. Fatkullin, and M. D. Fligel

N(h) Profiles from Ground and Interkosmos-19 Satellite Data
T. Pashova

Observed and Model *N(h)* Profiles for the Bulgarian Region
T. Pasheva, D. Samardziev, N. P. Benkova, N. A. Kochenova, and J. Kushnerevskij

Bottomside *N(h)* Profiles over Vietnam and Their Comparison with IRI
L. Hoang, K. B. Serafimov, I. Kutiev, and M. Karadimov

The State of the Art in D-Region IRI Modeling
K. Rawer and Y. V. Ramanamurty

Improvement of the Solar-Cycle Variation of IRI Lower Ionosphere Models by Means of Radio Wave Propagation Data
W. Singer, J. Bremer, and J. Taubenheim

Chapter 2 — PLASMA TEMPERATURE PROFILES

Solar Cycle Effects upon the Relationship of N_e and T_e in the F-Region
L. H. Brace and R. F. Theis

Chapter 3 — ION COMPOSITION

Chapter 4 — MISCELLANEOUS

5.5 Models of the Atmosphere and Ionosphere

K. Rawer, C. M. Minnis, K. S. W. Champion, M. Roemer (eds.)
Advances in Space Research, Volume 5, Number 7, 1-112, 1985.
Proceedings of the 1984 IRI Workshop in Graz (Austria).

Chapter 1 — THE INTERNATIONAL REFERENCE IONOSPHERE (Workshop VIII)

Section 1. Electron Density Profiles

5.6 International Reference Ionosphere—Status 1985/86

K. Rawer and Y. V. Ramanamurty (eds.)
Advances in Space Research, Volume 5, Number 10, 1-131, 1985.
Proceedings of the 1985 IRI Workshop in Louvain (Belgium).

The Interest of Information Obtained by Incoherent Scatter Technique
K. Rawer and D. Bilitza

Chapter 1 — TOPSIDE

Electron Density in the Equatorial Topside
D. Bilitza

Modeling the Plasmasphere for the International Reference Ionosphere
M. J. Rycroft and I. R. Jones

Comparison of Measured and Predicted F2-Peak Altitude
D. Bilitza

Latitudinal Asymmetry in Electron and Ion Density Distribution in Southern and Northern Hemispheres
K. B. Serafimov, I. S. Kutiev, and T. P. Dachev

On the Relative Abundance of Helium Ions in the Topside Ionosphere
R. Koleva and I. S. Kutiev

Chapter 2 — MIDDLE IONOSPHERE

Determining Electron Density Profiles for the Middle Ionosphere
K. Rawer

Reliability of Electron Density Profiles
A. K. Paul

Controlling Role of Maximum Usable Frequencies in Ionospheric Informatics
T. L. Gulyaeva

Practical Method for Routine Analysis of the Valley Parameters Between E- and F-Region of the Ionosphere
K. Bibl and M. Calandrella

Chapter 3 — LOWER IONOSPHERE

Chapter 4 — TEMPERATURES

5.7 International Reference Ionosphere—Status 1986/87

K. Rawer and P. A. Bradley (eds.)
Advances in Space Research, Volume 7, Number 6, 1-129, 1987.
Proceedings of the 1986 IRI Workshop in Toulouse (France).

5.8 Ionospheric Informatics

K. Rawer, T. L. Gulyaeva, and B. W. Reinisch (eds.)
Advances in Space Research, Volume 8, Number 4, 1-253, 1988.
Proceedings of the 1987 IRI Workshop in Novgorod (USSR).

Chapter 3 — REDUCTION OF MEASUREMENTS AND DATA

Annex 2: Formulas to "Use of Orthogonal Polynomials ..."
U. C. Upreti, S. Aggarwal, M. M. Gupta, and B. M. Reddy

Annex 3: Table to "Expansion of Ionospheric Characteristics ..."
N. I. Dvinskikh

Annex 4: Table of Incoherent Scatter Facilities
V. I. Taran

5.9 Ionospheric Informatics and Empirical Modeling

K. Rawer and P. A. Bradley (eds.)
Advances in Space Research, Volume 10, Number 8, 1-133, 1990.
Proceedings of the 1988 IRI Workshop in Espoo (Finland).

Chapter 6 — DATA HANDLING

Structure and Information Flows in the Distributed Solar-Terrestrial Physics Data Base System
C. C. Abston, N. E. Papitashvili, and V. O. Papitashvili

Chapter 7 — URSI WORKING GROUP G-4 ON IONOSPHERIC INFORMATICS

Chairman's Report

N(h) Profile Data at World Data Centers
J. H. Allen, R. Conkright, D. Bilitza, A. Y. Feldstein, and D. M. Willis

Discussion of the Valley Problem in *N(h)* Analysis of Ionograms
T. L. Gulyaeva, J. E. Titheridge, and K. Rawer

Digital Ionogram Data
B. W. Reinisch, A. Y. Feldstein, and H. Sizun

Oblique Propagation Studies
P. A. Bradley

5.10 Development of IRI-90

K. Rawer and W. R. Piggott (eds.)
Advances in Space Research, Volume 10, Number 11, 1990.
Proceedings of the 1989 IRI Workshop in Abingdon (United Kingdom).

Chapter 1 — VERTICAL PROFILES

Progress Report on IRI Status
D. Bilitza

New Options for IRI Electron Density in the Middle Ionosphere
D. Bilitza and K. Rawer

On a Characteristic Point at the Base of the F2-Layer
M. Mosert de Gonzales and S. M. Radicella

An Analytical Model of the Electron Density Profile in the Ionosphere
G. Di Giovanni and S. M. Radicella

Spatial and Temporal Variability of the Ionosphere During Solar Minima
T. L. Gulyaeva, M. Mosert de Gonzales, S. M. Radicella, and B. Zolesi

Temporal Variation of Median *foEs*
G. A. Moraitis

Global Models of N_e and T_e at Solar Maximum Based on DE 2 Measurements
L. H. Brace and R. F. Theis

Empirical Modeling of Ion Composition in the Middle and Topside Ionosphere
D. Bilitza

Chapter 2 — WORLDWIDE AND REGIONAL MAPPING

Application of the Expansion into Empirical Orthogonal Functions to Ionospheric Characteristics
W. Singer and J. Taubenheim

Discussion of a New Method for Mapping Ionospheric Characteristics
L. Bossy and K. Rawer

Proposed Improvement of the IRI Topside Profile Formula
K. Rawer

Arnold, F., K. Kissel, D. Krankowsky, H. Wieder, and J. Zähringer, Negative ions in the lower ionosphere, J. Atmos. Terr. Phys. 33, 1169, 1971.

Bilitza, D., Models for the relationship between electron density and temperature in the upper ionosphere, J. Atmos. Terr. Phys. 37, 1219, 1975.

Bilitza, D., Electron density in the D-region as given by the International Reference Ionosphere, World Data Center A for Solar-Terrestrial Physics, Report UAG-82, 7-10, Boulder, 1981a.

Bilitza, D., Models of ionospheric electron and ion temperature, World Data Center A for Solar-Terrestrial Physics, Report UAG-82, 11-16, Boulder, 1981b.

Bilitza, D., New descriptive temperature model, Adv. Space Res. 2 (10), 237-245, 1982.

Bilitza, D., Comparison between the IRI ion composition and incoherent scatter measurements and theoretical values, Adv. Space Res. 4(1), 107-109, 1984.

Bilitza, D., Electron density in the equatorial topside, Adv. Space Res. 5(10), 15-19, 1985a.

Bilitza, D., Implementation of the new electron temperature model in IRI, Adv. Space Res. 5(10), 117-121, 1985b.

Bilitza, D., International Reference Ionosphere: recent development, Radio Sci. 21, 343-346, 1986.

Bilitza, D., Empirical modeling of ion composition in the middle and topside ionosphere, Adv. Space Res., 10 (11), 47-56, 1990.

Bilitza, D., and W. R. Hoegy, Solar activity variation of ionospheric plasma temperatures, Adv. Space Res., 10(8), 81-90, 1990.

Bilitza, D., and K. Rawer, New options for IRI electron density in the middle ionosphere, Adv. Space Res., 10 (11), 7-16, 1990.

Bilitza, D., N. M. Sheikh, and R. Eyfrig, A global model for the height of the F2-peak using *M3000* values from the CCIR, Telecomm. J. 46, 549-553, 1979.

Bilitza, D., L. H. Brace, and R. F. Theis, Modeling of ionospheric temperature profiles, Adv. Space Res. 5(7), 53-58, 1985.

Bilitza, D., K. Rawer, S. Pallaschke, C. M. Rush, N. Matuura, and W. R. Hoegy, Progress in modeling the ionospheric peak and topside electron density, Adv. Space Res. 7(6), 5-12, 1987.

Bilitza, D., K. Rawer, and S. Pallaschke, Study of ionospheric models for satellite orbit determination, Radio Sci. 23, 223-232, 1988.

Booker, H. C., Fitting of multi-region ionospheric profiles of electron density by a single analytic function of height, J. Atmos. Terr. Phys. 39, 619, 1977.

Brace, L. H., and R. F. Theis, An empirical model of the interrelationship of electron temperature and density in the daytime thermosphere at solar minimum, Geophys. Res. Lett. 5, 275-278, 1978.

Brace, L. H., and R. F. Theis, Global empirical models of ionospheric electron temperature in the upper F-region and plasmasphere based on in situ measurements from Atmosphere Explorer C, ISIS 1 and ISIS 2 satellites, J. Atmos. Terr. Phys. 43, 1317-1343, 1981.

Bradley, P. A., Mapping the critical frequency of the F2-layer: Part 1—Requirements and developments to around 1980, Adv. Space Res. 10(8), 47-56, 1990.

Bradley, P. A., and J. R. Dudeney, Vertical distribution of electron concentration in the ionosphere, J. Atmos. Terr. Phys. 35, 2131-2146, 1973.

Briggs, B. H., J. Atmos. Terr. Phys. 39, 1023-1033, 1977.

Brinton, H. C., H. G. Mayr, R. A. Pickett, and H. A. Taylor, The effect of atmospheric winds on the O^+ - H^+ transition level, Space Research X, 652-662, North-Holland Publishing Company, Amsterdam, 1970.

Buonsanto, M. J., Comparison of incoherent scatter observations of electron density, and electron and ion temperature at Millstone Hill with the International Reference Ionosphere, J. Atmos. Terr. Phys. 51, 441-468, 1989.

Chiu, Y. T., An improved phenomenological model of ionospheric density, J. Atmos. Terr. Phys. 37, 1563, 1975.

CCIR, Comité Consultatif International des Radiocommunications, Reports 340, 340-2 and later supplements, Geneva, 1967.

CCIR, Comité Consultatif International des Radiocommunications, Report 252-2 and later supplements, Geneva, 1973.

CIRA 1961, North-Holland Publishing Company, Amsterdam, 1961.

CIRA 1965, North-Holland Publishing Company, Amsterdam, 1965.

CIRA 1972, Akademie-Verlag, Berlin, German Democratic Republic, 1972.

CIRA 1986, Adv. Space Res., 8(5-6), 1988, and 10(6), 1990.

Coster, A. J., M. Buonsanto, E. M. Gaposchkin, D. Tetenbaum, and L. E. Thornton, Ionospheric and tropospheric path delay observations obtained from GPS integrated phase, incoherent scatter and refractometer data and from IRI-86, Adv. Space Res. 10(8), 105-108, 1990.

Danilov, A. D., and V. K. Semenov, Relative ion composition model at midlatitudes, J. Atmos. Terr. Phys. 40, 1093-1102, 1978.

Danilov, A. D., and A. P. Yaichnikov, A new model of the ion composition at 75 to 1000 km for IRI, Adv. Space Res. 5(7), 75-79, 1985.

Demars, H. G., and R. W. Schunk, Temperature anisotropies in the terrestrial ionosphere and plasmasphere, Rev. Geophys. 25, 1659-1679, 1987.

Ducharme, E. D., L. E. Petrie, and R. Eyfrig, A method for predicting the F1-layer critical frequency, Radio Sci. 6, 369-378, 1971.

Ducharme, E. D., L. E. Petrie, and R. Eyfrig, A method for predicting the F1-layer critical frequency based on Zurich smoothed sunspot number, Radio Sci. 8, 837-839, 1973.

Dumbs, A., G. Emmenegger, R. Kist, D. Klumpar, E. Neske, J. Slavik, K. Spenner, and H. Wolf, Results from the plasma experiments on AEROS, J. Geomag. Geoelectr. 31, S125, 1979.

Feichter, E., R. Leitinger, and G. K. Hartmann, Untersuchungen über die Halbjahres- und die Jahreswelle in F-Schicht-Parametern, Kleinheubacher Ber. 31, 249-258, 1988.

Feichter, E., R. Leitinger, and G. K. Hartmann, Modell-Parameter für den Elektroneninhalt der Ionosphäre in mittleren Breiten, Kleinheubacher Ber. 32, 623-632, 1989.

Ferguson, B. G., and L. F. McNamara, Calculation of HF absorption using the International Reference Ionosphere, J. Atmos. Terr. Phys. 48, 41-49, 1986.

Goel, M. K., and B. C. N. Rao, Ion composition behaviour in low and midlatitudes during high solar activity, Adv. Space Res. 4(1), 111-118, 1984.

Goel, M. K., B. C. N. Rao, S. Chandra, and E. J. Maier, Satellite measurements of ion composition and temperatures in the topside ionosphere during medium solar activity, J. Atmos. Terr. Phys. 38, 389, 1976.

Gulyaeva, T. L., Progress in ionospheric informatics based on electron density profile analysis of ionograms, Adv. Space Res. 7(6), 39-48, 1987.

Gulyaeva, T. L., J. E. Titheridge, and K. Rawer, Discussion of the valley problem in N(h) analysis of ionograms, Adv. Space Res. 10(8), 123, 1990.

Hirao K., and K. Oyama, An improved type of electron temperature probe, J. Geomag. Geoelectr. 22, 393-402, 1970.

Johnson, C. Y., Ionospheric composition and density from 90 to 1200 kilometers at solar minimum, J. Geophys. Res. 71, 330, 1966.

Jones, W. B., and R. M. Gallet, The representation of diurnal and geographic variations of ionospheric data by numerical methods, Telecomm. J. 29, 129, 1962, and 32, 18, 1965.

Kazimirovsky, E. S., and E. I. Zhovty, A plan for compilation of experimental data on drifts for IRI, Adv. Space Res. 4(1), 149-151, 1984.

Kazimirovsky, E. S., E. I. Zhovty, and M. A. Chernigovskaya, Modeling of ionospheric drifts in view of IRI, Adv. Space Res. 5(7), 95-96 and 109-112, 1985.

Kelly, J. D., and V. B. Wickwar, Radar measurements of high-latitude ion composition between 140 and 300 km altitude, J. Geophys. Res. 82, 7617-7626, 1981.

Kleiner, B., and T. E. Graedel, Exploratory data analysis in the geophysical sciences, Rev. Geophys. Space Phys. 18, 699-717, 1980.

Kopp, E., Ion composition in the D- and lower E-regions with particular emphasis on cluster ions, World Data Center A for Solar-Terrestrial Physics, Report UAG-90, 140-149, Boulder, 1984.

Kopp, E., P. Eberhardt, and U. Iterrman, Summer daytime ion composition in the D-region above Wallops Island, Space Research XVIII, 245, 1978.

Kouris, S. S., and L. M. Muggleton, Diurnal variation in the E-layer ionization, J. Atmos. Terr. Phys. 35, 133-139, 1973a.

Kouris, S. S., and L. M. Muggleton, A proposed prediction method for monthly median *foE*, contribution No. 6/3/07 to Interim Working Party 6/3, CCIR Report 252-2, 1973b.

Kutiev, I., K. Serafimov, N. Karadimov, and R. Heelis, A proposed improvement of IRI using the O^+ - H^+ transition level, World Data Center A for Solar-Terrestrial Physics, Report UAG-90, 150-154, Boulder, Colorado, 1984a.

Kutiev, I., P. Marinov, and K. B. Serafimov, An approximation of the height of the O^+ – H^+ transition level for use in IRI, Adv. Space Res. 4(1), 119-121, 1984b.

Lathuillere, C., and A. Brekke, Ion composition in the auroral ionosphere as observed by EISCAT, Annales Geophysicae 3, 557-568, 1985.

Lathuillere, C., G. Lejeune, and W. Kofman, Direct measurements of ion composition with EISCAT in the high latitude F1-region, Radio Sci. 18, 887-893, 1983.

Leitinger, R., and E. Putz, Die Auswertung von Differenz-Doppler-Messungen an den Signalen von Navigationssatelliten, Technical Report, University of Graz, 1978.

Leitinger, R., and E. Putz, Ionospheric refraction errors and observables, in: Atmospheric Effects on Geodetic Space Measurements (F. K. Brunner, ed.), Monograph 12, School of Surveying, University of New South Wales, 81-102, 1988.

Leitinger, R., G. Schmidt, and A. Tauriainen, An evaluation method combining the differential Doppler measurements from two stations that enables the calculation of the electron content of the ionosphere, J. Geophysics (Zs. Geophysik) 41, 201-213, 1975.

Llewellyn, S. K., and R. B. Bent, Documentation and description of the Bent ionospheric model, Air Force Geophysics Laboratory, Report AFCRL-TR-73-0657, Hanscom AFB, Massachusetts, 1973.

Maeda, K. I., Midlatitude electron density profiles as revealed by rocket experiments, J. Geomag. Geoelectr. 21, 557, 1969.

Maeda, K. I., Midlatitude electron density profile in the lower solar activity, J. Geomag. Geoelectr. 22, 551, 1970.

Maeda, K. I., Study on electron density profile in the lower ionosphere, J. Geomag. Geoelectr. 23, 133, 1971.

Maeda, K. I., E-region electron density profile, Space Research XII, 1229, 1972.

Mahajan, K. K., and R. Kohli, Search of thickness parameter for the bottomside ionospheric F-region from incoherent-scatter electron-density profiles, Adv. Space Res. 7(6), 57-60, 1987.

Mahajan, K. K., R. Kohli, V. K. Pandey, and N. K. Sethi, Information about the E-region valley from incoherent scatter measurements, Adv. Space Res. 10(8), 17-20, 1990.

McNamara, L. F., Prediction of total electron content using the International Reference Ionosphere, Adv. Space Res. 4(1), 25-50, 1984.

McNamara, L. F., The use of total electron content measurements to validate empirical models of the ionosphere, Adv. Space Res. 5(7), 81-90, 1985.

McNamara, L. F., and P. J. Wilkinson, Prediction of total electron content using the International Reference Ionosphere, J. Atmos. Terr. Phys. 45, 169-174, 1983.

Mechtly, E. A., and D. Bilitza, Models of D-region electron concentrations, Institut fuer Physikalische Weltraumforschung, Report IPW-WB1, Freiburg, Federal Republic of Germany, 1974.

Miyazaki, S., Ion transition height distribution obtained with the satellite TAIYO, J. Geomag. Geoelectr. 31, S95-S112, 1979.

Oliver, W. L., Models of F1-region ion composition variations, J. Atmos. Terr. Phys. 37, 1065-1076, 1975.

Oyama, K. I., and T. Abe, Anisotropy of electron temperature in the ionosphere, Geophys. Res. Lett. 14, 1195-1198, 1987.

Oyama, K. I., K. Hirao, P. M. Banks, and P. R. Williamson, Is T_e equal to T_n at the heights of 100 to 120 km?, Planet. Space Sci. 28, 207-211, 1980.

Oyama, K. I., K. Hirao, and F. Yasuhara, Electron temperature probe on board Japan's 9th scientific satellite OHZORA, J. Geomag. Geoelectr. 37, 413-430, 1985.

Oyinloye, J. O., Equatorial HF radio wave absorption measurements and the IRI, J. Atmos. Terr. Phys. 50, 519-522, 1988.

Philbrick, C. R., and K. H. Bhavnani, F-region ion composition modeling, Adv. Space Res. 2(10), 253-257, 1983.

Philbrick, C. R., P. Lämmerzahl, E. Neske, and A. Dumbs, Comparison between plasma densities measured with the AEROS-B and S3-1 satellites and the IRI model, World Data Center A for Solar-Terrestrial Physics, Report UAG-90, 62-67, Boulder, 1984.

Pintado, O. I., S. M. Radicella, and P. M. Fernández, Experimental estimates of electron density variations at the reflection height of VLF signals, J. Atmos. Terr. Phys. 49, 129-133, 1987.

Raitt, W. J., R. W. Schunk, and P. M. Banks, A comparison of the temperature and density structure in high and low speed thermal proton flows, Planet. Space Sci. 23, 1103-1117, 1975.

Ramakrishnan, S., and K. Rawer, Model electron density profiles obtained by empirical procedures, Space Research XII, 1253-1259, Akademie-Verlag, Berlin, German Democratic Republic, 1972.

Rawer, K., in: Meteorological and Astronomical Influences on Radio Wave Propagation, B. Landmark (ed.), p. 221, Academy Press, New York, 1963.

Rawer, K. (ed.), Methods of Measurements and Results of Lower Ionosphere Structure, Akademie-Verlag, Berlin, German Democratic Republic, 1974.

Rawer, K., New description of the electron density profile, Adv. Space Res. 4(1), 11-15, 1984.

Rawer, K., Determining electron density profiles for the middle ionosphere, Adv. Space Res. 5(10), 43-49, 1986.

Rawer, K., Joint analytical profile of electron density profiles through the whole ionosphere, Adv. Space Res. 7(6), 25-33, 1987.

Rawer, K., Synthesis of ionospheric electron density profiles with Epstein functions, Adv. Space Res. 8(4), 191-200, 1988.

Rawer, K., and D. Bilitza, Electron density profile description in the International Reference Ionosphere, J. Atmos. Terr. Phys. 51, 781-790, 1989.

Rawer, K., and D. Bilitza, International Reference Ionosphere-plasma densities: Status 1988, Adv. Space Res. 10(8), 5-14, 1990.

Rawer, K., S. Ramakrishnan, and D. Bilitza, International Reference Ionosphere 1978, International Union of Radio Science, Special Report, Brussels, Belgium, 1978a.

Rawer, K., D. Bilitza, and S. Ramakrishnan, Goals and status of the International Reference Ionosphere, Rev. Geophys. 16, 177-181, 1978b.

Rawer, K., D. Bilitza, S. Ramakrishnan, and M. N. Sheikh, Intentions and buildup of the International Reference Ionosphere, in: Operational Modeling of the Aerospace Propagation Environment, AGARD-CPP-238, 6.1-6.10, 1978c.

Rawer, K. (chairman), J. V. Lincoln (ed.), R. O. Conkright (ed.), International Reference Ionosphere–IRI-79, World Data Center A for Solar-Terrestrial Physics, Report UAG-82, Boulder, 1981.

Rawer, K., D. Bilitza, and T. L. Gulyaeva, New formulas for the IRI electron density profile in the topside and middle ionosphere, Adv. Space Res. 5(7), 3-12, 1985.

Rush, C. M., M. PoKempner, and D. N. Anderson, F. G. Stewart, and J. Perry, Improving ionospheric maps using theoretically derived values of *foF2*, Radio Sci. 18, 95-107, 1983.

Rush, C. M., M. PoKempner, D. N. Anderson, J. Perry, F. G. Stewart, and R. Reasoner, Maps of *foF2* derived from observations and theoretical data, Radio Sci. 19, 1083-1097, 1984.

Rush, C. M., M. Fox, D. Bilitza, K. Davies, L. McNamara, F. G. Stewart, and M. PoKempner, Ionospheric mapping—An update of *foF2* coefficients, Telecomm. J. 56, 179-182, 1989.

Rycroft, M. J., and I. R. Jones, Modeling the plasmasphere for the International Reference Ionosphere, Adv. Space Res. 5(10), 21, 1985.

Rycroft, M. J., and I. R. Jones, A suggested model for the IRI plasmaspheric distribution, Adv. Space Res. 7(6), 13-22, 1987.

Serafimov, K. B., M. K. Serafimova, Y. V. Ramanamurty, and K. Rawer, A note on the use of absorption measurements for improving the IRI electron density distribution in the lower ionosphere, Adv. Space Res. 5(10), 99-102, 1985.

Shimazaki, T., Worldwide daily variability in the height of the maximum electron density of the ionospheric F2-layer, J. Radio Res. Labs. (Japan) 2, 85-97, 1955.

Singer, W., J. Bremer, and J. Taubenheim, Improvement of the solar-cycle variation of IRI lower ionosphere models by means of radio wave propagation data, Adv. Space Res. 4(1), 79-88, 1984.

Skedel, K., Vergleich von Empirischen Parametern der Ionosphäre mit Modelldaten der IRI (International Reference Ionosphere), Diplomarbeit (thesis for master's degree), Institut f. Meteorologie u. Geophysik, University of Graz, 1989.

Soboleva, T. N., Model profiles of the diurnal distribution of electron density of the quiet ionosphere at middle latitudes (Russian), IZMIRAN, Preprint No. 20, Moscow, 1972.

Soboleva, T. N., Diurnal variations in electron density distribution of the quiet ionosphere at middle latitudes, Geomagnetism and Aeronomy 13, 790, 1973.

Spenner, K., and R. Plugge, Empirical model of global electron temperature distribution between 300 and 700 km based on data from AEROS-A, J. Geophys. 46, 43-56, 1979.

Sridharan, R., R. Raghavaro, A. A. Pokhunkov, and V. A. Varfolomeev, Relative ion composition variation over the dip equator—A comparison of measurements with IRI, J. Atmos. Terr. Phys. 47, 1081-1084, 1985.

Suchy, K., and K. Rawer, Improvements in empirical modeling of the world-wide ionosphere, Air Force Geophysics Laboratory, Report AFGL-TR-87-0109, Hanscom AFB, Massachusetts, 1986.

Taylor, H. A., Observed solar geomagnetic control of the ionosphere: Implications for reference ionospheres, Space Research XII, 1275, 1972.

Thomas, L., The neutral and ion chemistry of the upper atmosphere, in: Encyclopedia of Physics, Volume XLIX/6, Geophysics III/6, K. Rawer (ed.), Springer-Verlag, Berlin, 1982.

Titheridge, J. E., Determination of ionospheric electron content from the Faraday rotation of geostationary satellite signals, Planet. Space Sci. 20, 353-369, 1972.

Titheridge, J. E., Ion transition heights from topside electron density profiles, Planet. Space Sci. 24, 229-245, 1976.

Torr, D. G., and M. R. Torr, Chemistry of the thermosphere and ionosphere, J. Atmos. Terr. Phys. 41, 797, 1979.

Vergasova, G. V., E. I. Zhovty, and E. S. Kazimirovsky, Planet Space Sci. 26, 387-398, 1979.

Whitehead, J. D., Recent work on midlatitude and equatorial sporadic-E, J. Atmos. Terr. Phys. 51, 401-424, 1989.

NATIONAL SPACE SCIENCE DATA CENTER

National Aeronautics and Space Administration

Goddard Space Flight Center,
Greenbelt, Maryland 20771